NEUROSENSORY DEVELOPMENT IN THE ZEBRAFISH INNER EAR

A Dissertation

by

SHRUTI VEMARAJU

Submitted to the Office of Graduate Studies of
Texas A&M University
in partial fulfillment of the requirements for the degree of

DOCTOR OF PHILOSOPHY

December 2011

Major Subject: Biology

NEUROSENSORY DEVELOPMENT IN THE ZEBRAFISH INNER EAR

A Dissertation

by

SHRUTI VEMARAJU

Submitted to the Office of Graduate Studies of
Texas A&M University
in partial fulfillment of the requirements for the degree of

DOCTOR OF PHILOSOPHY

Approved by:

Chair of Committee,	Bruce B. Riley
Committee Members,	Mark J. Zoran
	Brian D. Perkins
	Rajesh C. Miranda
Head of Department	Uel Jackson McMahan

December 2011

Major Subject: Biology

ABSTRACT

Neurosensory Development in the Zebrafish Inner Ear. (December 2011)

Shruti Vemaraju, B.Tech., Guru Gobind Singh Indraprastha University

Chair of Advisory Committee: Dr. Bruce B. Riley

The vertebrate inner ear is a complex structure responsible for hearing and balance. The inner ear houses sensory epithelia composed of mechanosensory hair cells and non-sensory support cells. Hair cells synapse with neurons of the VIIIth cranial ganglion, the statoacoustic ganglion (SAG), and transmit sensory information to the hindbrain. This dissertation focuses on the development and regulation of both sensory and neuronal cell populations. The sensory epithelium is established by the basic helix-loop-helix transcription factor Atoh1. Misexpression of *atoh1a* in zebrafish results in induction of ectopic sensory epithelia albeit in limited regions of the inner ear. We show that sensory competence of the inner ear can be enhanced by co-activation of *fgf8/3* or *sox2*, genes that normally act in concert with *atoh1a*. The developing sensory epithelia express several factors that regulate differentiation and maintenance of hair cells. We show that *pax5* is differentially expressed in the anterior utricular macula (sensory epithelium). Knockdown of *pax5* function results in utricular hair cell death and subsequent loss of vestibular (balance) but not auditory (hearing) defects. SAG neurons are formed normally in these embryos but show disorganized dendrites in the utricle following loss of hair cells. Lastly, we examine the development of SAG. SAG

precursors (neuroblasts) are formed in the floor of the ear by another basic helix-loop-helix transcription factor *neurogenin1* (*neurog1*). We show that Fgf emanating from the utricular macula specifies neuroblasts, that later delaminate from the otic floor and undergo a phase of proliferation. Neuroblasts then differentiate into bipolar neurons that extend processes to hair cells and targets in the hindbrain. We show evidence that differentiating neurons express *fgf5* and regulate further development of the SAG. As more differentiated neurons accumulate, increasing level of Fgf terminates the phase of neuroblast specification. Later on, elevated Fgf stabilizes the transit-amplifying phase and inhibits terminal differentiation. Thus, Fgf signaling regulates SAG development at various stages to ensure that proper number of neurons is generated.

ACKNOWLEDGEMENTS

I would like to thank my advisor, Dr. Bruce Riley for his constant guidance and encouragement that helped my professional and personal growth. I am very grateful to my committee members, Dr. Mark Zoran, Dr. Brian Perkins and Dr. Rajesh Miranda for their invaluable input through the years.

I am thankful to all current and past members of the Riley lab for their feedback on my work, and for creating an environment conducive to research and scientific interaction. I am extremely thankful to Sujin Kwak who mentored me in the initial years of my graduate career and introduced me to the SAG. It was a pleasure to work with her on the *pax5* paper. I would also like to thank Elly Sweet for all the intellectually stimulating discussions over the years and collaboration on the *atoh1* paper. Work done by Mahesh Padanad and Dr. Hye-Joo Kwon in characterizing expression patterns of all known Fgfs in zebrafish was instrumental in identifying *fgf5* in the SAG. I would like to thank members in other zebrafish labs, especially Anand Narayanan and Michelle Ramsey, for in-depth discussions, sharing reagents and help with troubleshooting experiments. Anand and Elly have also been a constant source of motivation and support to me. I greatly appreciate Mugdha Deshpande for helpful cryosectioning tips and for welcoming me into her home during my long visits to College Station. On a separate note, I would like to extend my gratitude to Prof. K. Kannan for painstakingly designing my undergraduate program that has helped me build a strong foundation.

I am grateful to my parents, extended family and friends for their encouragement and involvement in numerous ways during this journey. I would especially like to thank my brother, Ravi Vemaraju, for inspiring me to pursue research in the field of neuroscience and being a pillar of strength my entire life. Lastly, I am thankful to Rico for all the laughs and dog therapy that was very critical in relieving stress. And special thanks to my husband, Sudeep Potharaju, for being extremely patient and providing unending support to complete my graduate study and in writing this dissertation.

This work was supported by the National Institutes of Health NIDCD grant R01-DC03806.

TABLE OF CONTENTS

CHAPTER Page

LIST OF FIGURES

FIGURE Page

LIST OF TABLES

CHAPTER I

INTRODUCTION

CLINICAL IMPLICATION AND RELEVANCE

The vertebrate inner ear is a complex structure that is responsible for hearing and maintaining balance. Hearing impairment and balance disorders such as vertigo can have several underlying causes ranging from genetic conditions to environmental factors. The most common form of permanent hearing deficit results from loss of inner ear sensory hair cells. Although humans have lost the ability to regenerate hair cells, most non-mammalian vertebrates have retained the capacity to replace hair cells lost during normal growth or following injury. In some cases of ear dysfunction, the peripheral nerve connecting the inner ear to the central nervous system itself is damaged. A better understanding of the molecular players involved in neurosensory development and regeneration is critical for designing therapeutic strategies to restore proper inner ear function.

CRANIAL PLACODES

The peripheral nervous system in vertebrate embryos is derived from two cell populations- neural crest and cranial placodal cells, which form at the border of the

---

This dissertation follows the style of Developmental Biology.

neural plate and epidermis. Cranial placodes are specialized regions of vertebrate ectoderm that contribute to cranial ganglia and paired sense organs associated with olfaction, vision, hearing and balance in the head. These ectodermal thickenings form at distinct anteroposterior positions along the developing neural tube. Cranial placodes include the anterior lobe of the pituitary gland (adenohypophyseal), olfactory, lens, trigeminal, profundal, otic, lateral line, epibranchial and hypobranchial placodes. Most of these placodes are present in all vertebrates. Despite the diversity of structure and cell types derived from these placodes, all cranial placodes are thought to arise from a common field called the preplacodal ectoderm (reviewed in Baker and Bronner-Fraser, 2001, Schlosser, 2010, Streit, 2004).

STRUCTURE OF THE INNER EAR

The inner ear is a complex three-dimensional structure that houses neuronal, sensory and non-neurosensory cell-types that are involved in hearing and balance. The earliest visible sign of inner ear development is the appearance of the otic placode. This placode cavitates to form a hollow structure called the otic vesicle in zebrafish (Fig. 1.1A). In other vertebrates such as chick and mouse this process occurs via invagination. The vesicle then undergoes a series of morphological changes that form interconnected chambers and canals (Lewis et al., 1985) (Fig. 1.1C). Each of these structures is associated with sensory patches, called maculae and cristae, which are important for auditory (hearing) and vestibular (balance) function. These patches called sensory

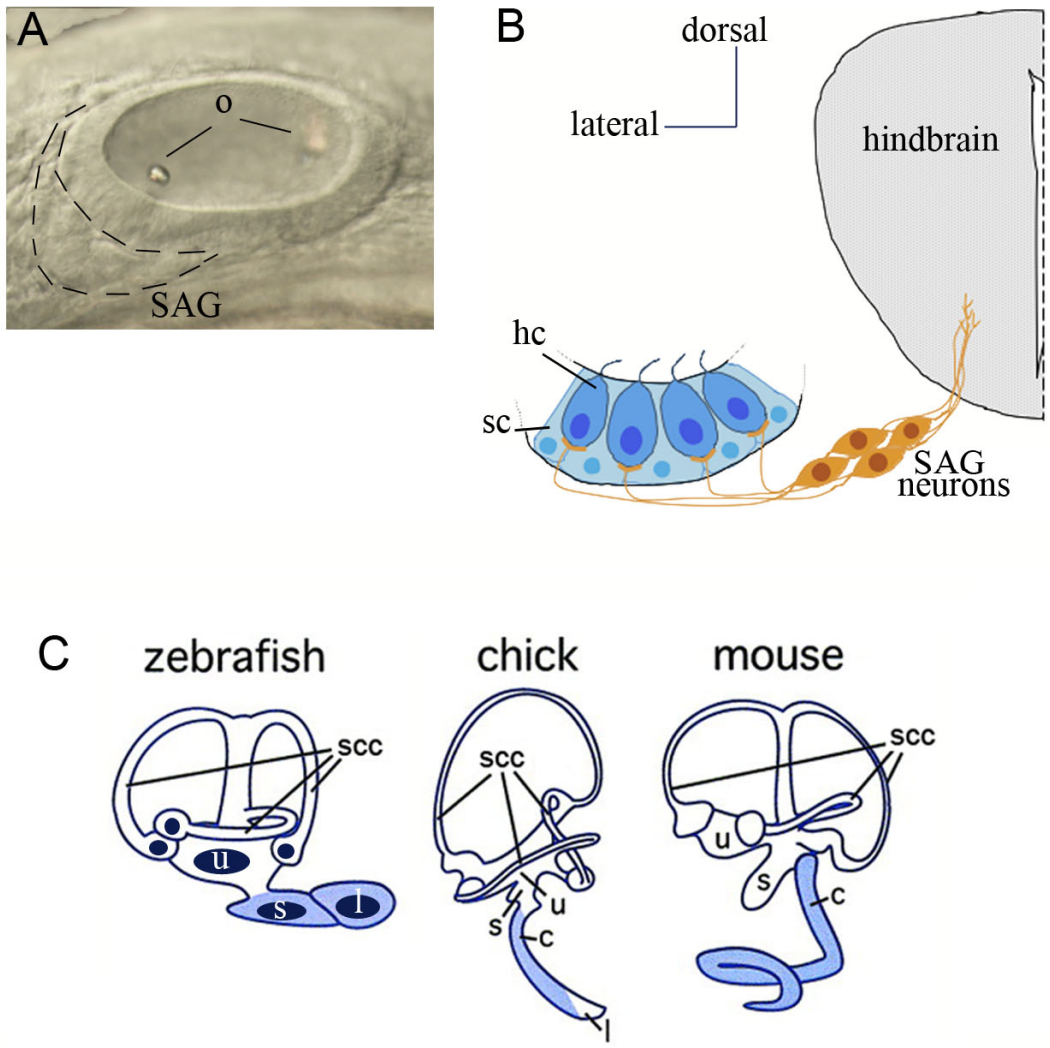

Figure 1.1. Structure of the inner ear.
(A) Otic vesicle at 24 hpf showing otoliths (o) overlaying the sensory epithelia in the anterior and posterior regions. Neuronal precursor cells delaminate from the otic floor and accumulate outside the vesicle to form the SAG. (B) Illustration showing hair cells (hc) and support cells (sc) in the sensory epithelium. Bipolar SAG neurons innervate the hair cells peripherally and hindbrain nuclei centrally. (C) Illustration of adult inner ear structure. Chambers colored in blue are auditory endorgans; all others constitute the vestibular apparatus. Black patches represent sensory epithelium associated with each chamber or canal. Abbreviations: u, utricle; s, saccule; l, lagena; scc, semicircular canals (adapted and modified from Riley and Phillips, 2003).

epithelia are composed of mechanosensory hair cells and non-sensory support cells (Fig. 1.1B). Hair cells perceive sound and motion through lateral deflection of ciliary bundles that project into the lumen of the ear. Maculae are present in the sensory epithelia of the utricle, saccule and lagena. They are associated with dense calcium carbonate crystals called otoliths that facilitate detection of linear acceleration, gravity and sound. Cristae, sensory epithelia in the semicircular canals, lack otoliths and instead long ciliary bundles of hair cells act as sensors of rotational acceleration. Sensory information from hair cells is transduced to nuclei in the hindbrain via neurons of the VIIIth cranial ganglion (Fig. 1.1A, B), called the statoacoustic ganglion (SAG), that synapse with hair cells (Haddon and Lewis, 1996, Riley and Philips, 2003; Whitfield et al., 2002). The vestibular apparatus, constituting the utricle and semicircular canals, is present in all vertebrates and is highly conserved. The auditory sense organs, on the other hand, show considerable diversity. The primary auditory endorgans in fish are the saccule and the lagena whereas in birds and mammals it is the cochlea (Fig. 1.1C). The saccule serves a vestibular function in birds and mammals, and there is no known counterpart of the cochlea in fish (Riley and Phillips, 2003).

ROLE OF FGF IN OTIC INDUCTION

Induction of the otic placode depends on signals from the hindbrain and the mesoderm underneath the presumptive otic tissue. Several members of the fibroblast growth factor (Fgf) gene family have been identified as primary otic inducers. In zebrafish, *fgf3* and *fgf8* are expressed in the developing hindbrain adjacent to the pre-otic domain and act in

a redundant manner to induce otic tissue. Knockdown of either *fgf3* or *fgf8* results in a smaller otic vesicle and disrupting both *fgf* functions causes complete loss of otic tissue (Phillips et al., 2001; Leger and Brand, 2002; Maroon et al., 2002). In mouse, *Fgf3* from hindbrain acts redundantly with *Fgf10* from subotic mesoderm to induce the otic placode. *Fgf3*/*Fgf10* double mutants fail to form otic vesicles or form microvesicles (Alvarez et al., 2003; Wright and Mansour, 2003). In chick, *Fgf19* expressed in the mesoderm adjacent to the prospective otic placodal tissue has been shown to play a role in otic induction (Ladher et al., 2000). Recent studies in mouse and chick have reported that *Fgf8* is involved in otic induction albeit in an indirect manner. It is expressed in the endoderm and also in the periotic region of mouse. *Fgf8* is necessary for the expression of mesodermal otic inducer *Fgf10* in mouse and *Fgf19* in chick (Ladher et al., 2005). These studies support a central role of Fgfs in otic placode induction. Fgfs continue to be expressed in surrounding tissue and the otic vesicle at later stages. Their role in otic vesicle patterning and neurosensory development will be discussed later.

AXIAL PATTERNING OF THE INNER EAR

Following otic induction several genes are expressed asymmetrically in the placode and vesicle stages. As a result, the anterior-posterior (A-P), dorso-ventral (D-V) and medio-lateral (M-L) axes are established in the ear. Signals from adjacent tissue play an important role in regional specification of the ear. Paired domain transcription factor *pax2a* is expressed in preotic cells and is later restricted to the ventromedial wall of the otic placode, adjacent to the hindbrain, and finally maintained in sensory hair cells

(Riley et al., 1999; Leger and Brand, 2002). Medial expression of *Pax2* is also observed in chick and mouse (Nornes et al., 1990; Herbrand et al., 1998; Hutson et al., 1999). Hutson et al., (1999) showed that *Pax2* is expressed on the medial side of the developing ear closest to the hindbrain and absent from the lateral wall. By rotating the otic field 180^{O} about the A-P axis the (now) medially positioned lateral epithelium upregulated *Pax2* expression supporting a role for hindbrain signals in otic patterning.

In the zebrafish hindbrain, *fgf3* is strongly expressed in rhombomere 4 (r4) during placodal stages (Maroon et al., 2002) and regulates anterior fates in the placode. *hmx3* and *pax5* are expressed in the anterior part of the otic placode as early as 14 hpf and 17 hpf, respectively (Pfeffer et al., 1998; Adamska et al., 2000). Loss of *fgf3* eliminates expression of these anterior markers. Expansion of *fgf3* expression domain in the hindbrain of *valentino* (*val*) mutants shows the opposite effect. The *val* gene, orthologous to mouse MafB Kreisler gene, encodes a bZIP transcription factor that is expressed in r5 and r6 (Cordes and Barsh, 1994). *val* mutants show mispatterning of the hindbrain resulting in expanded *fgf3* expression, from r4 through r5/r6. *hmx3* and *pax5* are expressed throughout the medial wall and posterior marker *pou3f3b* is eliminated suggesting anteriorization of the otic vesicle. Fgf3 also regulates specification of the anterior sensory macula (utricle) and in *val* ectopic hair cells are produced in the medial wall adjacent to the expanded *fgf3* domain in r5/6, which is normally devoid of hair cells (Kwak et al., 2002). Similar altered otic patterning is seen in *vhnf1* mutants. *vhnf1* codes for a homeodomain transcription factor that is expressed in the same hindbrain segments as *val* (Sun and Hopkins, 2001). Vhnf1 acts in synergy with Fgf3 from r4 to activate *val*

expression in r5 and r6, and also represses *hoxb1a* so as to limit its expression to r4 (Hernandez et al., 2004). In *vhnf1* mutant embryos anterior markers, such as *hmx3* and *pax5*, are expanded posteriorly. In addition, these embryos show expansion of ventrally expressed *atoh1* in the nascent maculae at the cost of dorsal marker suggesting a role in D-V patterning. As a result, sensory epithelia are distributed abnormally along the A-P and D-V axes. Precursor cells of the SAG are specified in the anteroventral part of the otic placode and express *neurog1* and *neurod*. Expression of these genes is expanded posteriorly and failed to downregulate at later stages in mutant embryos. However, no ectopic posterior ganglion was observed suggesting that mechanisms independent of *vhnf1* regulate ganglion size (Lecaudey et al., 2007).

Fgf8 is expressed strongly in r4 during early somitogenesis but is not detected in the hindbrain after 14 hpf. Instead, *fgf8* is expressed in the presumptive anterior and posterior maculae in the otic vesicle starting at 18 hpf (Leger and Brand, 2002). Loss of *fgf8* (*ace*) does not alter *hmx* expression in the vesicle but severely impairs hair cell and SAG development. Expression of SAG markers is reduced which may reflect a direct role of *fgf8* in SAG development or secondary effects resulting from a small otic vesicle in *ace* mutant embryos (Adamska et al., 2000; Leger and Brand, 2002).

DEVELOPMENT OF SENSORY EPITHELIUM

Sensory epithelia are composed of mechanosensory hair cells and non-sensory support cells that detect auditory and vestibular stimuli. The basic helix-loop-helix transcription factor *Atoh1* is both necessary and sufficient for sensory epithelia development. Two

Atoh1 genes, *atoh1a* and *atoh1b*, are present in zebrafish. *Atoh1* (*atoh1b* in zebrafish at 10.5 hpf) is initially broadly expressed in cells throughout the presumptive sensory epithelium. These are precursor cells that have equal potential to give rise to both hair cells and support cells. At later stages, these cell-types emerge in a salt-and-pepper pattern as a result of lateral inhibition within this domain. Some cells (prospective hair cells) within the equivalence group upregulate expression of *Atoh1* followed by Notch-signaling ligands like *Delta1* and *Jagged2*. This results in Notch activation in neighboring cells that eventually attain the alternate support cell fate. In zebrafish, both *atoh1a* and *atoh1b* are expressed in sensory epithelia primordium at 14 hpf. At later stages, *atoh1a* is expressed predominantly in the sensory epithelia and at higher levels in the hair cell layer compared to the basal support cell layer (Millimaki et al., 2007). Zebrafish *mindbomb* (*mib*) mutants, defective in Delta-Notch signaling, fail to restrict the initial, broad *atoh1* expression domain and this results in excess hair cells at the expense of support cells (Haddon et al., 1998; Millimaki et al., 2007). Loss of *Atoh1* results in complete absence of both hair cells and support cells (Woods et al., 2004; Millimaki et al., 2007). *Atoh1* misexpression can induce hair cell production in non-sensory regions of the ear and attract auditory neurons in some cases (Zheng and Gao, 2000; Kawamoto et al., 2003; Izumikawa et al., 2005; Millimaki et al., 2007; Huang et al., 2009). However, the ability to induce ectopic hair cells is limited. Some of these ectopic cells are disorganized, show abnormal morphology, and fail to survive. This might reflect the absence of certain factors normally present during sensory epithelia

development or the presence of inhibitory factors at ectopic locations. The effects of *atoh1a* misexpression will be investigated in Chapter II.

Several studies have shown that Notch signaling specifies the sensory progenitors in mouse and chick much before expression of *Atoh1*. Activation of Notch-signaling in non-sensory regions of the otic vesicle results in induction of ectopic sensory patches (Daudet and Lewis, 2005; Hartman et al., 2010; Pan et al., 2010). The prosensory domain also expresses Sox2, a high mobility group (HMG) box domain transcription factor belonging to the SoxB1 subfamily of proteins (Uchikawa et al., 1999). Members of this group are known for maintaining stem-cell-like state and inhibiting neuronal differentiation (Bylund et al., 2003; Graham et al., 2003). In chick and mouse ear, Sox2 is expressed in both neuronal and sensory progenitors. In the developing sensory epithelium, *Sox2* expression in downregulated in cells that will differentiate into hair cells while it is maintained in support cells (Neves et al., 2007; Dabdoub et al., 2008). Support cells are involved in regenerative response after hair cell damage in birds either by proliferation or by trans-differentiation where a support cell differentiates into a hair cell (reviewed in Matsui and Ryals, 2005). In zebrafish, *sox2* is expressed in the otic placode a few hours after the initial specification of the prosensory domain. Its expression is lost from mature hair cells but maintained in support cells, like in chick and mouse. Knockdown of *sox2* function results in cell death in the sensory epithelia and impairs recovery following hair cell loss consistent with its expression in support cells (Millimaki et al., 2010).

Fgf signaling regulates specification of the prosensory region by activating *Atoh1* expression. Inhibition of Fgf signaling at early stages causes failure to induce *atoh1* expression and causes a reduction in the number of hair cells and support cells. Fgfs are also expressed in newly formed sensory epithelia. Blocking Fgf signaling at later stages results in a failure to expand the sensory epithelium by possibly impairing recruitment of additional cells (Pirvola et al., 2002; Jacques et al., 2007; Millimaki et al., 2007; Puligilla et al., 2007; Hayashi et al., 2008).

Developing hair cells express genes that are essential for proper differentiation and survival. *pax2a* and *pax2b* are expressed in differentiating hair cells and are downstream targets of *atoh1* (Riley et al., 1999; Millimaki et al., 2007). Another paired domain transcription factor, *pax5*, is differentially expressed in the anterior part of the otic vesicle (Pfeffer et al., 1998) and its function in sensory epithelium development will be explored in Chapter III. Differentiating hair cells in all sensory epithelia express a Pou-domain transcription factor, *Pou4f3* (*Brn3c*). *Brn3c*-null mice express early hair cell differentiation markers but these immature cells undergo apoptosis soon after (Xiang et al., 1998). This suggests a role in hair cell maturation and survival. *Brn3c* upregulates the expression of a zinc-finger transcription factor *Gfi1* (Hertzano et al., 2004). *Gfi1* mutant embryos show a similar phenotype as *Brn3c* mutant embryos. However, rapid degeneration is seen only in the cochlea, and although vestibular sensory patches are disorganized no signs of cell death are observed. In these embryos, neurons of the cochlear ganglion show progressive degeneration following hair cell loss (Wallis et al., 2003). Another survival factor Barhl1, a homeodomain protein, is also expressed in hair

cells of all epithelia but shows a gradual loss of hair cells only in the cochlea much later in development (Li et al., 2002). These studies suggest that maintenance of sensory epithelia is differentially regulated.

DEVELOPMENT OF THE STATOACOUSTIC GANGLION (SAG)

Sensory neurons of the statoacoustic ganglion (SAG), also called the cochleovestibular ganglion (CVG), innervate hair cells in the sensory epithelia. SAG development is a sequential process involving several stages discussed below and illustrated in Fig.1.2. SAG precursor cells, called neuroblasts, are specified in the otic floor by *neurogenin1* (*neurog1*), a bHLH factor homologous to *atoh1*. Loss of *neurog1* leads to a complete loss of SAG neurons (Ma et al., 1998, Ma et al., 2000; Andermann et al., 2002). Overexpression of *neurog1* in *Xenopus* and zebrafish results in formation of ectopic neurons in the ectoderm supporting a role in neuronal specification (Ma et al., 1996; Blader et al., 1997). In zebrafish, neuroblasts are first specified during placodal stages (Haddon and Lewis, 1996; Andermann et al., 2002; Radosevic et al., 2011). These neuroblasts leave the otic floor in a process called delamination from the anterolateral margin of the vesicle and from the middle of the floor more posteriorly up until 42 hpf (Haddon and Lewis, 1996). Expression of *neurog1* is transient in the precursors and is followed by strong upregulation of neuronal differentiation bHLH gene *neurod* (Korzh et al., 1998, Andermann et al., 2002). Delta-Notch signaling regulates the number of cells committed into entering neuronal differentiation via lateral inhibition. Members of Notch signaling pathway are expressed in the neurogenic domain of the otic vesicle and

disruption of Notch signaling in zebrafish *mindbomb* mutant or in chick by blocking Notch intracellular cleavage leads to excess sensory neuronal precursors (Adam et al., 1998; Haddon et al., 1998; Alsina et al., 2004; Abello et al., 2007).

In chick and mouse, neuroblasts undergo a brief phase of proliferation to expand the precursor population (D'Amico-Martel, 1982; Begbie et al., 2002; Alsina et al., 2003; Matei et al., 2005). This stage of transit-amplification is characterized by the expression of *neurod* and proliferation markers (Camerero et al., 2003). Mitotic cells are observed in the SAG well after delamination has ceased in chick (D'Amico-Martel, 1982). In some fish such as the oscar, *Astronotus ocellatus*, neurons are added to the SAG throughout adulthood suggesting that a pool of neuronal precursor cells is maintained (Popper and Hoxter, 1984; Presson and Popper, 1990). In zebrafish, hair cells form throughout life (Bang et al, 2001; Higgs et al., 2001) and it is likely that the SAG continues to grow in order to accommodate the expanding sensory epithelia. Following proliferation, neuroblasts exit the cell cycle and differentiate into bipolar neurons that innervate hair cells in the sensory epithelia and processing centers in the hindbrain. Maturing neurons in zebrafish express LIM domain/homeodomain transcription factors Islet-1/2 (Korzh et al., 1993; Inoue et al., 1994; Haddon et al., 1998). In chick and mouse, Islet-1 is expressed in the otic epithelium in addition to the developing SAG (Li et al., 2004b; Radde-Gallwitz et al., 2004).

Differentiating neurons express a gamut of other markers related to extension of neurites to peripheral and central targets, synaptogenesis and survival. Otic neurons in chick and mouse are spatially segregated into auditory (cochlear or spiral ganglion

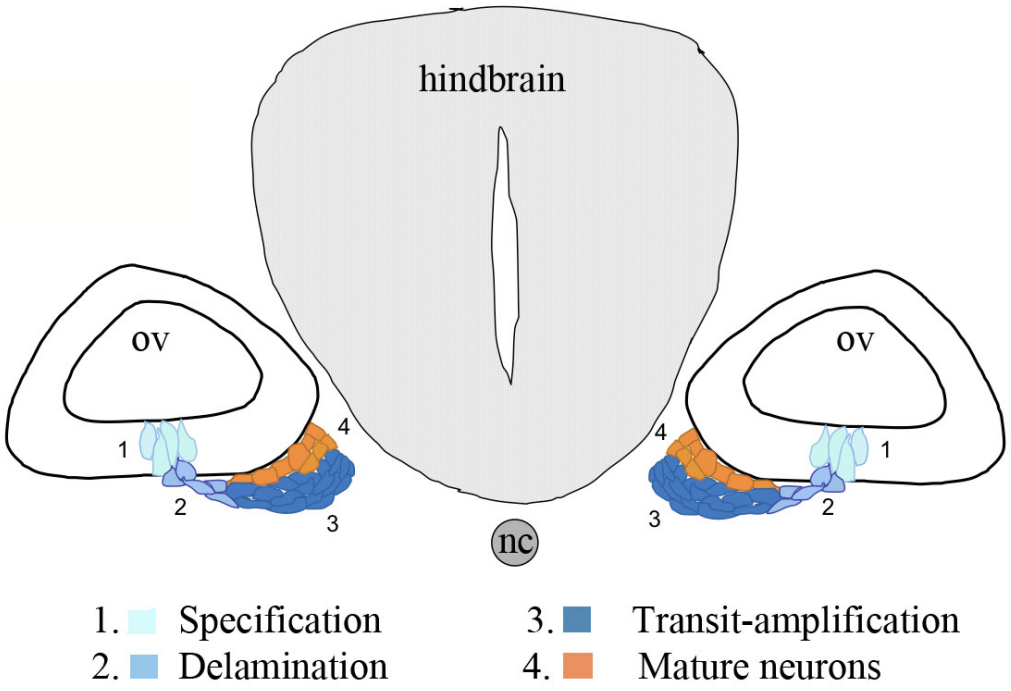

Figure 1.2. Stages of statoacoustic ganglion (SAG) development.
Illustration depicting the various stages of SAG development. SAG precursor cells called neuroblasts form in the floor of the otic vesicle (1, specification). These cells leave the ear (2, delamination) and migrate ventromedially. Upon delamination, neuroblasts undergo proliferation (3, transit-amplification) and eventually differentiate into neurons (4, mature neurons). Abbreviations: nc, notochord; ov, otic vesicle. Transverse section posterior to the utricular macula is shown, with dorsal on top.

neurons, SGN) and vestibular ganglia, which innervate endorgans with respective functions (Maklad and Fritzsch, 1999; Koundakjian et al., 2007; Bell et al., 2008). Dye-tracing experiments in zebrafish embryos show spatial segregation of SAG into anteroventral and posteromedial parts. This reflects functional segregation as well for the most part. The anteroventral part of the SAG innervates sensory epithelia responsible for vestibular function (utricle, anterior and lateral cristae). The posteromedial part of the SAG innervates the auditory endorgan (saccule). One exception is the posterior crista

that is innervated by the posterior part of the SAG and not the anteroventral part along with other vestibular endorgans (our unpublished observation, Sapede and Pujades, 2010). Whether vestibular and auditory neurons segregate further during later stages of development is not known.

FACTORS REGULATING SAG DEVELOPMENT

Sensory neurons depend on neurotrophins for survival and differentiation. Inner ear sensory epithelia and delaminating neuroblasts express brain-derived neurotrophic factor (BDNF) and neurotrophin-3 (NT-3). Their action is mediated by high-affinity tyrosine kinase receptors TrkB (BDNF) and TrkC (NT-3) that are expressed in SAG neurons. Studies in chick and mouse suggest selective dependency of vestibular and cochlear neurons on BDNF and NT-3, respectively. In embryos doubly homozygous for *BDNF*/*NT-3* or *TrkB*/*TrkC* all SAG neurons are lost (reviewed in Fritzsch et al., 2004; Sanchez-Calderon et al., 2007b, reviewed in Appler and Goodrich, 2011).

Insulin-like growth factor (IGF-1) and its receptor (IGF1R) are expressed in the inner ear of chick and mouse. IGF affects nervous system development and otic neurogenesis by modulating cell proliferation and survival. Exogenous IGF-1 in cultured chick SAG increases proliferation, neurite outgrowth and expression of differentiation markers. Blocking IGF-1, on the other hand, impairs SAG development by reducing proliferation, differentiation and increasing cell death (Camarero et al., 2003). IGF-1 acts in a similar fashion in mice. *IGF-1* null mice show delay in differentiation of cochlear neurons and apoptotic cell death during postnatal development resulting in loss of

hearing. *IGF-1* mutation in humans leads to hearing loss as well (Camarero et al., 2002; reviewed in Varela-Nieto et al., 2004). In zebrafish, *IGF1R* is expressed in the ear primordium and knockdown of IGF1R function results in arrested development, increased neuronal apoptosis and a small otic vesicle (Ayaso et al., 2002; Schlueter et al., 2007).

Several studies in chick and mouse have implicated the role of Fgf signaling at different stages of otic neurogenesis. *Fgf2* (*bFgf)* is expressed in chick otic placode (Vendrell et al., 2000) and ectopic Fgf2 increases the number of migrating and differentiating SAG neurons (Hossain et al., 1996; Zhou et al., 1996; Adamska et al., 2001). *Fgf2* promotes *TrkB* receptor expression in culture that allows these neurons to respond to BDNF that has been shown to accelerate SAG precursor proliferation and their migration (Brumwell et al., 2000). *Fgf3* is expressed in the sensory epithelium and the SAG in mouse. *Fgf3* mutants have smaller SAG and since the ear shows morphogenetic defects in this background it is difficult to deduce its role in otic neurogenesis (Wright and Mansour, 2003). *Fgf8* is expressed in the chick otic vesicle and in the SAG. Delaminating neuroblasts are observed at the boundary of *Fgf8* domain in the vesicle. Ectopic application of Fgf8 enhances expression of SAG markers (Adamska et al., 2001). Knockdown of *fgf3* and *fgf8* in zebrafish shows impairment of SAG development, as discussed previously, but detailed analysis is lacking (Leger and Brand, 2000). Another Fgf, *Fgf10*, is expressed in the presumptive neural and sensory regions of the otic placode in chick and mouse. In mouse, *Fgf10* is also expressed in the SAG and delaminating neural precursors (Pirvola et al., 2000; Alsina et al., 2004).

Overexpression of *Fgf10* in chick increases the number of *Neurod*-positive cells in the neurogenic domain of the vesicle and in the SAG without inducing ectopic site of delamination. No increase in *Neurog1*/*Delta1* expression or cell proliferation is observed in the otic epithelium suggesting that Fgf10 promotes neuronal determination (characterized by *Neurod* expression) and not specification. However, inhibition of all Fgf signaling using SU5402 results in a dramatic reduction in *Neurog1* and *Neurod* supporting a role for Fgfs in early stages of SAG precursor specification and determination (Alsina et al., 2004). Mouse *Fgf10* null mutants do not show defects in formation of SAG neurons although neurons innervating the posterior crista are lost later in development (Pauley et al., 2003). *Fgf19* is expressed in delaminating neuroblasts and the SAG in chick, and its role in otic neurogenesis is unknown. Homologue of chick *Fgf19* in mouse, *Fgf15*, is not expressed in the SAG (Wright et al., 2004; Sanchez-Calderon et al., 2007a). Detailed analysis of zebrafish SAG development and its regulation by Fgf will be examined in Chapter IV.

ESTABLISHMENT OF NEURAL AND SENSORY DOMAINS

The anterior ventromedial region of the otic vesicle gives rise to both sensory neurons and the sensory epithelia. In chick and mouse, neurosensory development occurs in a sequential manner- SAG precursors are specified first followed by delamination, and then sensory epithelia precursors form in the same region. In zebrafish, neuronal and sensory populations begin to develop concurrently during placodal stages and are segregated spatially instead of temporally. Both of these scenarios require that the

expression domains of *Neurog1* and *Atoh1* be restricted within the common neurosensory field. Raft et al. (2007) showed that expression of neurogenic markers (*Neurog1*, *Neurod*) persists while *Atoh1* expression is upregulated in the utricle and saccule, but not in the cochlea of mouse. They show evidence of mutual antagonism between *Neurog1* and *Atoh1*, such that expression domain of each is expanded in *Atoh1* and *Neurog1* mutants, respectively. Cross-regulation of bHLH genes to generate progenitor cells with alternative fates has been shown elsewhere in the nervous system (Gowan et al, 2001; Bertrand et al., 2002; Akagi et al., 2004). Similar cross-regulation is thought to occur in the zebrafish inner ear but is not fully understood.

Upon specification of precursors, the question remains as to how precursors from the same neurosensory region give rise to different branches of the SAG and to various sensory epithelia. Recent studies in chick have shown that neuronal precursors of vestibular and cochlear ganglion are temporally and spatially segregated within the otic placode. Early-born precursors from the anterior region of the neurogenic domain give rise to neurons that innervate vestibular endorgans. One exception is precursors of neurons that project to the posterior cristae, which are present in the posterior neurogenic domain. Later-born precursors from the posterior part of the neurogenic region mainly contribute to the cochlear ganglion. Sensory epithelia precursors show similar spatial segregation. Fate maps reveal that precursors of vestibular and auditory endorgans emerge from the anterior and posterior-medial part of the neurosensory domain in the otic floor, respectively (Bell et al., 2008). This suggests that both neuronal and sensory precursors acquire similar positional identity in the otic floor and that neurons formed in

a specific region of the ear eventually innervate sensory epithelia derived from the same region. Overall these data suggest that a complex and dynamic relationship exists between sensory epithelia and SAG formation in the inner ear.

DISSERTATION OBJECTIVES

The objective of this dissertation is to study the development and regulation of neuronal and sensory components of the zebrafish inner ear.

Several studies have shown that Atoh1 is necessary for induction of sensory epithelia and sufficient to form ectopic hair cells. However, whether *atoh1* can induce the entire sensory epithelium, including hair cells and support cells, has been addressed only by few. Studies in chick and mouse have shown that the competence of otic tissue to form ectopic hair cells is restricted. This may be either due to changes in developmental plasticity or absence of other necessary factors. Chapter II, a collaborative effort with the first author, my former colleague Elly M. Sweet, shows that *atoh1* is sufficient to induce ectopic sensory epithelium with maximal effects during placodal stages. However, there is a degree of spatial restriction even at this early stage that can be overcome by misexpressing *fgf3/8* and *sox2*, factors normally involved in sensory epithelia development.

During otic differentiation, many factors are expressed asymmetrically in response to signals from adjacent tissues. Fgf3 from the hindbrain induces expression of *pax5* in the anterior macula (utricle). Chapter IV is in collaboration with the first author, my former colleague, Sujin Kwak and addresses the role of *pax5* in sensory epithelia

development. We show that *pax5* is necessary for survival of hair cells in the utricle but not the posterior macula (saccule). As a secondary consequence dendrties of statoacoustic ganglion (SAG) neurons are disorganized. Since the utricle is responsible for vestibular function, embryos knocked down for *pax5* show balance defects but no auditory impairment.

Chapter V focuses on the development of the statoacoustic ganglion (SAG). We show that precursor cells are specified in the floor of the ear by a moderate to low dose of Fgf, emanating from the adjacent hindbrain and the utricle. Upon leaving the otic vesicle, these precursor cells undergo proliferation, followed by differentiation. Differentiating neurons express *fgf5*, which increases the overall level of Fgf signaling and results in termination of precursor specification. In addition, Fgf stabilizes precursor cells in a proliferative state and delays differentiation. This feedback inhibition mediated by Fgf from mature neurons regulates neurogenesis and thus, the total number of neurons formed in the ganglion.

CHAPTER II

SOX2 AND FGF INTERACT WITH ATOH1 TO PROMOTE SENSORY COMPETENCE THROUGHOUT THE ZEBRAFISH INNER EAR*

OVERVIEW

This is published work describing the effects of *atoh1a* misexpression and factors influencing sensory competence of otic tissue. It is primarily the work of my colleague, E. M. Sweet. I include it here as a record of my work because I contributed towards portions of Figure 2.6 and the entirety of Figures 2.1, 2.7, 2.9, 2.10, 2.11.

INTRODUCTION

Sensory epithelia of the inner ear, comprising hair cells and support cells, mediate the senses of hearing and balance. One of the most important regulatory factors controlling development of sensory epithelia is the basic helix-loop-helix transcription factor, Atoh1, expression of which is both necessary and sufficient for development of sensory epithelia (Chen et al., 2002; Millimaki et al. 2007; Millimaki et al., 2010; Woods et al., 2004). Atoh1 is best known for its role in differentiation of hair cells. Atoh1 expression is maximal in differentiating hair cells, and conditions that maintain elevated expression promote hair cell differentiation at the expense of support cells

---

(Dabdoub et al., 2008; Jones et al., 2006; Woods et al., 2004; Zheng and Gao, 2000). However, Atoh1 also acts at an earlier stage to establish the prosensory domain from which both hair cells and support cells emerge. Accordingly, Atoh1 is initially expressed in a broad domain containing precursors of both hair cells and support cells (Woods et al., 2004; Yang et al., 2010). Only later does Atoh1 become restricted to differentiating hair cells by a self-limiting process termed lateral inhibition (reviewed by Cotanche and Kaiser, 2010). Disruption of Atoh1 prevents development of both hair cells and support cells, whereas misexpression of Atoh1 can stimulate formation of ectopic sensory epithelia containing both cell types (Millimaki et al., 2007; Woods et al., 2004). Thus, Atoh1 exhibits potent tissue-organizing activity that goes beyond its ability to promote hair cell differentiation.

The basis for Atoh1's broader organizing activity lies in its ability to activate downstream signaling pathways that diversify cell fates. For example, Atoh1 activates expression of various Notch ligands that facilitate lateral signaling required for support cell specification (Millimaki et al., 2007; Woods et al., 2004). Notch signaling in this context works in part by repressing Atoh1 expression in a subset of precursor cells, resulting in the alternating pattern of hair cells and support cells seen in mature sensory epithelia. Newly formed sensory epithelia also express a number of Fgf genes. It appears that Fgf signaling serves to recruit additional cells into the developing sensory epithelium: Discrete subsets of hair cells and support cells that normally form after the first wave of hair cell production fail to form when Fgf signaling is impaired (Hayashi et al., 2007; Hayashi et al., 2008; Jacques et al., 2007; Millimaki et al., 2007; Pirvola et al.,

2002; Puligilla et al., 2007). Notch and Fgf also appear to function upstream to activate Atoh1 expression (Hayashi et al., 2008; Millimaki et al., 2007; Woods et al., 2004), suggesting a complex feedback network that is only partially understood. How these signals influence the effects of Atoh1 misexpression remains to be established.

Despite the organizing effects of Atoh1, competence to respond properly to Atoh1 is not uniform. For example, some regions of the otic vesicle appear to be completely refractory to the effects of Atoh1, failing to produce sensory epithelia even after high-level Atoh1 misexpression (Huang et al., 2009; Kawamoto et al., 2003; Millimaki et al., 2010; Woods et al., 2004; Zheng and Gao, 2000). Even in regions capable of forming ectopic sensory epithelia, ectopic hair cells induced by Atoh1 misexpression often exhibit aberrant morphology or a diminished capacity to survive after differentiation (Izumikawa et al., 2005; Kawamoto et al. 2003; Millimaki et al., 2007). In such cases, it is likely that cells in foreign sites lack essential cofactors needed for normal Atoh1 activity or, alternatively, other regionally expressed factors may interfere with Atoh1. Because Atoh1 is a promising candidate for gene therapy to restore hearing (Izumikawa et al., 2005; Shou et al., 2003), identifying the factors that influence sensory competence remains an important goal of inner ear research.

Here we investigate the effects of *atoh1a* misexpression in zebrafish by examining temporal and spatial parameters that influence Atoh1 function. We demonstrate that misexpression of *atoh1a* at various stages of otic development can induce ectopic sensory epithelia composed of both hair cells and support cells. Competence to respond to *atoh1a* misexpression is already spatially restricted during

placodal stages and becomes increasingly restricted after formation of the otic vesicle. Co-misexpressing *atoh1a* with *fgf3*, *fgf8* or *sox2*, genes that normally act in the same gene network with *atoh1a*, promotes sensory development throughout the otic vesicle. These data elucidate a genetic network that is sufficient to enhance competence to respond to Atoh1.

MATERIALS AND METHODS

Strains

The wild-type strain was derived from the AB line (Eugene, OR). The *brn3c:gfp* line was developed by Xiao et al. (Xiao et al., 2005) and *hsp70:dkk1-GFP*^{w32} was developed by Stoick-Cooper et al., (Stoick-Cooper et al., 2007). *hsp70:atoh1a*^{x20}, *hsp70:fgf8*^{x17} and *hsp70:sox2*^{x21} lines were previously described (Millimaki et al., 2010). We also generated two new lines, *Tg (hsp70:pax2a)*^{x23} and *Tg(hsp70:fgf3)*^{x27}, using previously described techniques (Millimaki et al., 2010).

Misexpression and gene-knockdown

To assess the effects of gene misexpression or gene knockdown, at least 30 embryos were observed for each time-point. Except where noted in the text, phenotypes were fully penetrant. For most misexpression experiments using heat shock-inducible transgenic lines, embryos were incubated in a water bath at 39°C for 30 minutes at time points described in the results. For experiments involving *hsp70:pax2a*^{x23} or both *hsp70:pax2a*^{x23} and *hsp70:atoh1a*^{x20}, embryos were activated at 36°C for 30 minutes.

Activation of *hsp70:pax2a*^{x23} at higher temperatures causes elevated cell death, whereas activation of both transgenes is highly effective at 36°C (data not shown). Injection of morpholino oligomers to knockdown *pax2a*, *pax2b* or *pax8* was performed as previously described (Bricaud and Collazo, 2006; Mackereth et al., 2005).

In situ hybridization

In situ hybridization was performed as described previously (Jowett and Yan, 1996; Phillips et al., 2001).

Immunostaining

Antibody staining was performed as described by Riley et al. (Riley et al., 1999). Primary antibodies: anti-Pax2 (Covance diluted at 1:100), anti-GFP (Santa Cruz Biotechnology diluted 1:200) and anti-Caspase 3 (R&D systems diluted 1:100). Secondary antibodies: Alexa 546-conjugated goat anti-rabbit IgG (Molecular Probe diluted 1:200) or HRP-conjugated goat anti-rabbit IgG (Vector laboratories PI-2000 diluted 1:200).

Sections

For cryosectioning of *brn3c:gfp*, embryos were fixed overnight in MEMFA (0.1 M Mops at pH7.4, 2 mM EGTA, 1 mM $MgSO_4$, 3.7% formaldehyde). Embryos were then washed twice for 5 minutes in 1x PBS followed by two one hour long washes in PBT with 0.5% Triton-X and finally washed twice for 5 minutes in 1x PBS and transferred

into a 30% sucrose solution made in PBS. Embryos were embedded in tissue freezing medium (Triangle Biomedical Sciences, H-TFM) and cut into 10 μm sections using a cryostat. Slides were dried overnight, washed in PBS, and then mounted in ProLong Gold (Invitrogen). The same protocol was used for cryosectioning of embryos following wholemount in situ hybridization except that PBT washes were omitted. For double labeling of *sox2* and *brn3c:gfp*, embryos were first stained by wholemount situ hybridization for *sox2*, then 10 μm cryosections were immunostained for GFP. For resin-sections of *sox2* and *brn3c:gfp,* embryos were stained in wholemount by immunolocalization of GFP followed by in situ hybridization for *sox2,* then embedded in Immunobed resin (Poly- sciences No. 17324) and cut into 7 μm sections.

RESULTS

Effects of *hs:atoh1a* misexpression in the nascent otic vesicle

We showed previously that zebrafish *atoh1a* is necessary and sufficient for hair cell development (Millimaki et al., 2007). To further investigate the effects of *atoh1a* misexpression and determine the temporal requirements for *atoh1a,* we utilized a heat shock-inducible transgenic line to misexpress *atoh1a* (Millimaki et al., 2010). Induction of the *hsp70* heat shock promoter typically results in elevated transcript levels of the transgene for 90 minutes, followed by a gradual decay over the next few hours (Hans et al., 2007). However, activation of transgenic *hs:atoh1a* led to robust expression of *atoh1a* transcript for at least 6 hours, with moderate upregulation still evident through 9 hours post-activation (Fig. 2.1E, F). This extended period of upregulation likely occurs

through auto-regulatory activation of the endogenous *atoh1a* locus (Helms et al., 2000; Sun et al., 1998; our unpublished observations). For the purposes of this study it is important to note that the *hs:atoh1a* transgene is expressed globally, including throughout the otic vesicle (Fig. 2.1A-D).

We began our analysis by activating *hs:atoh1a* at 18 hpf, the time when the otic vesicle first forms. Production of mature hair cells was monitored by following expression of *brn3c:gfp* (Xiao et al., 2005), which can first be detected in nascent hair cells around 9 hours after activation of *hs:atoh1a* (Millimaki et al., 2010). Activation of *hs:atoh1a* at 18 hpf led to production of hair cells throughout the ventromedial quadrant of the ear at 30 hpf (Fig. 2.2A, B). This region includes the areas normally occupied by the utricular and saccular maculae plus intervening tissue. Ectopic hair cells were stably maintained through at least 42 hpf, and additional hair cells continued to accumulate around the edges of the expanded sensory epithelium (Fig. 2.2C, D). To further characterize hair cell differentiation under these conditions, we examined Pax2 expression, which normally upregulates during development of all utricular hair cells, as well as the first 2-3 hair cells to form in the saccule (Riley et al., 1999; Kwak et al., 2006). Nearly all cells within the otic vesicle that expressed *brn3c:gfp* became positive for Pax2 within 15 hours of *hs:atoh1a* activation (Fig. 2.2E, F). Additionally, expression of general macular markers *fgf3* and *fgf8* also expanded following activation of *hs:atoh1a*, as did the utricular marker *pax5* (Fig. 2.2G-L). Thus, misexpression of *atoh1a* induced formation of excess and ectopic hair cells in the ventromedial portion of the otic vesicle, with most hair cells expressing markers consistent with an anterior

(utricular) fate. In contrast, only a small number of hair cells were seen in the dorsal epithelium and none in the lateral epithelium, indicating that sensory competence is already spatially restricted at the early otic vesicle stage.

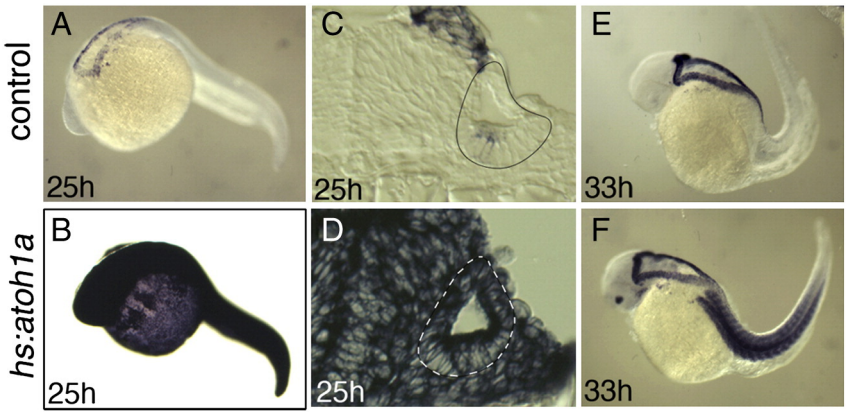

Figure 2.1. *atoh1a* expression following *hs:atoh1a* activation at 24 hpf. Expression of *atoh1a* at indicated times in control embryos (A, C, E) and *hs:atoh1a* transgenic embryos (B, D, F). Images of wholemount specimens (A-B, E-F) are dorsolateral views with anterior to the left and transverse sections (C-D) with dorsal to the top. The otic vesicles are outlined in C-D.

Effects of *hs:atoh1a* misexpression at later stages

We next characterized the effects of activating *hs:atoh1a* at 24 hpf, by which time the first mature hair cells have formed and maculae have started to expand (Haddon and Lewis, 1996; Riley et al., 1999). We showed previously that activation of *hs:atoh1a* at this time leads to production of hair cells throughout the ventromedial wall in a manner comparable to activating *hs:atoh1a* at 18 hpf (Millimaki et al., 2010). We extended that work by examining early markers of macular development. Some of the earliest targets of *atoh1a/b* in the zebrafish otic placode and vesicle are Notch pathway genes *deltaA* and *deltaD* (Millimaki et al., 2007). Accordingly, activation of *hs:atoh1a* at 24 hpf led

to a rapid expansion of the macular domains of *deltaA* to cover the entire ventromedial wall of the otic vesicle by 26 hpf (Fig. 2.3A, B). This was followed by expansion of *fgf3* into the medial wall at 28 hpf, including medial expansion of utricular expression and upregulation in the saccular macula (Fig. 2.3C, D). Expression of *sox2*, which normally follows *atoh1a/b* and initially marks both hair cells and support cells, showed intense expression throughout the ventromedial wall of the otic vesicle by 30 hpf, 6 hours after

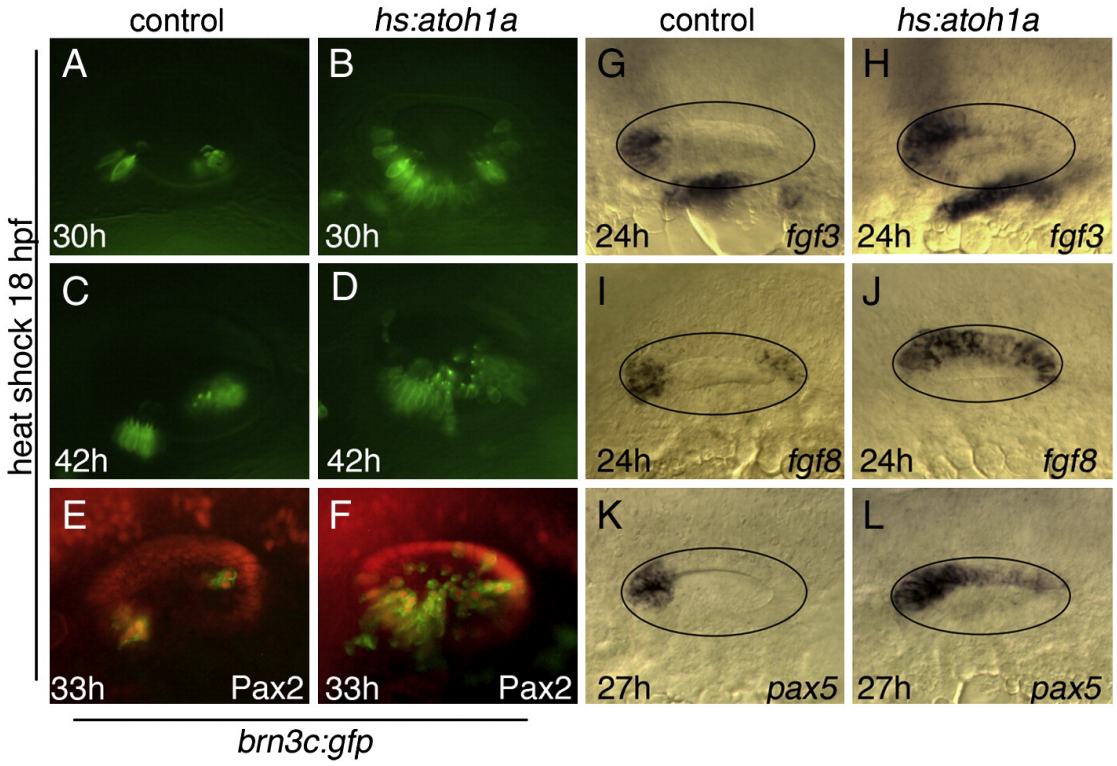

Figure 2.2. Otic vesicle patterning following *hs:atoh1a* activation at 18 hpf. (A-F) Expression of *brn3c:gfp* (green) in the utricle and saccule of control embryos (A, C, E) and in *hs:atoh1a* transgenic embryos (B, D, F) at indicated times. (E, F) Co-staining with anti-Pax2 in red. (G-L) Otic expression of *fgf3, fgf8,* and *pax5* in control embryos (G, I, K) and expanded expression in *hs:atoh1a* transgenic embryos (H, J, L). All images show dorsolateral views with anterior to the left and dorsal up (A-H) or dorsal views with anterior to the left and medial up (I-L).

heat shock (Fig. 2.3E, F; Millimaki et al., 2010). Because *sox2* is also induced by Fgf and Notch (Millimaki et al., 2010), it is possible that Atoh1a induced *sox2* indirectly through activation of Fgf and Notch pathways. Ectopic hair cells marked with *brn3c:gfp* were first observed by 33 hpf, 9 hours after activation of *hs:atoh1a* (Millimaki et al., 2010, and data not shown). Transverse sections of embryos differentially stained for *brn3c:gfp* and *sox2* confirmed that *atoh1a* misexpression expanded production of both hair cells and support cells (Fig. 2.3G, H). Many hair cells in the anterior half of the ear, and a few randomly scattered hair cells in the posterior, became Pax2-positive by 39 hpf (Fig. 2.3I, J; Millimaki et al., 2010). The timeframe of responses of various macular genes to *hs:atoh1a* activation is summarized in Fig. 2.3K.

Although many genes showed similar responses to *hs:atoh1a* activation at 18 hpf compared to 24 hpf, there were several notable exceptions. For example, activation of *hs:atoh1a* at 24 hpf or later did not expand the domains of *fgf8* and *pax5* expression as it did with earlier *hs:atoh1a* activation (data not shown). Similarly, upregulation of *pax2a* was limited mostly to anterior hair cells following *hs:atoh1a* activation at 24 hpf, whereas virtually all hair cells expressed *pax2a* following *hs:atoh1a* activation at 18 hpf (compare Figs. 2.2F and 2.3J). These data suggest that *atoh1a* misexpression at 24 hpf does not expand anterior otic fates as it does at earlier stages. The reason for this change is not clear.

The effects of *atoh1a* misexpression diminished after 24 hpf. For example, compared to the broad medial expansion of hair cells following activation of *hs:atoh1a* at 24 hpf (Fig. 2.4B, F), activation of *hs:atoh1a* at 36 hpf resulted in production of two

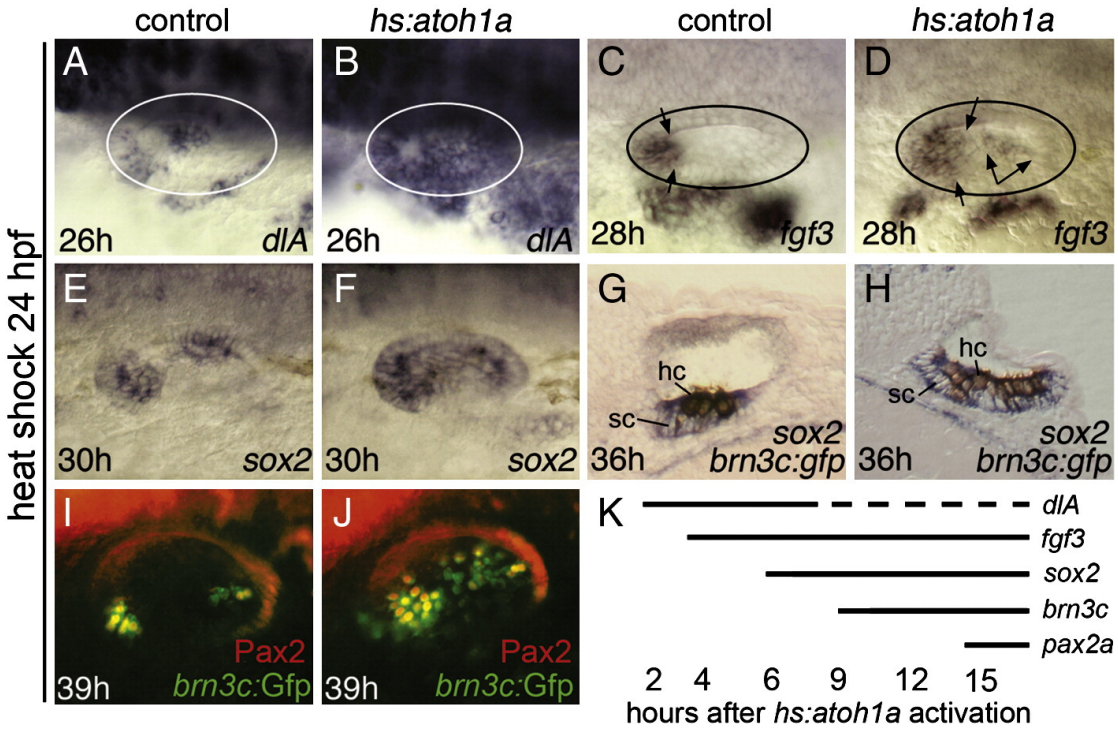

Figure 2.3. Otic vesicle patterning following *hs:atoh1a* activation at 24 hpf. (A-F) Expression at the indicated times of *dlA*, *fgf3* and *sox2* in control embryos (A, C, E) and *hs:atoh1a* transgenic embryos (B, D, F). To assist in interpretation of images, otic vesicles are outlined in A-D and the spatial limits of *fgf3* expression are marked by arrows (C, D). (G, H) Transverse sections showing expression of *sox2* (blue) and anti-GFP (brown) at 36 hpf in a control embryo (G) and a *hs:atoh1a* transgenic embryo (H). Positions of hair cells (hs) and support cells (sc) are indicated. (I, J) Expression of *brn3c:gfp* (green) and Pax2 (red) in otic hair cells at 39 hpf in a control embryo (I) and a *hs:atoh1a* transgenic embryo (J). (K) Summary of the onset of expanded or ectopic expression of various otic markers following activation of *hs:atoh1a* at 24 hpf. Most markers were stably expressed, except for *dlA*. Expression of *dlA* was lost in a subset of cells after several hours, presumably reflecting the process of lateral inhibition. Images of wholemount specimens (A-F, I, J) are dorsolateral views with anterior to the left and dorsal to the top.

discrete but enlarged maculae, with an intervening region devoid of hair cells (Fig. 2.4C, G). Activation of *hs:atoh1a* at 48 hpf caused only a slight increase in hair cell production within the endogenous maculae and cristae but did not promote sensory development in ectopic locations (Fig. 2.4D, H). These data indicate that competence to respond to *hs:atoh1a* becomes increasingly restricted at later developmental stages.

Effects of *hs:atoh1a* misexpression at placodal stages

In zebrafish, a broad prosensory domain is established in the preplacode by 10.5 hpf and the first hair cells are specified by 14 hpf, just as the otic placode becomes morphologically visible (Millimaki et al., 2007). We reasoned that competence to respond to Atoh1a may be more widespread at these early stages. Misexpression at

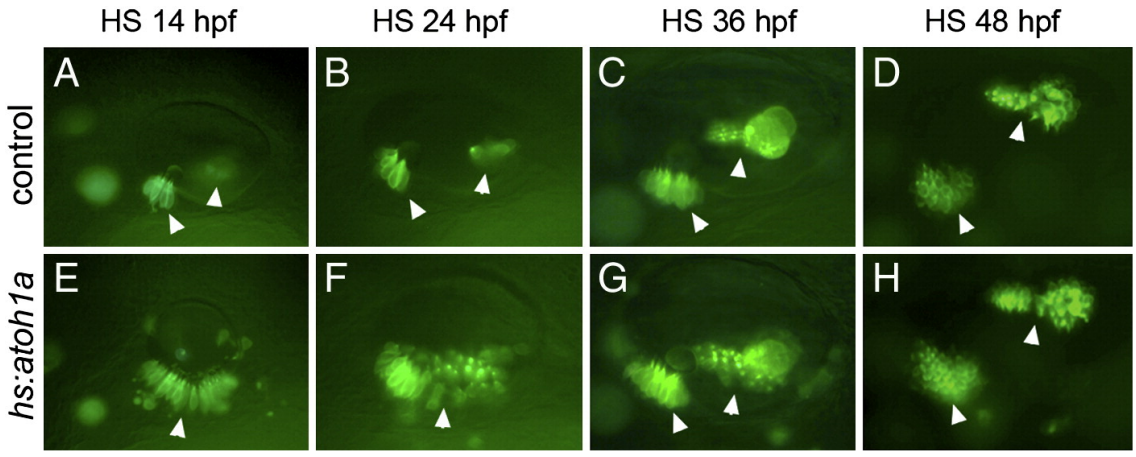

Figure 2.4. Spatial restriction of competence to respond to *hs:atoh1a* at different stages. Expression of *brn3c:gfp* in control embryos (A-D) and *hs:atoh1a* transgenic embryos (E-H). Embryos were heat shocked at the times indicated across the top and photographed 12-13 hours later. Arrowheads mark positions of endogenous and expanded sensory epithelia. Images show dorsolateral views with anterior to the left and dorsal to the top.

different times showed that activating *hs:atoh1a* at 14 hpf had the greatest effect on sensory development (Fig. 2.4A, E). In contrast, activation of *hs:atoh1a* at 12 hpf resulted in a more modest expansion of sensory epithelia; and heat shock initiated at 10 hpf had little or no effect on macular development (data not shown). The likely reason for the weak response to transgene activation at 10 hpf or 12 hpf is that the endogenous *atoh1b* locus normally shows widespread expression in the otic placode at these times (Millimaki et al., 2007), such that a brief pulse of transgene activity is superfluous. We therefore focused on transgene activation at the most sensitive stage to assess the spatial limits of sensory competence. Although heat shock at 14 hpf caused a dramatic expansion of sensory epithelium, the sensory epithelium was generally limited to the ventral epithelium of the otic vesicle (Fig. 2.4A, E). In rare cases, a small number of ectopic hair cells were observed in more dorsal positions (Fig. 2.4E), though none were detected in the lateral wall. The same results were obtained when embryos were subjected to serial heat shocks at 14 hpf and 16 hpf to prolong expression of *hs:atoh1a* (Fig. 2.5A, B, and data not shown). Transverse sections revealed few if any cells on the dorsal, medial, or lateral walls of the otic vesicle (Fig. 2.5I, J). Thus, the zone of sensory competence is already spatially restricted at the earliest stages when embryos are maximally responsive to *hs:atoh1a*.

Enhancement of sensory competence by misexpression of Fgf8 or Sox2

Fgf is one of the factors required to activate *atoh1a/b* in the developing otic placode and vesicle (Millimaki et al., 2007). We speculated that Fgf might influence sensory

competence by activating additional factors that work in concert with Atoh1. To test this, we examined the effects of co-misexpression of *hs:atoh1a* and *hs:fgf8*. A single heat shock at 14 hpf yielded a large sensory epithelium in the ventral floor, as well as a few scattered hair cells in the lateral wall (not shown). Prolonging misexpression by serial co-activation of *hs:atoh1a* and *hs:fgf8* at 14 hpf and 16 hpf led to a much more dramatic expansion of hair cells throughout the otic vesicle, including the dorsal and lateral walls (Fig. 2.5C). Similar results were obtained by serial co-activation of *hs:atoh1a* and *hs:fgf3* (Fig. 2.6F). Transverse sections of *hs:atoh1a;hs:fgf8* embryos confirmed the presence of a contiguous sensory epithelium covering the entire vesicle, with the exception of a small region in the medial wall (Fig. 2.5K, L). Absence of hair cells in this region correlated with notable thinning of the epithelium and the presence of multiple microvesicles in adjacent hindbrain tissue, suggesting some degree of tissue disruption. Nevertheless, these data show that early co-misexpression of *hs:atoh1a* and either *hs:fgf8* or *hs:fgf3* can dramatically expand sensory competence into virtually all regions of the otic vesicle. Moreover, regions of ectopic sensory development exhibited a thickened pseudostratified morphology typical of normal sensory epithelia. In contrast, activation of *hs:fgf8* or *hs:fgf3* alone was not sufficient to induce ectopic sensory epithelia, though the saccular macula was broken into 2 discrete domains in these backgrounds (Fig. 2.6B, C).

We next examined the ability of *sox2* to enhance hair cell production following activation of *hs:atoh1a*. *sox2* is normally induced by Fgf and Notch and is co-expressed with *atoh1a/b* in developing sensory epithelia (Millimaki et al., 2010). Similar to

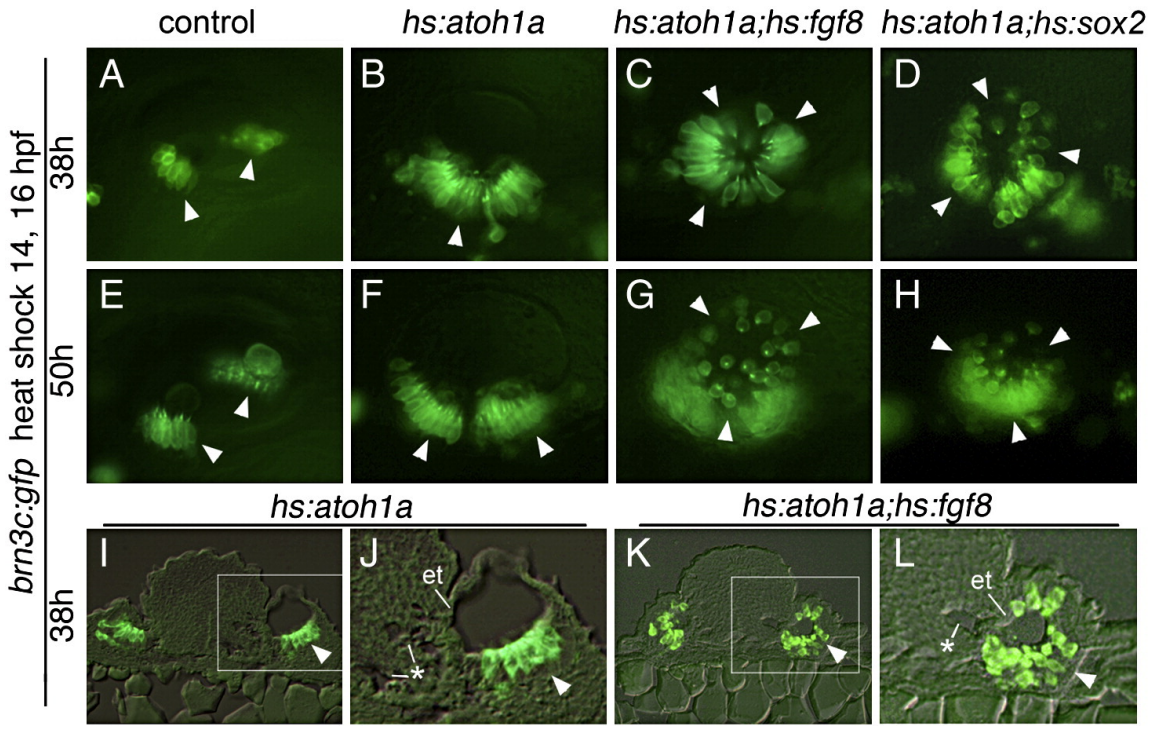

Figure 2.5. Co-misexpression of *atoh1a* with *fgf8* or *sox2*.
(A-J) Expression of *brn3c:gfp* after serial heat shock at 14 and 16 hpf in a control (A, E), *hs: atoh1a* (B, F, I, J), *hs:atoh1a;hs:fgf8* (C, G, K, L) and *hs:atoh1a;hs:sox2* (D, H) embryos. Embryos were fixed and processed at the indicated times. Arrowheads mark positions of endogenous and ectopic sensory epithelia. Images in I-L show transverse sections. The boxed areas in I and K are enlarged in J and L, respectively. The hindbrain shows sporadic formation of microvesicles (asterisks), suggesting tissue disruption, and the adjacent wall of the otic vesicle shows marked epithelial thinning (et). All other images show dorsolateral views of live embryos, with anterior to the left and dorsal to the top.

co-misexpression of *atoh1a* and *fgf8*, serial activation of *hs:atoh1a* and *hs:sox2* at 14 hpf and 16 hpf produced hair cells located throughout the otic vesicle (Fig. 2.5D). Serial activation of *hs:sox2* alone had little effect on hair cell production (Fig. 2.6A). Hair cells produced after misexpression of *atoh1a* with either *fgf8* or *sox2* were still present at 50 hpf, indicating these cells are relatively stable. Although hair cells in the lateral wall

appeared more widely separated at later stages (Fig. 2.5G, H), this appears to result from expansion of intervening tissue rather than death of hair cells based on monitoring GFP patterns over time. Anti-Caspase 3 staining confirmed that double-transgenic embryos did not exhibit an elevated number of apoptotic cells (Fig. 2.7).

We also examined the ability of *pax* genes to influence sensory competence. Expression of *pax8* and *pax2a* are also regulated by Fgf during otic development and are known to affect development and survival of hair cells (Kwak et al., 2006; Millimaki et al., 2007; Riley et al., 1999). However, serial co-activation of *hs:atoh1a* with either *hs:pax2a* or *hs:pax8* did not alter the production of hair cells compared to activation of *hs:atoh1a* alone (Fig. 2.6D, E, I, and data not shown). Likewise, disruption of either *pax8* or *pax2a* and *pax2b* did not diminish the ability of *hs:atoh1a* to induce ectopic hair cells following heat shock activation at 14 hpf or 24 hpf (Fig. 2.6G, H, and data not shown).

Patterning associated with global sensory development

The nearly global expansion of sensory development following co-misexpression of *hs:atoh1a* with either *hs:fgf8* or *hs:sox2* suggested dramatic changes in axial patterning within the otic vesicle. To test this, we examined expression of numerous spatial markers after serial activation of *hs:atoh1a* alone or in combination with *hs:fgf8*. Several anterior markers, *fgf8*, *fgf3* and *pax5* were all expanded posteriorly following activation of *hs:atoh1a* alone and were more strongly expressed following co-misexpression of *hs:atoh1a* and *hs:fgf8* (Fig. 2.8A-C''). Consistent with anteriorization

of the otic vesicle, the posterior marker *pou3f3b* (previously *zp23*) was reduced by activation of *hs:atoh1a* and nearly absent following activation of *hs:atoh1a* and *hs:fgf8*, while the posterior marker *fsta* was completely absent after misexpression of *atoh1a* or a*toh1a* and *fgf8* (Fig. 2.8D-E''). Expression of the dorsal marker *dlx3b* was reduced in *hs:atoh1a* and nearly absent after co-activation of *hs:atoh1a* and *hs:fgf8* (Fig. 2.8F-F''). An anterior/ventral marker *hmx3* (previously *nkx5.1*) was somewhat expanded by activating *hs:atoh1a* alone and was expressed nearly globally in *hs:atoh1a; hs:fgf8* double transgenic embryos (Fig. 2.8G-G''). Expression of the neuronal specifier *neurog1* was restricted to a small antero-lateral patch following activation of *hs:atoh1a* (Fig. 2.8H, H'). This is consistent with data from mouse showing Neurog1 and Atoh1 antagonize one another (Raft et al., 2007). In *hs:atoh1a; hs:fgf8* embryos the domain of *neurog1* was similarly reduced but shifted to a slightly more posterior position (Fig. 2.8H''). The lateral/posterior marker *otx1* was severely diminished in the otic vesicles of *hs:atoh1a* embryos and completely eliminated in double transgenic animals (Fig. 2.8I-I''). Consistent with loss of lateral markers we observed expansion of the medial marker *pax2a* into more lateral regions in *hs:atoh1a* and more strongly so in *hs:atoh1a*; *hs:fgf8* double transgenic embryos (Fig. 2.8J-J''). Nevertheless, expansion of medial fate was incomplete, since *pax2a* expression was not as strong laterally as medially (Fig. 2.8J'') and *pax5* did not show appreciable lateral expansion (Fig. 2.8C''). In contrast to the above results, serial activation of *hs:fgf8* alone led to ectopic expression of some anterior markers in posterior domains but otherwise did not strongly affect axial patterning in the otic vesicle (Fig. 2.9). Taken together, these data indicate that *atoh1a* misexpression can

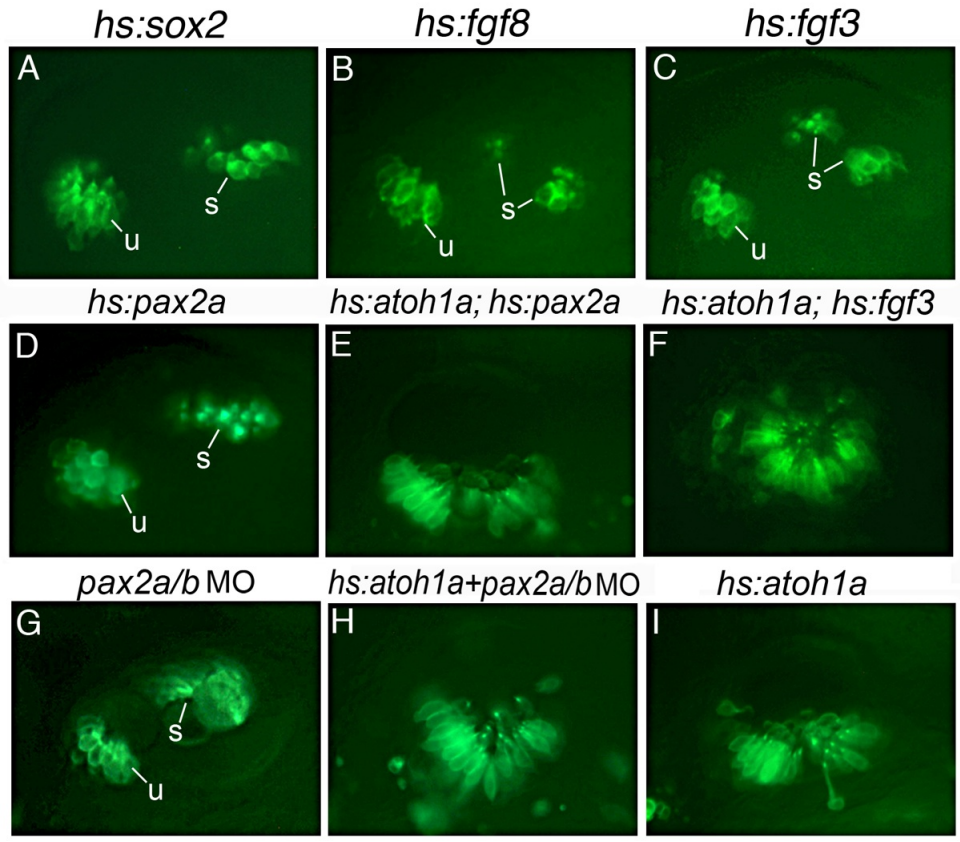

Figure 2.6. Ability of *fgf*, *sox* and *pax* genes to influence sensory competence. Expression of *brn3c:gfp* after serial heat shock at 14 and 16 hpf in the indicated transgenic (A-F, H, I) and non-transgenic (G) backgrounds. Embryos in G and H were also injected at the one-cell stage with 5 ng each of *pax2a* and *pax2b* morpholino (*pax2a/b* MO). Embryos were fixed and processed at 38 hpf. All images are dorsolateral views with anterior to the left and dorsal to the top.

expand anterior/ventral/medial identity within the otic vesicle but only to a certain extent on its own. Co-activation of *hs:fgf8* and *hs:atoh1a* enhances this activity.

Expansion of sensory competence at later stages

Because the effects of *atoh1a* misexpression become severely limited at later stages of development, we asked whether co-misexpression of *fgf8* or *sox2* can enhance sensory

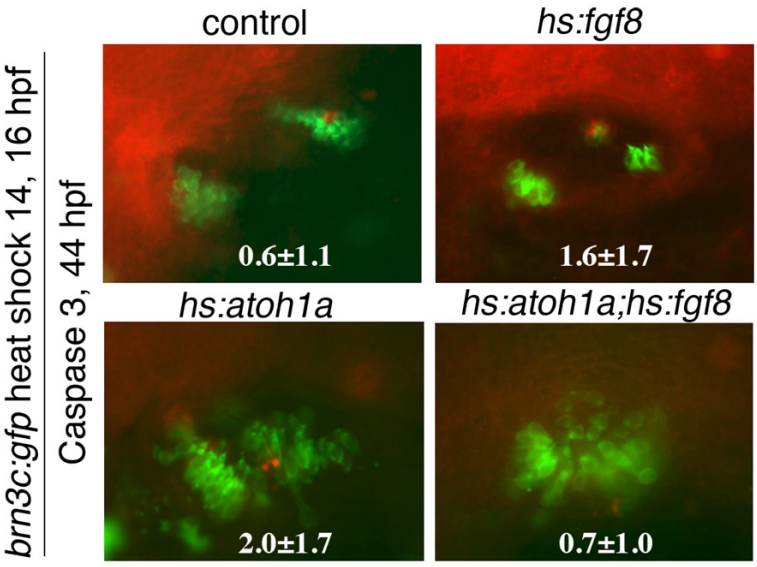

Figure 2.7. Analysis of cell death following co-misexpression of *atoh1a* and *fgf8*. Expression of *brn3c:gfp* (green) and Caspase 3 (red) at 44 hpf following serial heat shock at 14 and 16 hpf in a control embryo (A), *hs:fgf8* (B), *hs:atoh1a* (C) and *hs:atoh1a;hs:fgf8* (D). Means and standard deviations of the number of Caspase-positive cells is indicated for each background. Sample sizes and p-values from t-tests (relative to controls) were as follows: controls, n=17. *hs:atoh1a*, n=17, p=0.01. *hs:fgf8,* n=13, p=0.07. *hs:atoh1a;hs:fgf8*, n=20, p=0.94. Thus, only *hs:atoh1a* embryos showed a statistically significant, albeit small, increase in cell death. All images are dorsolateral views with anterior to the left and dorsal to the top.

competence after 24 hpf. In an initial series of experiments, we observed that delivering two heat shocks separated by either a 2- or 3-hour rest interval was optimal for increasing hair cell production, whereas two heat shocks separated by a 4-hour rest interval gave results that were indistinguishable from a single heat shock. Delivering a third heat shock offered no advantage relative to two heat shocks. For all experiments below, embryos were subjected to two heat shocks separated by a 3-hour rest interval, and sensory development was examined 24 hours after the final heat shock.

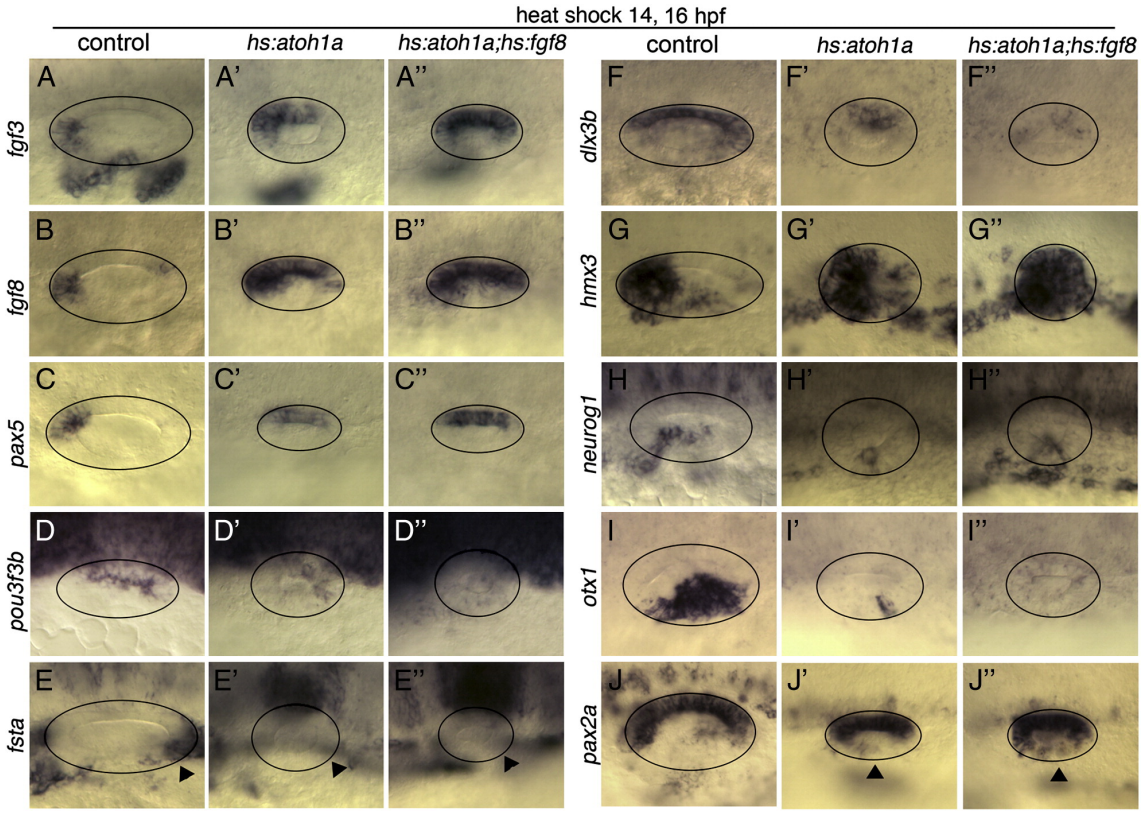

Figure 2.8. Axial patterning following co-activation of *hs:atoh1a* and *hs:fgf8*. Expression of various otic markers in control embryos (A-J) *hs:atoh1a* transgenic embryos (A'-J') and *hs:atoh1a;hs:fgf8* double transgenic embryos (A"-J"). Embryos were serially heat shocked at 14 hpf and 16 hpf and fixed for processing at 26 hpf. Images show dorsal views (A-C") or dorsolateral views (D-J"), with anterior to the left. Circles outline the otic vesicle. Arrowheads in E-E" mark expected location of *fsta* in the posterior otic vesicle. Arrowheads in J-J" indicate expanded domains of *pax2a* in the lateral wall of the otic vesicle.

Serial activation of *hs:atoh1a* at 24 hpf or 45 hpf yielded greater production of excess and ectopic hair cells than a single heat shock. However, production of ectopic hair cells was still mostly seen in the medial and ventral portions of the otic vesicle (Fig. 2.10D, E). Formation of hair cells in the lateral wall was rare, with an average of about 2 ± 2 lateral-wall hair cells per otic vesicle (n=13) (Fig. 2.11). Semicircular canals failed to form normally under these conditions, suggesting perturbation of non-sensory

development. Serial co-activation of *hs:atoh1a* and *hs:fgf8* after 24 hpf did not appreciably expand the domain of sensory development compared to serial activation of *hs:atoh1a* alone (not shown). In contrast, serial co-activation of *hs:atoh1a* and *hs:sox2* beginning at 24 hpf or 45 hpf led to a marked increase in hair cell production, including in the lateral wall of the otic vesicle (Fig. 2.10G, H). On average 9 ± 3 hair cells were observed in the lateral wall per otic vesicle (n=12) (Fig. 2.11). Ectopic hair cells usually formed as widely scattered single cells or small clusters.

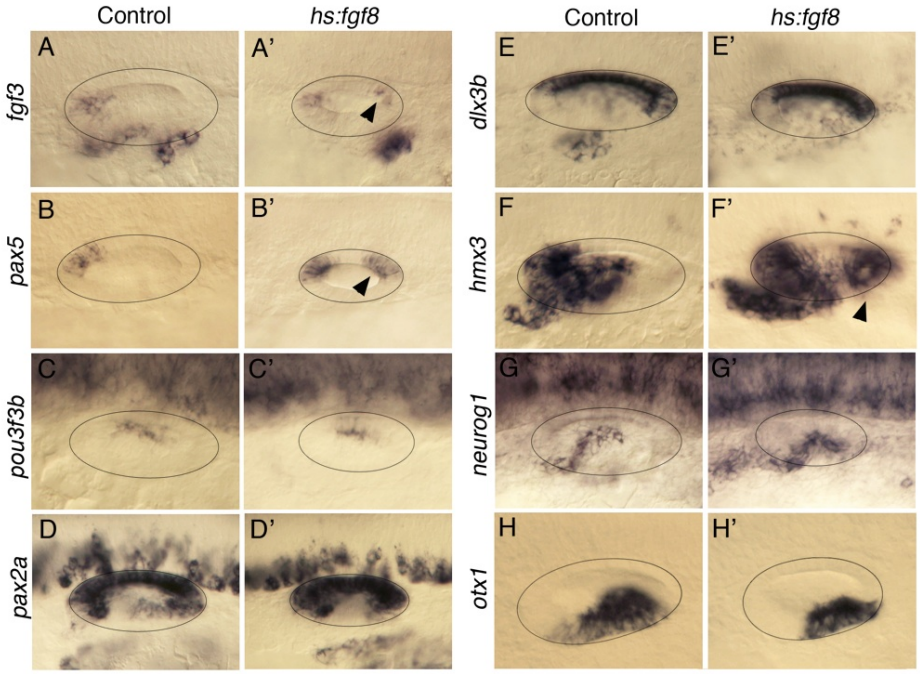

Figure 2.9. Axial patterning following activation of *hs:fgf8*. Expression of various otic markers in control (A-H) and *hs:fgf8* transgenic embryos (A'-H'). Embryos were serially heat shocked at 14 hpf and 16 hpf and fixed for processing at 26 hpf. Images show dorsal views (A-B'') or dorsolateral views (C-H''), with anterior to the left. Circles outline the otic vesicle.

The epithelium surrounding ectopic hair cells was notably thickened and exhibited a pseudostratified morphology (compare Fig. 2.10C, F, I). Additionally, small patches of *sox2* expression were usually detected near ectopic hair cells, suggesting the presence of support cells (Fig. 2.10I). Excess and ectopic hair cells were not observed following activation of *hs:sox2* alone, nor in control embryos (Fig. 2.11 and Millimaki et al., 2010). Thus, co-misexpression of *sox2* plus *atoh1a* can significantly enhance sensory competence at later stages of development.

Finally, we examined the effects of co-misexpressing *atoh1a* with either *pax2a* or the Wnt-inhibitor *dkk1*. Despite the involvement of *pax2a* in sensory development (Kwak et al., 2006; Riley et al., 1999), co-activation of *hs:atoh1a* and *hs:pax2a* after 24 hpf did not lead to production of ectopic hair cells, similar to results obtained at earlier stages (Fig. 2.6E and data not shown). Wnt signaling is thought to induce non-sensory fates in the otic vesicle (Lecaudey et al., 2007; Riccomagno et al., 2005), raising the possibility that blocking Wnt via *dkk1* misexpression might enhance sensory competence. However, the effects of co- activating *hs:atoh1a* and *hs:dkk1* were indistinguishable from activating *hs:atoh1a* alone (data not shown). Thus, not all genes associated with medial sensory development or lateral non-sensory development can affect sensory competence under the conditions used here.

DISCUSSION

We have characterized the effects of Atoh1 misexpression and identified important cofactors that potentiate its ability to promote sensory development in the zebrafish inner

ear. Misexpressing *atoh1a* greatly expands the spatial domain of sensory development, typically resulting in formation of a single large macula covering the ventral/medial region of the otic vesicle. Responsiveness to *atoh1a* misexpression is maximal during placodal through early otic vesicle stages and diminishes soon thereafter, presumably

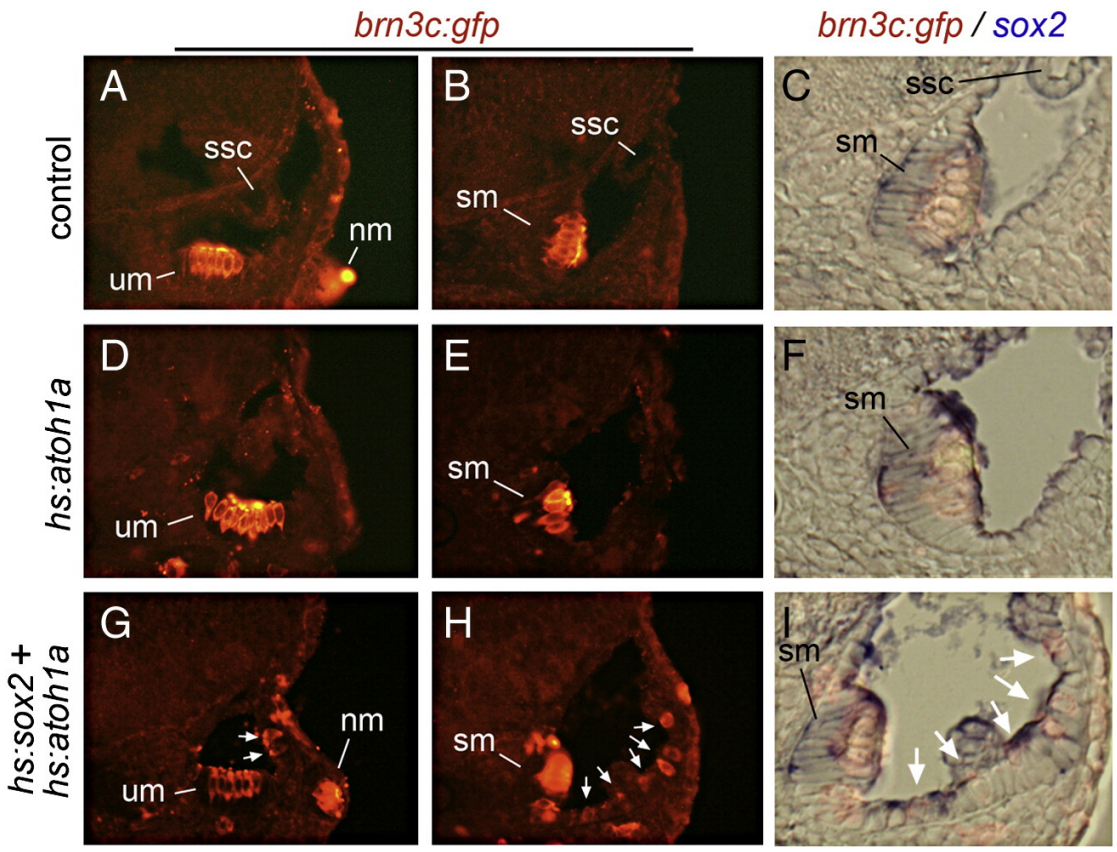

Figure 2.10. Sox2 expands sensory competence at later stages. Transverse sections showing otic expression of *brn3c:gfp* (red) and *sox2* (blue) in a control embryo (A-C), a *hs:atoh1a* transgenic embryo (D-F) and a *hs:atoh1a;hs:sox2* double transgenic embryo. Embryos were serially heat shocked at 45 hpf and 48 hpf and fixed at 72 hpf for staining and sectioning. Shown are sections passing through the anterior end (A, D, G) or the posterior end (B, C, E, F, H, I) of the otic vesicle. Positions of the utricular macula (um), saccular macula (sm), semicircular canals (ssc) and lateral line neuromasts (nm) are indicated. White arrows (G-H) mark ectopic hair cells. Specimens in (C, F, I) are enlargements of images (B, E, H) and are shown in brightfield with fluorescence to clarify the spatial relationships between hair cells and *sox2* expression.

reflecting progressive differentiation of non-sensory fates in the developing inner ear. Even during placodal stages, cells in the lateral portion of the otic placode are refractory to the effects of Atoh1a. By co-misexpressing the upstream regulator *fgf8*, which normally predominantly affects ventral/medial (sensory and neural) fates (Alsina et al., 2004; Hatch et al., 2007; Kwak et al., 2002; Kwak et al., 2006; Vasquez-Echeverria et al., 2008), the entire otic epithelium is rendered competent to respond appropriately to *atoh1a*. Likewise, co-misexpressing *sox2*, which is normally induced in parallel with *atoh1a/b* in response to Fgf and Notch (Millimaki et al., 2010), globally expands sensory development during placodal stages. At later stages *sox2* can still potentiate the ability

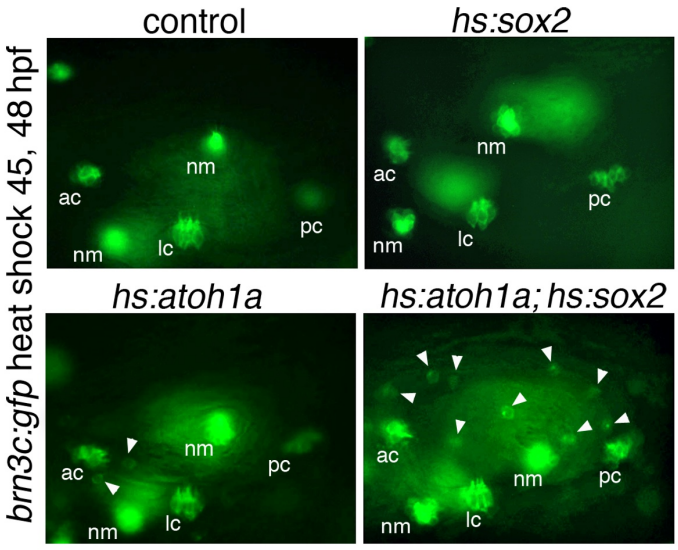

Figure 2.11. Hair cells in the plane of the lateral wall after serial heat shock. Expression of *brn3c:gfp* at 72 hpf following serial heat shock at 45 and 48 hpf in a control (A), *hs:sox2* (B), *hs:atoh1a* (C) and *hs:atoh1a;hs:sox2* (D). White arrowheads indicate ectopic hair cells in the lateral wall. Hair cells are also evident in the anterior crista (ac), lateral crista (lc), posterior crista (pc), and neuromasts of the lateral line (nm). Images show lateral views with anterior to the left and dorsal up.

of *atoh1a* to promote ectopic sensory development, whereas *fgf8* loses this ability. These findings refine our understanding of the genetic network that influences Atoh1 function and sensory competence.

Profile of gene expression in expanded and ectopic sensory epithelia

A highly conserved feature of *Atonal* gene regulation in insects and vertebrates is a robust auto-amplification loop that acts during the initial stages of proneural/prosensory development (Helms et al., 2000; Sun et al., 1998; our unpublished observations). This is followed by a non-autonomous negative feedback loop in which upregulation of Delta mediates lateral inhibition/lateral specification (Millimaki et al, 2007; Woods et al., 2004). Accordingly, we find that a relatively brief pulse of transgenic *atoh1a* expression is sufficient to activate prolonged expression of endogenous *atoh1a/b* genes within 1 hour, and *delta* genes are activated within 2 hours (Figs. 2.1, 2.3B and data not shown). Thus efficient induction of both feedback loops accounts for why transient expression of *hs:atoh1a* causes a dramatic increase in both hair cells and support cells. An expanded domain of *sox2* expression is seen within 6 hours and *brn3c:gfp* expression is detected in new hair cells within 9-10 hours (Fig. 2.3), a timeframe similar to the course of normal sensory development. A notable difference in ectopic sensory development, however, is that upregulation of *pax2a* in hair cells is not observed until 15 hours after *hs:atoh1a* activation. Normally *pax2a* expression precedes or coincides with hair cell differentiation, as both processes are initially coordinately regulated by localized Fgf signaling from the hindbrain. In contrast, the first exposure to local Fgf signaling in

ectopic sensory patches comes 4-6 hours after activation of *hs:atoh1a* as expanded macular domains of *fgf3* and *fgf8* begin to form. Hence the delay in expression of *pax2a* could reflect the distinctive timing of Fgf signaling in ectopic sensory epithelia.

Mechanisms that promote sensory competence

Our findings implicate Fgf and Sox2 as important mediators of sensory competence in zebrafish. Neither factor alone is sufficient to promote ectopic sensory development, but they synergize with Atoh1a to promote global sensory development. How Fgf and Sox2 function in this context is not clear. Fgf signaling influences axial fates in the otic placode and vesicle (Alsina et al., 2004; Hatch et al., 2007; Kwak et al., 2002; Kwak et al., 2006; Vásquez-Echeverría et al., 2008), raising the possibility that transgenic Fgf8 expands a regional identity compatible with sensory development. Indeed, analysis of regional markers in the otic vesicle following co-misexpression of *atoh1a* and *fgf8* indicates there is a near global expansion of ventral/medial/anterior identity, which is normally associated with the utricular macula. Similar but less pronounced changes in axial markers are seen following misexpression of *atoh1a* alone, including expansion of the domains of *fgf3* and *fgf*8 expression. Nevertheless, expansion of endogenous *fgf*3/8 expression by *hs:atoh1a* is not sufficient to promote sensory development in dorsal/lateral regions of the otic vesicle. It is possible that transgenic Fgf8 boosts the overall level of Fgf signaling above the threshold required for more complete axial respecification. Transgenic Sox2 also strongly promotes sensory competence, although its role in axial specification in the inner ear is unknown. A distinct alternative model is

that Fgf8 and Sox2 promote sensory competence by inducing a state of increased pluripotency. Both factors can promote formation of stem cells or multi-potent progenitors associated with early stages of tissue development (Graham et al., 2003; Nyeng et al., 2011; Tucker et al., 2010; reviewed by Lanner and Rossant, 2010). Thus, elevating Fgf8 or Sox2 could reverse early stages of differentiation of non-sensory cell types, thereby making cells more susceptible to Atoh1 activity. Whether Fgf and Sox2 are required before Atoh1 to enhance sensory competence, or instead act simultaneously with Atoh1 to form an optimal combinatorial code, remains to be established.

Studies in mouse and chick suggest that a somewhat different mechanism operates in amniotes, though there is likely to be some conservation of function as well. Misexpression of *Atoh1* in rodents induces formation of ectopic sensory epithelia but only in regions close to endogenous sensory epithelia, indicating that competence to respond to *Atoh1* is spatially restricted in mammals, too. Mammalian and avian sensory epithelia are normally specified by Jag1-Notch signaling (Brooker et al., 2006; Daudet et al., 2007; Kiernan et al., 2001; Kiernan et al., 2006). Notch plays a dual role in sensory development in birds and mammals, with an initial prosensory phase followed by a robust inhibitory phase associated with lateral inhibition/lateral specification (Brooker et al., 2006; Daudet and Lewis, 2005; Daudet et al., 2007). In mouse early misexpression of NICD, the intracellular domain of Notch, leads to global expression of prosensory markers *Jag1* and *Sox2* throughout the otic epithelium (Hartman et al., 2010; Pan et al., 2010). Under these conditions otic development arrests and mature hair cells and support cells are not observed. However, localized Cre-mediated expression of NICD at

later stages results in formation of scattered ectopic sensory epithelia, even in non-sensory regions far from endogenous sensory epithelia. Thus prosensory Notch activity in mammals can reprogram virtually any otic cell to adopt a sensory fate. In chick, misexpression of NICD or Jag1 can induce formation of ectopic sensory epithelia, but not within the dorsal half of the otic vesicle (Daudet and Lewis, 2005; Neves et al., 2011). However, misexpression of the Notch target gene *Sox2* can yield scattered sensory epithelia in virtually any part of the otic vesicle in chick (Neves et al., 2011). In zebrafish, activation of NICD strongly upregulates *sox2* expression throughout the medial wall, but this is not sufficient to activate hair cell formation, nor does NICD activate *sox2* expression in lateral cells (Millimaki et al., 2010). Despite these species-differences, Sox2 appears to be an important effector of sensory-competence in all vertebrates: Sox2 is essential for sensory development in mammals (Kiernan et al., 2005), it is sufficient to activate sporadic sensory development in chick (Neves et al., 2011), and it is sufficient to render all otic cells competent to respond to Atoh1 in zebrafish (this work). Whether Fgf signaling can also promote Sox2 expression or ectopic sensory development in mammals and birds has not been reported.

Implications for regeneration

In non-mammalian vertebrates, hair cell regeneration is efficiently mediated by support cells, which can transdifferentiate directly into hair cells or undergo asymmetric cell division to yield new hair cell-support cell pairs (Millimaki et al., 2010; Schuck and Smith, 2009; reviewed by Brignull et al., 2009; Cotanche and Kaiser, 2010). However,

regeneration fails to occur in the adult mammalian cochlea because support cells lose the ability to divide or transdifferentiate during neonatal development. This transition correlates with a significant decline in *Sox2* expression during cochlear maturation (Smeti et al., 2011). Because Sox2 is essential for hair cell regeneration in zebrafish (Millimaki et al., 2010), it seems likely that the decline in Sox2 levels in the mammalian cochlea contributes to loss of regenerative capacity. Interestingly, forced expression of *Atoh1* in rodents can stimulate transdifferentiation of support cells and thereby foster some regeneration, though recovery of hair cells is inefficient and morphology is often abnormal (Izumikawa et al., 2005; Kawamoto et al., 2003; Shou et al., 2003; Zheng and Gao., 2000). Whether *Sox2* can augment *Atoh1*-mediated regeneration in mammals remains an open question. In apparent contradiction, one study in mouse showed that co-misexpression of *Sox2* and *Atoh1* induced many fewer ectopic hair cells than did *Atoh1* alone (Dabdoub et al., 2008). However that study utilized vectors designed to promote strong constitutive expression, conditions that clearly override normal feedback mechanisms. Based on our studies, we speculate that transient co-misexpression would allow endogenous *Atoh1* and *Sox2* promoters to respond freely to natural regulatory mechanisms and potentiate sensory development and hair cell regeneration (e.g. see Woods et al. 2004).

CHAPTER III

ZEBRAFISH PAX5 REGULATES DEVELOPMENT OF UTRICULAR MACULA AND VESTIBULAR FUNCTION*

OVERVIEW

This is a published account of the role of *pax5* in sensory epithelia development. It is primarily the work of my colleague, S. J. Kwak. Because I contributed to portions of Figures 3.2, 3.4, 3.5, 3.6, 3.7 and Table 2, I include it here as a record of my work.

INTRODUCTION

The vertebrate inner ear is a conserved organ system comprising a series of interconnected chambers, each of which primarily mediates either vestibular or auditory function. Each chamber contains a sensory patch consisting of sensory hair cells and supporting cells. Hair cells synapse with neurons of the statoacoustic ganglion (SAG), or the VIIIth cranial nerve, axons of which project to processing nuclei in the hindbrain (reviewed by Lewis et al., 1985).

All sensory patches originate from a prosensory region in the ventromedial wall of the otic vesicle, and each sensory patch subsequently differentiates with specific

---

*Reprinted with permission from "Zebrafish *pax5* regulates development of the utricular macula and vestibular function" by Kwak, S.J., Vemaraju, S., Moorman, S.J., Zeddies, D., Popper, A.N., Riley, B.B., 2006. Dev. Dyn. 235, 3026-3038. Copyright [2006] Wiley-Liss, Inc.

structural and functional attributes (Lewis et al., 1985; Fekete and Wu, 2002; Riley and Phillips, 2003; Barald and Kelley, 2004). Hair cells in the semicircular canals have very long cilia embedded in a gelatinous cupula that senses angular acceleration through fluid motion in the canal. Hair cells in the cochlea of mammals and birds have shorter cilia embedded in a tectorial membrane that transmits sound vibrations. Hair cells in the sensory maculae of the utricle, saccule, and lagena bear cilia that contact crystalline otoliths that transmit forces caused by linear acceleration, gravity and, in fish, sound vibrations (Fay and Popper,1980; Popper and Fay, 1993).

Despite the dual sensory capacity of fish maculae, studies in zebrafish (*Danio rerio*) and the closely related goldfish (*Carassius auratus*) suggest that the functions of different maculae are not identical. Although it is likely that all maculae contribute to hearing, the saccule is the primary auditory sensor, particularly at frequencies above several hundred Hz (Popper et al., 2003). Zebrafish, like other ostariophysan fishes, utilize a series of bones (Weberian ossicles) that are thought to transmit sound vibrations from the swim bladder to the saccule (Popper et al., 2003). Disruption of the Weberian ossicles or swim bladder results in partial loss of hearing (Fay and Popper, 1973; Bang et al., 2002; Zeddies and Fay, 2005). The utricle probably also has some role in hearing, possibly in sound source localization (Popper et al., 2003). However, unlike the saccule, the utricle is essential for vestibular function in zebrafish larvae, as shown by analysis of *monolith* (*mnl*) mutants (Riley et al., 1997; Riley and Moorman, 2000). These mutants usually form saccular otoliths but not utricular otoliths, which ablates all discernable vestibular function and is lethal during larval stages. However, experimental

manipulations that restore utricular otoliths rescue both vestibular function and viability in *mnl* mutants, even if saccular otoliths are ablated instead. Thus, in zebrafish the utricle is especially important for vestibular function while the saccule has a more pronounced role in hearing. Sensory cristae within the semicircular canals are also devoted to vestibular function but these do not become functional until after 30 dpf (Beck et al., 2004).

Differential gene activity in the otic vesicle presumably underlies development of the characteristic structure and function of each chamber and sensory epithelium. Indeed, many candidate genes have been identified that show expression in only one or a small subset of sensory patches. However, loss of function of such genes often causes severe morphogenetic defects that preclude assessment of functional output. For example, *Otx1* is expressed in the presumptive lateral crista and *Otx1*$^{-/-}$ mutant mice do not produce the lateral crista or a normal lateral semicircular canal (Morsli et al., 1999). Thus, it is not clear whether *Otx1* plays an ancillary role in programming the lateral crista or its associated neurons to specialize as a vestibular endorgan.

In zebrafish, sensory epithelia form at an early stage before extensive morphogenesis of the various chambers of the inner ear (Haddon and Lewis, 1996; Whitfield et al., 2002). The nascent otic vesicle contains only two sensory patches corresponding to the utricular (anterior) and saccular (posterior) maculae. We have been interested in identifying genes required for regulating functional specialization of these two sensory epithelia. One candidate gene, *pax5*, is initially expressed in the anterior end of the nascent otic vesicle (Pfeffer et al., 1998) and later becomes localized to the

utricular macula. This pattern suggested that *pax5* might be involved in development, maintenance or functional organization of the utricular macula. To investigate *pax5* function, we cloned the full sequence of *pax5* cDNA and performed loss of function studies using antisense morpholinos. Knocking down *pax5* caused vestibular defects in zebrafish larvae without altering morphogenesis of the ear or the ability to hear. We show that vestibular deficits result from defects in maintaining utricular hair cells, with secondary defects in the pattern of SAG neuronal processes in the utricular macula.

MATERIAL AND METHODS

Fish strains and staging

Wild-type zebrafish strains were derived from the AB line (Eugene, OR). Mutants alleles used in this study include *noi*^{tu29a} (Lun and Brand, 1998), *lia*^{t24152} (Herzog et al., 2004) and *mnl*^{z2} (Riley and Grunwald, 1996). Embryos and larvae were maintained in an incubator at 28.5˚ C and staged as described by Kimmel et al. (1995). Ages are denoted as hours post-fertilization (hpf) or days post-fertilization (dpf). Embryos normally hatch by 3 dpf, after which they are referred to as larvae. In some case, 0.2 mM phenylthiourea (PTU) was added to prevent melanin formation.

Cloning of *pax5*

Comparison of zebrafish (http://www.ensembl.org) and *Fugu* genomic sequences identified the putative missing 5' and 3' ends of zebrafish *pax5*. The identified sequence was confirmed by RT-PCR followed by cloning and sequencing using primers for the

putative full length ORF; *pax5*(-6): 5'GGGAATTCAACACGATGGAAATCCACTG3', *pax5*(1128):5'GGTCTAGATTATTTCGTGCCTCCCACTC3'.

Behavioral analysis

Vestibular function was assayed by three tests between 3 and 7 dpf as previously described (Riley and Moorman, 2000). Balance was assessed by the ability of larvae to rest with their dorsal sides up one minute after initiating a startle response by tapping Petri dishes containing larvae. Each specimen was tested three times and was scored as negative if it failed all three trials. To test motor coordination, individual larvae were observed following a startle response, induced by tapping the plate or gentle physical stimulation of the tail. Normally, larvae rapidly traverse a 6 cm Petri dish in a straight line. Larvae with vestibular dysfunction swim in circles, vertical loops, spirals, or in erratic zigzags. Specimens failing three consecutive trials were scored as negative. Swim bladder inflation was observed under a dissecting microscope (Riley and Moorman 2000). Normally, larvae must swim to the surface to obtain air for swim bladder inflation. Vestibular deficits impede this motion and thereby prevent swim bladder inflation. Acoustic-evoked behavioral responses (AEBR) were tested in larval fish 7-12 dpf as described by Zeddies and Fay (2005). Briefly, larval fish were placed in the 8 central wells (one fish per well) of a 24-well plate affixed to a plastic platform. A TDT System 3 (TDT, Inc, Gainsville, FL) was used to deliver tonal pulses to the platform via a vertically oriented Bruel & Kjaer type 4810 shaker. Eight frequencies from 100-1200Hz were tested at seven different levels (ranging from 0 to -42 dB re 1g).

Five-second long video sequences of the larvae were digitally recorded such that the tone was presented 2.5 s after the start of the video recording. A frame-by-frame subtraction method was then employed to analyze the video sequences and compare the movement of the larval fish in quiet to their movement when the stimulus is present. A positive response was registered when the movement during the tone was significantly different ($p<.0001$) than in quiet. A complete experiment consisted of the presentation of two randomized presentations of the 56 trials. The lowest level that resulted in a positive response at each frequency was then considered the threshold level for that frequency.

Morpholino injection

Splice- and translation-blocking morpholino oligomers (Nasevicius and Ekker, 2000; Draper et al., 2001) were generated to knock down *pax5*. Translation blocker for splice variant 1 (TB1): 5'CAGTGGATTTCCATCTGTTTTAAA3'; translation blocker for splice variant 2 (TB2): 5'CTCGGATCTCCCAGGCAACATGGT3'; splice blocker for exon-intron boundary of exon 2 (SB1): 5'TACTCATAACTTACCTGCCCAGTA3'; splice blocker for exon-intron boundary of exon 3 (SB2): 5'ATGTGTTTTACACACCTGTTGATTG3'; splice blocker for exon-intron boundary of exon 5: 5'TTGACCCTTACCTAAATTATGCGCA3'. A cocktail of all five morpholinos was prepared in Danieaux solution (Nasevicius and Ekker, 2000) to a concentration of 12 µg/µl (3µg/µl each TB1 and TB2; and 2 µg/µl each SB1, 2 and 3). Approximately 1 nl was injected into wild-type zebrafish embryos at one-cell stage to generate *pax5* morphants.

Injection of *pax5* RNAs

Two splice variants, *pax5*-v1and *pax5*-v2 were cloned in pCS2p+. RNAs for both variants were synthesized in vitro and ~200 pg of *pax5*-v1 and *pax5*-v2 RNA mixture (100 pg each) was injected into embryos at the one- to two-cell stage.

Immunohistochemistry

Embryos raised in PTU were fixed and processed as previously described (Riley et al., 1999). Primary antibodies: mouse anti-Pax2 (Berkeley Antibody Company, 1:100 dilution), anti-acetylated tubulin (Sigma T-6793, 1:100) and anti-Islet-1/2 (Developmental Studies Hybridoma Bank 39.4D5, 1:100). Secondary antibodies: Alexa 546 goat anti-rabbit IgG (Molecular Probes A-11010, 1:50) and Alexa 488 goat anti-mouse IgG (Molecular Probes A-11001, 1:50).

Rhodamine-Phalloidin staining

Larvae raised in PTU were fixed between 3 and 7 dpf. Fixed larvae were rinsed in PBS containing 0.1% Triton-X-100 for 15 minutes and then permeabilized by incubation in PBS containing 2-3% Triton-X-100 for 4 hours at room temperature and then overnight at 4˚C. Permeabilized embryos were incubated in Rhodamine-Phalloidin (Molecular Probes R415, 1:30 dilution in 1% Bovine Serum Albumin in PBS) for 2 hours at room temperature, washed four times in PBS with 0.5% Triton-X-100 for 30 minutes each.

DiI labeling

Larvae were fixed between 3 and 7 dpf and then washed in PBS. Fixed larvae were mounted in 0.6% low-melting-temperature agarose made in PBS. To examine the neuronal projections from the statoacoustic ganglion (SAG), DiI (1,1-dioctadecyl-3,3,3,3 -tetramethylin-docarbocyanine perchlorate, Molecular probes D-282, 4mg/ml in 100% ethanol) was injected into the utricular macula. Glass micropipettes were backfilled with the DiI solution and directed to the utricular macula using a micromanipulator. Injected larvae were incubated at 33˚C overnight and observed.

Whole-mount in situ hybridization

Whole-mount in situ hybridizations were carried out as described previously (Phillips et al. 2001) using the following riboprobes: *nkx5.1* (Adamska et al., 2000), *otx1* (Li et al., 1994), *zp23* (Hauptmann and Gerster, 2000), *dlx3b* (Ekker et al., 1992a), *krox20* (Oxtoby and Jowett, 1993), *msxC* (Ekker et al., 1992b), *pax5* (Pfeffer et al., 1998), *fgf8* (Reifers et al., 1998) and *fgf3* (Kiefer et al., 1996).

Cell death analysis

Embryos were dechorionated and incubated in acridine orange (1µg/ml) in PBS for 1 hour at room temperature and washed twice (10 minutes each) in PBS prior to observation. In situ TUNEL assay (TdT-mediated dUTP Nick-End Labeling) was performed as suggested by the manufacturer (Promega TUNEL assay kit).

RESULTS

Cloning of zebrafish *pax5*

The known sequence for zebrafish *pax5* cDNA was incomplete, with sequences missing from both the 5' and 3' cDNA ends (Pfeffer et al., 1998). We completed cloning of the *pax5* sequence (see Experimental Procedures). Analysis of multiple cDNA clones revealed two distinct splice isoforms, *pax5*-variant 1 (*pax5*-v1) and *pax5*-variant 2 (*pax5*-v2) (Fig. 3.1A). *pax5*-v1 corresponds to full-length *pax5* cDNA. *pax5*-v2 has a partial paired domain caused by splicing out the second exon (nucleotides 47-212). This splice variant is predicted to use an alternative translation start codon in exon 3. In mouse, six splice variant forms are known. The two zebrafish variants, *pax5*-v1 and *pax5*-v2, are homologous to mouse splice variants *Pax-5a* and *Pax-5b*, respectively, suggesting that mechanisms for alternative splicing of *pax5* have been conserved (Zwollo et al., 1997). The relative abundance of cloned cDNAs suggests that *pax5*-v1 (8 out of 10 clones) is more prevalent than *pax5*-v2 (2 out of 10 clones).

Expression of *pax5* in the otic vesicle

pax5 is first detected in the anterior end of the otic placode at about 17 hpf, just before formation of the otic vesicle (Fig. 3.1B). By 24 hpf, the anterior quarter of the otic vesicle shows a uniformly high level of *pax5* expression (Fig. 3.1C). Expression is subsequently restricted to the anterior (utricular) macula and remains in the macula until at least 72 hpf (Fig. 3.1D, E). At these later stages, all cells in the utricular macula

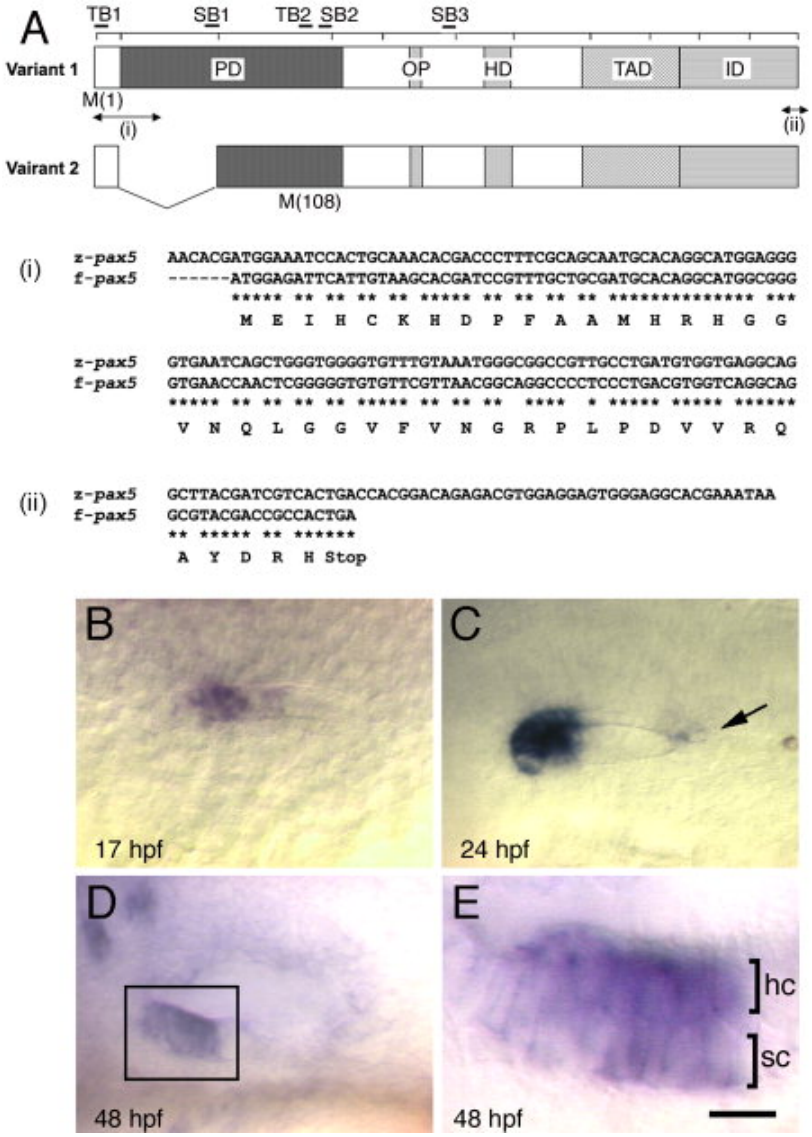

Figure 3.1. cDNA structure and expression of *pax5*.
(A) General structure of *pax5* splice variants. Brackets indicate exon-boundaries. Conserved functional domains, paired (PD), octapeptide (OP), homeo (HD), transactivation (TAD) and inhibitory (ID) are marked. Putative translation start sites (M) are indicated. Binding sites for translation-blocking (TB1 and 2) and splice-blocking (SB1, 2 and 3) morpholinos are shown. Newly identified 5'(i) and 3'(ii) sequences are shown in comparison with *fugu pax5*. Zebrafish and f*ugu* sequences are 100% identical at the amino acid level. (B-E) Expression of *pax5* in the otic placode at 17 hpf (B), in the otic vesicle at 24 hpf (C) and in the utricular macula at 48 hpf (D,E). (E) Enlarged view of boxed area in (D). Hair cell (hc) supporting cell layers are marked. Arrow, weak expression in the saccule. (A) Dorsal, (B) dorsolateral and (C,D) lateral views, with anterior to the left.

express *pax5*, but hair cells show higher expression than supporting cells (Fig. 3.1E). In addition to the predominant domain in the utricle, a small number of saccular hair cells also express *pax5* (Fig. 3.1C). This posterior expression is maintained through at least 48 hpf (not shown).

Vestibular defects in *pax5*-depleted larvae

To study *pax5* function in the inner ear development, two morpholinos were designed to block translation from two putative translation start sites and three were designed to block splicing of sequences encoding the paired domain or the homeodomain (Fig. 3.1A). Each of these morpholinos, used individually, disrupted vestibular function (discussed below) but varied in efficiency. However, a cocktail of all five morpholinos proved most efficient and was used for the remainder of this study. Embryos injected with *pax5*-MO cocktail (*pax5* morphants) show no obvious morphological defects. The otic vesicle is normal in size and otoliths form in the correct positions at the right time. Because of the predominant expression of *pax5* in the utricle, we assayed the vestibular-dependent functions of balance, motor coordination, and swim bladder inflation (Riley and Moorman, 2000). For comparison we also examined *monolith* (*mnl*) mutants, which show a severe and permanent loss of vestibular function due to the lack of utricular otoliths (Riley and Grunwald, 1996; Riley et al., 1997; Riley and Moorman, 2000). By all three assays, *pax*5 morphants are delayed by a day or more in development of vestibular function (Fig. 3.2A-C). This does not reflect a general developmental delay since morphological and molecular milestones occur on time (see below). Although

many *pax5* morphants eventually display normal vestibular behavior, about 20% never do so and continue to show severely impaired vestibular function through at least 7 dpf (Fig. 3.2). These data support the hypothesis that *pax5* is required for development and/or function of the vestibular system.

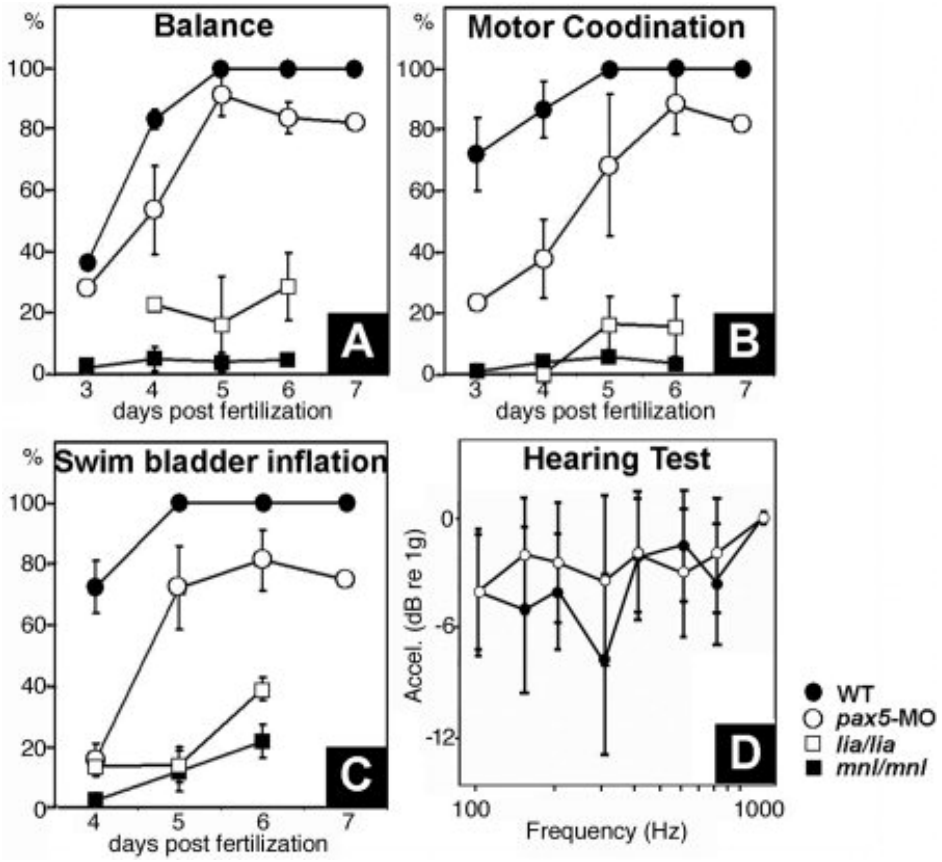

Figure 3.2. Assessment of vestibular and auditory function.
Development of balance (A), motor coordination (B) and swim bladder inflation (C) in wild-type (n=173), *pax5*-morphant (n=330), *lia/lia* (n=110) and *mnl/mnl* (n=238) embryos between 3 and 7 dpf. Data show the means and standard errors of two independent experiments. (D) Frequency range and sensitivity of hearing in wild-type larvae and *pax5* morphants at 5 dpf. Only *pax5* morphants with severe vestibular deficits were used in (D).

In contrast to vestibular function, acoustic function appears normal in *pax5* morphants. Zeddies and Fay (2005) recently described an assay to test acoustically-evoked behavioral responses (AEBR) in zebrafish larvae and adults. Beginning at 5 dpf, wild-type larvae respond at the same levels over the same frequency range as adult zebrafish. Because *pax5* shows only minor expression in the saccular macula, we hypothesized that hearing should be relatively normal. Indeed, even *pax5* morphants with severe and persistent vestibular deficits appear to respond normally to sound on 5 dpf and later (Fig. 3.2D and data not shown). These data suggest that the vestibular deficits in *pax5* morphants are not caused by global or nonspecific defects but instead reflect a specific requirement in the utricular epithelium for vestibular function.

Otic vesicle patterning in *pax5* morphants

The vestibular defects in *pax5* morphants could be caused by perturbation of general patterning of the otic vesicle. To test this possibility, we examined several markers of otic vesicle patterning. *nkx5.1*, which marks the anterior end of the otic vesicle, is expressed normally in *pax5* morphants (Fig. 3.3A, B), as is *zp23,* a marker of the posterior medial wall adjacent to r5 and r6 of hindbrain (Fig. 3.3C, D). Patterning of dorsoventral and mediolateral axes also appear normal as demonstrated by expression of a dorsomedial marker, *dlx3b*, and a ventrolateral marker, *otx1* (Fig. 3.3E, F, G, H). In addition, sensory maculae and cristae appear to form on time and express appropriate markers (Fig. 3.3I-L). Several aspects of inner ear patterning, including otic expression of *pax5*, depend on Fgf3 from the hindbrain (Kwak et al., 2002), so we also examined

hindbrain patterning. Expression of *fgf3*, as well as other hindbrain markers such as *krox20*, are normal in *pax5* morphants (Fig. 3.3M-P, and data not shown). Thus, hindbrain patterning and general features of otic vesicle patterning appear normal in *pax5* morphants.

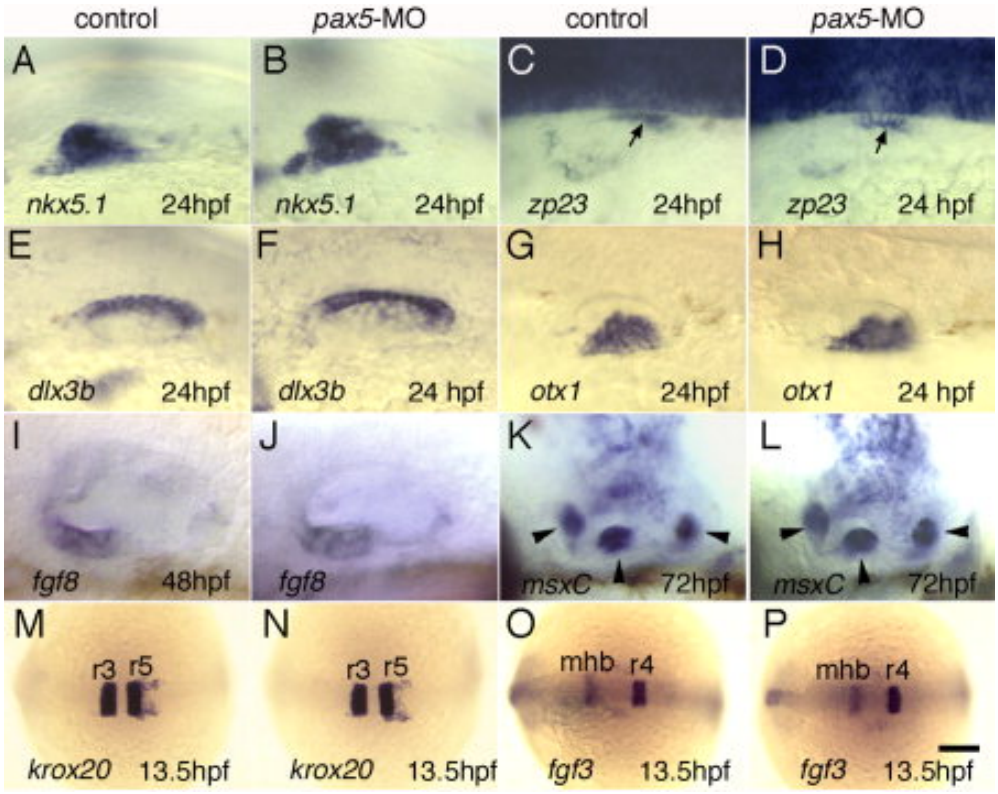

Figure 3.3. Inner ear and hindbrain patterning in *pax5* morphants.
Expression of *nkx5.1*, *zp23* (arrows mark otic domain), *dlx3b* and *otx1* in the otic vesicle of uninjected control embryos (A,C,E,G) and *pax5*-morphants (B,D,F,H) at 24 hpf. (I,J) Macular expression of *fgf8* in control (I) and *pax5*-morphant (J) at 48 hpf. (K,L) Expression of *msxC* in cristae (arrowheads) of control (K) and *pax5*-morphant (L) at 72 hpf. (M-P) *krox20* and *fgf3* expression at 13.5 hpf (9-somite stage) in the hindbrain of uninjected control embryos (M,O) and *pax5* morphants (N,P). Images show dorsolateral (A-F), lateral (I-L) and dorsal (G-H, M-P) views with anterior to the left. Abbreviations: MHB, midbrain-hindbrain border; r3, rhombomere 3; r4, rhombomere 4. Scale bar, 35 µm (A-J), 65 µm (K,L), 160 µm (M-P).

Formation of SAG neurons in *pax5* morphants

Another possible cause of vestibular deficits is failure to form the statoacoustic ganglion (SAG). SAG neuroblasts are initially specified in the ventral region of the otic vesicle in a region that partially overlaps with the domain of *pax5* expression (Haddon and Lewis, 1996). Neuroblasts delaminate from the otic vesicle and migrate to a position between the anteromedial wall of the otic vesicle and hindbrain. *neurogenin1*(*ngn1*) encodes a bHLH transcription factor required for SAG specification and is first expressed at 18 hpf (Andermann et al., 2002). *ngn1* is expressed normally in *pax5* morphants (Fig. 3.4A, B). After delamination, SAG neuroblasts express *nkx5.1* (Adamska et al., 2000) and this pattern is also normal in *pax5* morphants (Fig. 3.3A, B). Similarly, the number and position of SAG neuroblasts is normal at 30 hpf as shown by anti-Islet staining (Fig. 3.4C, D). Thus, depletion of *pax5* does not alter production or migration of SAG neurons.

Neuronal targeting of SAG neurons in *pax5* morphants

SAG neurons are bipolar neurons, sending processes into the hindbrain and sensory patches of the ear. Axonal processes to the hindbrain were visualized by injecting a lipophilic tracer, DiI, into utricular maculae at 3 dpf or later. Utricular SAG neurons initially extend their axons in a bundle to the hindbrain in a dorsoposterior direction. This axonal bundle splits into two main branches in the hindbrain, one ascending and the other descending (Fig. 3.4G). In some specimens, ascending and descending branches are compact and well organized (Fig 3.4G, type-1). In about 60% of control larvae, the

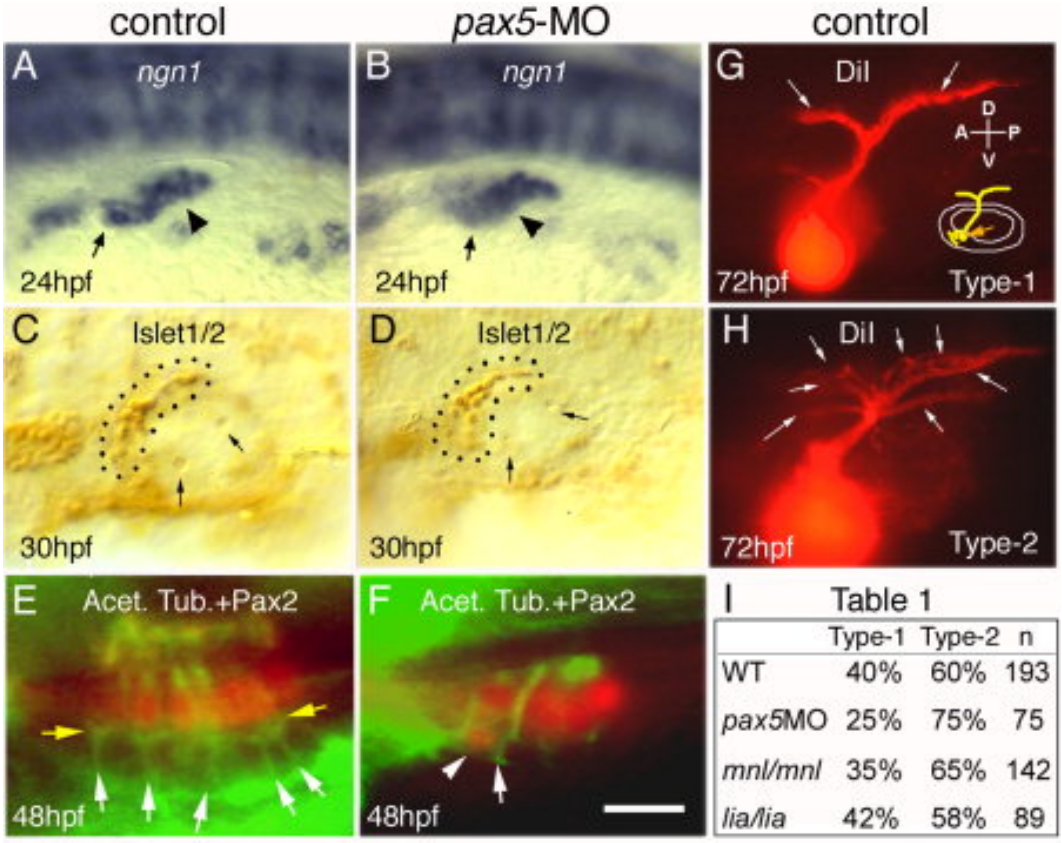

	Type-1	Type-2	n
WT	40%	60%	193
*pax5*MO	25%	75%	75
mnl/mnl	35%	65%	142
lia/lia	42%	58%	89

Figure 3.4. Development of the statoacoustic ganglion (SAG).
(A-B) Expression of *ngn1* in the otic vesicle (arrowheads) and SAG (arrows) in a control embryo (A) and *pax5*-morphant (B) at 24 hpf. (C, D) Anti-Islest1/2 staining of SAG neuroblasts (outlined) at 30 hpf. An average of 16.5±4.2 neuroblasts were detected in control embryos (C) compared to 15.7±3.5 in *pax5* morphants (D). Arrows mark otoliths. (E, F) Utricular maculae of a 48 hpf control embryo (E) and *pax5* morphant (F) showing acetylated tubulin (green) relative to Pax2 in hair cell nuclei (red). White arrows in (E) mark axonal process projecting to hair cells and broader regions of staining (yellow arrows) are observed at the basal regions of hair cells, possibly associated with synapses. Specimen in (F) shows a misplaced hair cell (arrowhead) associated with a single thick SAG process (arrow). (G, H) Central projections of SAG neurons visualized by injecting DiI into the utricular macula at 72 hpf. Schematic in (G) shows the site of DiI injection (orange arrow) and SAG projections relative to the ear. Wild-type larvae show either two discrete axonal bundles in the hindbrain (G, type-1) or more diffuse projection patterns (H, type-2), including smaller secondary branches indicated by arrows. (I) Table 1**,** percentage of larvae showing type-1 or type-2 projection patterns in control embryos, *pax5* morphants, *mnl/mnl* mutants and *lia/lia* mutants. Images show dorsolateral (A-B, E-F), dorsal (C, D) and lateral (G-K) views, with anterior to the left. Scale bar, 50µm (A,B,E,F), 30µm (C,D), 12.5µm (G-K).

main branches are more diffuse and there are several additional minor branches projecting in parallel to the main branches (Fig. 3.4H, type-2). A similar distribution of type-1 vs. type-2 patterns is seen at 7 dpf, even though all control larvae show fully integrated vestibular function by 5 dpf (Fig. 3.2). Moreover, virtually identical patterns are observed in *mnl* mutants (Fig. 3.4I, Table 1), which are null for vestibular function (Riley and Moorman, 2000). Thus, the distribution of type-1 vs. type-2 patterns is not influenced by the status of vestibular signaling or early maturation of the larval hindbrain. Similar SAG projections are seen in *pax5* morphants, though type-2 patterns are slightly more frequent than in control larvae (Fig. 3.4I, Table 1). At present, we do not understand the significance of the two different projection patterns. Nevertheless, vestibular deficits in *pax5* morphants do not appear to be caused by aberrant projections in the hindbrain.

We also examined SAG processes in developing maculae. Acetylated tubulin is localized in the cortex and cilia of hair cells, as well as axonal processes of SAG neurons (Fig. 3.4G, H). Acetylated tubulin staining is especially prominent in the basal part of hair cells where SAG neurons synapse (Fig. 3.4E). While some *pax5* morphants appear normal, half or more show a variety of defects in neural patterning in the utricle. For example, about half of *pax5* morphants show loss of putative synapse-staining on utricular hair cells and the number of SAG processes is reduced (Fig. 3.4F). Occasionally, processes can be seen projecting at oblique angles and fail to innervate any hair cells (not shown). In addition, about 20% of *pax5* morphants show thick bundles of dendrites reaching to the luminal surface without contacting any hair cells

(Fig. 3.4F). Anti–NCAM staining shows similar patterns of SAG axonal processes (data not shown). Innervation of the saccular macula is difficult to visualize because of its close proximity to the brightly stained hindbrain. However, SAG innervation of hair cells in cristae is normal in *pax5* morphants (data not shown). Thus, variable defects in hair cell innervation primarily affect the utricle in *pax5* morphants and could contribute to the observed vestibular deficits in *pax5* morphants.

Formation of hair cells

We hypothesized that *pax5* might also regulate development of utricular hair cells. To test this, embryos were stained with anti-Pax2 antibody, which labels nuclei of mature hair cells (Riley et al., 1999). In *pax5* morphants, hair cells are produced normally in the utricular and saccular maculae at 24 hpf, but at later stages the number of utricular hair cells is consistently reduced by 20-30% relative to uninjected controls ($p<0.05$) (Fig. 3.5A-C). In contrast, the number of saccular hair cells is normal through at least 72 hpf (Fig. 3.5C). To confirm these results, we used two other markers to stain hair cell cilia, anti-acetylated tubulin and phalloidin. The number of utricular hair cells detected by phalloidin or acetylated tubulin-staining is slightly greater than Pax2-staining at all time points (Fig. 3.5G), probably because cilia form before high level accumulation of Pax2 in differentiating hair cells. However these markers confirmed a 20-30% decrease in utricular hair cells in *pax5* morphants (Fig. 3.5G). In the saccule, the number of Pax2-postivie cells does not change after 30 hpf (Fig. 3.5C), yet the number of hair cells

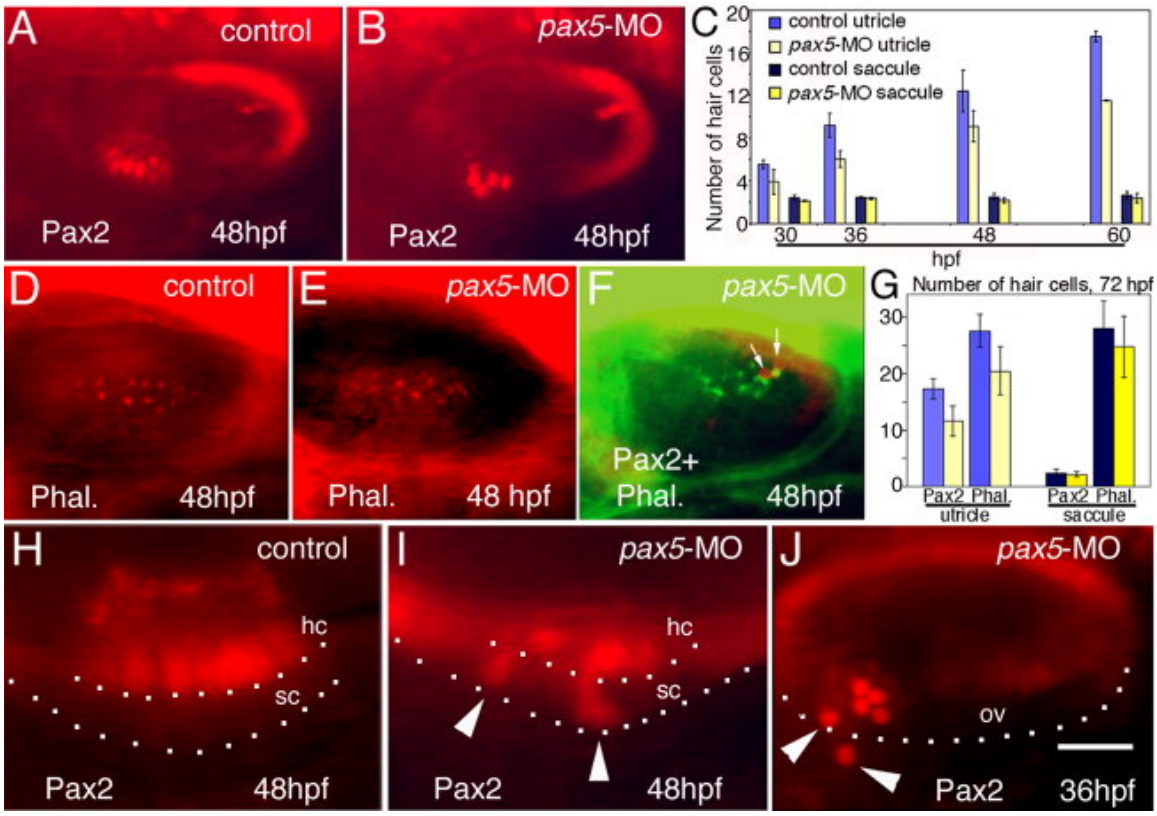

Figure 3.5. Assessment of hair cell development.
(A, B) Anti-Pax2 staining in the otic vesicle in a control embryo (A) and *pax5* morphant (B) at 48 hpf. (C) Number of Pax2+ hair cells at the indicated stages (means and standard errors of at least three experiments, with at least15 specimens/time-point/experiment). p-values for the comparison of control embryos vs. *pax5* morphants are: utricle, p=0.042 (30 hpf), p=0.009 (36 hpf), p=0.0007 (48 hpf), p=0.017 (60 hpf), saccule, p=0.136 (30 hpf), p=0.138 (36 hpf), p=0.05 (48 hpf), p=0.28 (60 hpf). (D, E) Rhodamine-phalloidin staining in the saccular macula of a control embryo (D) and *pax5* morphant (E) at 48 hpf. In control embryos (n=23), there were 21.5±5.0 hair cells in the utricular macula and 17.8±9.7 in the saccular macula. In *pax5* morphants (n=42), there were 16.8±4.5 hair cells in the utricle and 14.8±7.5 in the saccule. (F) Saccular maculae stained with anti-acetylated tubulin (green) and anti-Pax2 (red) in a *pax5* morphant at 48 hpf. Only two hair cells are Pax2-positive (arrows). (G) Hair cell numbers detected by anti-Pax2 or phalloidin staining in *pax5* morphants and uninjected controls at 72 hpf. Data bars are color-coded as in (C). (H, I) Enlarged view of the utricular macula stained with anti-Pax2 at 48 hpf in a control embryo (H) and *pax5* morphant (I). Basal edges of hair cell (hc) and supporting cell (sc) layers are indicated. (J) Otic vesicle of *pax5* morphant stained with anti-Pax2 at 36 hpf. Arrowheads mark misplaced hair cells. The ventral limit of the otic vesicle (ov) is indicated. Images show dorsolateral (A, B, D-F, J) and lateral (H, I) views with anterior to the left. Scale bar, 40µm (A,B, D-F), 12.5µm (H,I), 25µm (J).

detected by acetylated tubulin or phalloidin-staining increases steadily (Fig. 3.5D-G). At 72 hpf, for example, there are only 2-4 Pax2-positive cells in the saccule, whereas 28 ± 4.8 hair cells are detected by phalloidin-staining (Fig. 3.5G). We do not know the functional significance of the small number of Pax2-positive hair cells in the saccule but note that the pattern of Pax2-staining is similar to the pattern of *pax5* expression. In any case, the number of saccular hair cells in *pax5* morphants is not significantly different from the control (Fig. 3.5G). Thus, the deficiency of hair cells in *pax5* morphants is limited to the utricle.

Anti-Pax2 staining also demonstrates that *pax5* morphants have irregular arrangements of hair cells in utricular macula. In a variable fraction (22.9 ± 8.3%) of *pax5* morphants, one or two hair cell nuclei are localized in the basal supporting cell layer or even outside of the otic vesicle (Fig. 3.5I, J). Interestingly, misplaced hair cells are usually accompanied by the appearance of abnormal SAG processes (Fig. 3.4F). Ejection of hair cells undergoing apoptosis has been previously described in several species. In mouse and guinea pig, for example, apoptotic hair cells sink to the basal layer within the sensory epithelium (Sobkowicz et al., 1992; Sobkowicz et al., 1997; Quint et al., 1998). Similarly, hair cells in zebrafish *mind bomb* (*mib*) mutants begin to die after 36 hpf and are extruded from otic vesicle to the underlying mesenchyme (Haddon et al., 1998). Therefore, the reduced number and misplaced position of hair cells in *pax5* morphants could reflect elevated apoptosis.

***pax5* and cell death in the utricle**

To examine the pattern of cell death, embryos were stained with the vital dye acridine orange (AO). Control embryos show very little AO staining in the otic vesicle between 30 and 72 hpf (Fig. 3.6A). Summing the patterns of 30 embryos shows a "hot spot" of cell death near the anteromedial wall of the otic vesicle, although some of these cells may lie outside the otic vesicle (Fig. 3.6G). Staining in other regions is very sparse. Only 5.4 to 7.7% of control embryos (depending on the stage) show AO-positive cells in the utricle. The overall pattern of AO staining is very similar in *pax5* morphants, except that there are roughly five-fold more labeled cells in the utricular macula (Fig. 3.6G; 34 labeled cells in *pax5* morphants vs. 7 in control embryos). On average, 31.2 to 37.1% of *pax5* morphants (at 30 hpf and 48 hpf, respectively) show labeled cells in the utricular macula (Fig. 3.6B, E). Similarly, wholemount TUNEL assays show that 40% of *pax5* morphants have apoptotic cells in utricle at 48 hpf (Fig. 3.6C, D). The saccular macula shows little cell death in either uninjected embryos or *pax5* morphants (Fig. 3.6G), showing that *pax5*-depletion specifically affects the utricular macula. We hypothesized that dying cells seen in the utricle of *pax5* morphants correspond to misplaced hair cells. To test this, AO-stained embryos were photographed at 48 hpf to record positions of dying cells, then fixed and stained for Pax2. *pax5* morphants with no cell death show normal hair cell arrangements (n=14). In contrast, misplaced Pax2-positive hair cells were frequently detected in the corresponding position where AO positive cells had been detected (12 out of 19 embryos, Fig. 3.6E, F). The remainder of AO staining was detected in normally positioned hair cells in the utricular macula (3/19) or Pax2-negative

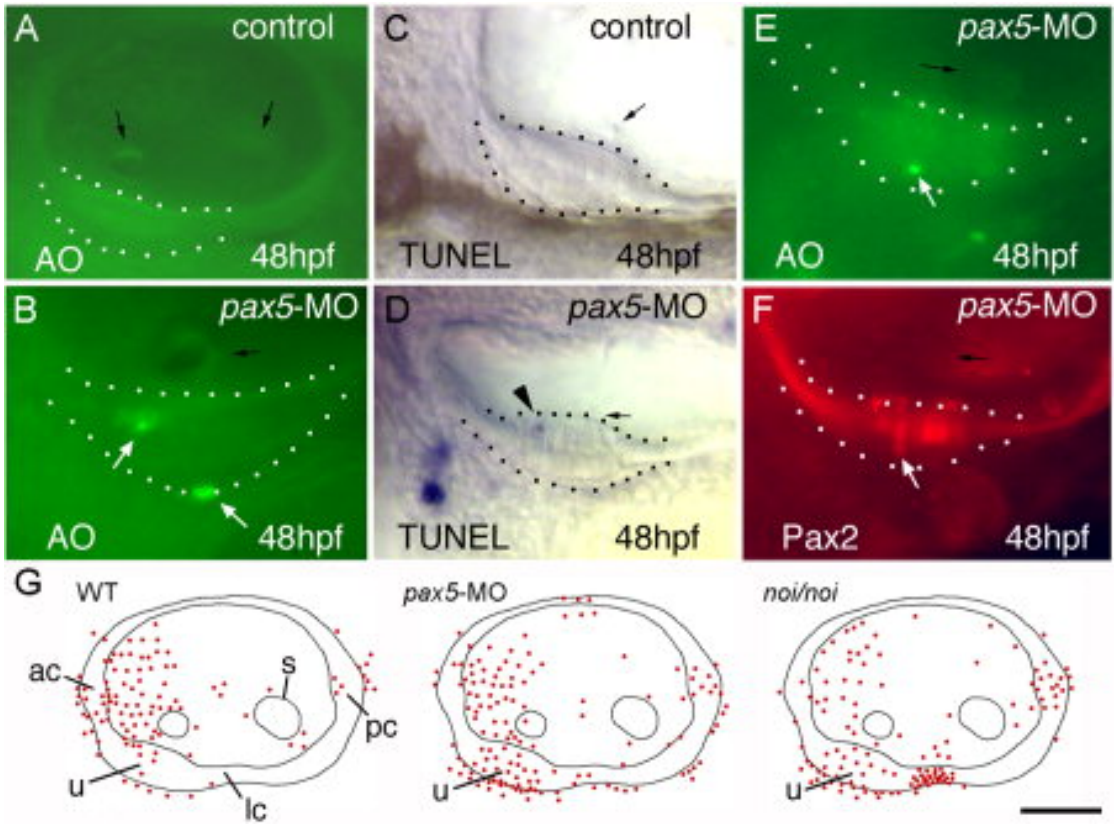

Figure 3.6. Analysis of cell death in *pax5* morphants.
(A, B) Acridine orange staining in the otic vesicle of a control embryo (A) and in the utricle of a *pax5* morphant (B) at 48 hpf. White arrows indicate AO-positive cells, black arrows show otoliths. (C, D) TUNEL staining in the utricle of a control embryo (C) and a *pax5* morphant (D) at 48 hpf. Arrowhead shows a TUNEL-positive cell (E). (E, F) A *pax5*-morphant stained with acridine orange at 48 hpf (E) and subsequently stained with anti-Pax2 (F). An AO-positive cell appears in the same position as a misplaced hair cell (white arrows). The utricular macula is outlined in (A-F). (G) Cumulative data (n=30) representing the frequency and distribution of AO-labeled cells in the otic vesicle of a wild-type control embryo, a *pax5* morphant and a *noi/noi* mutant at 48 hpf. The positions of labeled cells (red spots) were projected onto schematic maps of the otic vesicle. Positions of the utricular macula (u), saccular macula (s), anterior crista (ac), lateral crista (lc) and posterior crista (pc) are indicated. All images show lateral views, with anterior to the left. Scale bar, 40µm (A), 25µm (B-D), 30µm (E,F), 50 µm (G).

cells within the basal layer (presumptive support cells or nascent hair cells, 4/19) (data not shown). These data support the hypothesis that utricular hair cells in *pax5* morphants undergo an elevated rate of apoptosis and that dying hair cells are ejected from the utricular macula. Elevated AO staining persists through 3 dpf in *pax5* morphants but declines to normal by 4 dpf (not shown). This is probably reflects diminishing capacity of the injected morpholinos to knock down *pax5* function.

***pax5* mRNA rescues early defects in *pax5* morphants.**

To confirm specificity of gene knockdown by *pax5*-MO, we coinjected *pax5*-MO with *pax5*-v1 and *pax5*-v2 mRNAs to try to rescue *pax5* morphants. These mRNAs are impervious to splice-blocking MOs and when injected at high levels can overwhelm the effects of translation-blocking MOs. In control (non-morphant) embryos, misexpression of *pax5* has no effect on morphology. However, *pax5* mRNA restores hair cell numbers to normal in *pax5* morphants at 32 hpf ($p=0.47$, wild-type vs. rescued embryos, Table 2). The fraction of embryos showing cell death in the utricular macula (21.7%) is reduced to half of the level otherwise seen in *pax5* morphants, a significant difference ($p\leq0.032$). At 48 hpf, the effects of *pax5* mRNAs are less evident (Table 2). This is probably because injected RNAs rarely persist beyond 24 to 30 hpf, whereas morpholinos often continue to function for at least 3 days. The ability to rescue balance and coordination could not be evaluated due to the limited stability of injected mRNA. However, the finding that *pax5* mRNA rescues early defects in the *pax5* morphants validates the specificity of *pax5*-MO.

Distinct roles for *pax2a* and *fgf3* in regulating *pax5* and vestibular function

Previous studies identified *pax2a* and *fgf3* as upstream regulators of *pax5*. Knocking down *fgf3* by morpholino injection diminishes expression of *pax5* in the ear (Kwak et al., 2002). *noi* (*pax2a*) null mutants show a complete loss of *pax5* expression in the ear (Pfeffer et al., 1998; and Fig. 3.7A). Therefore, we speculated that these mutants might display defects similar to those of *pax5* morphants.

noi mutants initially produce more hair cells than normal due to weakened lateral inhibition (Riley et al 1999). Thus, *noi* mutants produce an average of 6.0 ± 0.8 utricular hair cells by 30 hpf, compared to 4.9 ± 0.8 in the wild-type. However, *noi* mutants later show a deficit of utricular hair cells similar to that seen in *pax5* morphants: At 48 hpf, *noi* mutants have 16 ± 3.4 utricular hair cells (n=29), a 27% decrease compared to the wild-type (22 ± 2.7 hair cells, n=22) (Fig. 3.7I, J). Moreover, about 35% of *noi* mutants show dying cells in the utricular macula at 48 hpf (Fig. 3.7C). Summing data from 30 *noi* mutants shows nearly a four-fold increase in the number of AO stained cells in the utricular macula (Fig. 3.6G; 26 labeled cells in *noi/noi* vs. 7 in +/+ embryos). *noi* mutants also show elevated cell death in primordia of the posterior and lateral cristae (Fig. 3.6G). TUNEL assays give similar results (Fig. 3.7D). SAG projections to the utricular macula are difficult to discern and, when present, are highly disorganized (data not shown). SAG projections to the hindbrain are also disorganized (Fig. 3.7B). Since the morphology of *noi* mutants is severely altered and embryos begin to die by 3 dpf, balance and coordination cannot be tested. Thus there are a number of similarities

Table 2. Rescue of *pax5* morphants by *pax5* mRNA injection.

		Control	pax5-MO	pax5-MO +pax5 RNA	pax5 RNA
Number of hair cells in the utricular macula†	32 hpf	**100** % 6.8 ± 0.8 (n=92)	**79.5** % 5.4 ± 0.4 (n=90) *p=0.008	**101.5** % 6.9 ± 0.7 (n=35) *p=0.474 ‡p=0.013	**107.4** % 7.3 ± 0.7 (n=48) *p=0.254
	48 hpf	**100** % 14.6 ± 1.1 (n=30)	**70.5** % 10.3 ± 0.7 (n=28) *p=0.023	**79.5** % 11.6 ± 0.8 (n=19) *p=0.045 ‡p=0.118	not determined
Number of hair cells in the saccular macula†	32 hpf	**100** % 2.3 ± 0.3 (n=92)	**100** % 2.3 ± 0.2 (n=90) *p=0.492	**100** % 2.3 ± 0.1 (n=35) *p=0.434 ‡p=0.242	**100** % 2.3 ± 0.3 (n=48) *p=0.493
	48 hpf	**100** % 2.1 ± 0.1 (n=30)	**104.8** % 2.2 ± 0.3 (n=28) *p=0.386	**95.2** % 2.0 ± 0.2 (n=19) *p=0.242 ‡p=0.242	not determined
Percentage of embryos with AO-positive cells in the utricular macula ††	32 hpf	**5.4** % ± 1.77 (n=39)	**37.1** % ± 4.91 (n=59)	**21.7** % ± 10.9 (n=50) ‡p=0.032	**4.0** % (n=35)
	48 hpf	**7.7** % (n=13)	**31.2** % ± 11.4 (n=44)	**26.2** % ± 4.5 (n=52) ‡p=0.268	not determined

† Based on the number of Pax2-positive hair cells; mean of 2-3 experiments ± standard error (n=total number of embryos examined). Percentages in boldface reflect values relative to the control.

†† Mean (± standard error) of 2 experiments, except for 48 hpf control and 32 hpf mRNA-injection, which are means of one experiment each.

p-values are based on T-tests in comparison with control (*) or with *pax5* morphants (‡).

between *noi* mutants and *pax5* morphants, but *noi* mutants have a wider range of defects. This is probably because *noi* mutants lack expression of *pax5* as well as numerous other down stream genes.

A null mutation in *fgf3*, *lim absent* (*lia*) was recently identified (Wiebke et al., 2004). Consistent with the results of *fgf3*-MO injection (Kwak et al., 2002), *lia* mutants display decreased *pax5* expression in the otic vesicle (Fig. 3.7E) and in some cases, *pax5* transcripts are almost ablated (Fig. 3.7F). *lia* mutants produce fewer hair cells in the utricular macula (2.6 ± 0.5, 30 hpf, n=11) than wild-type (5 ± 0.6, 30 hpf, n=38) (Fig. 3.7K, L). Projections of SAG neurons to the hindbrain are similar to wild-type (Fig. 3.4, Table 1). Despite having strongly reduced *pax5* expression, *lia* mutants do not show increased cell death in the utricular macula (Fig. 3.7G, H) or misplaced hair cells (data not shown), and SAG projection patterns in the utricle are normal. The reduced number of hair cells in *lia* probably reflects a reduced rate of production, as Fgf3 is implicated in hair cell specification (Kwak et al., 2002). Vestibular function is more severely impaired in *lia* mutants than *pax5* morphants (Fig. 3.2). However, we note that utricular and saccular otoliths fuse in *lia* mutants by 48 hpf. Combined with the reduced number of utricular hair cells, the late stage otolith defects are likely to contribute to the severe vestibular deficits in *lia* mutants. Thus, loss of *fgf3* perturbs vestibular function by a mechanism distinct from that seen in *noi* mutants and *pax5* morphants. The implications of these findings are discussed below.

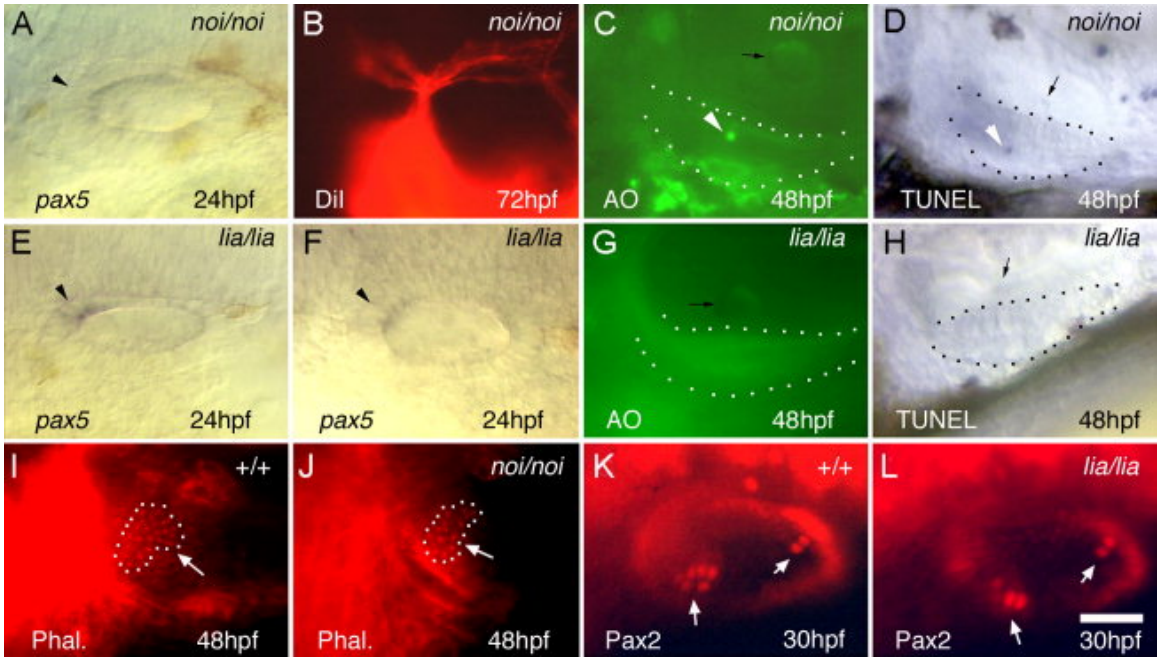

Figure 3.7. Otic development in *noi* (*pax2a*) and *lia* (*fgf3)* mutants.
Otic expression of *pax5* in *noi/noi* (A) and *lia/lia* (E,F) mutants at 24 hpf. Arrowheads mark the *pax5* expression domain. (B) SAG projections in a *noi/noi* mutant labeled by injecting DiI into the utricular macula at 72 hpf. (C, G) Acridine orange staining in *noi/noi* (C) and *lia/lia* (G) mutants at 48 hpf. (D, H) TUNEL staining in *noi/noi* (D) and *lia/lia* (H) mutants at 48 hpf. White arrowheads indicate apoptotic cells (C, D) and black arrows mark otoliths. Utricular maculae are outlined in (c, D, G, H). (I, J) Rhodamine-phalloidin labeling of the utricular macula (outlined) in wild-type (I) and *noi/noi* (J) embryos at 48 hpf. (K, L) Anti-Pax2 staining of the otic vesicle in wild-type (K) and *lia/lia* (L) embryos at 30 hpf. White arrows indicate hair cell patches (I-L). Images show dorsolateral (A, B, E, F, I-L) and lateral (C, D, G, H) views, with anterior to the left. Scale bar, 30µm (A, E, F, K, L), 50µm (B), 25µm (C, D, G, H, I, J).

DISCUSSION

In this report, we have shown that *pax5* regulates the maintenance and function of the utricular macula, which is essential for vestibular function during larval development (Riley and Moorman, 2000). In *pax5* morphants, utricular hair cells appear to form normally but begin to die by 30 hpf, resulting in variable disorganization of the macula.

There is not a wholesale loss of hair cells, possibly because of ongoing developmental expansion of the macula or regeneration of lost hair cells. In addition, it is likely that the phenotype is ameliorated by loss of *pax5*-MO activity during later stages of development, as suggested by a return to normal rates of cell death by 4 dpf. Globally misexpressing *pax5* rescues early cell death in the utricular macula of *pax5* morphants, resulting in restoration of utricular hair cell number. Together, these data suggest that *pax5* regulates maintenance rather than formation of hair cells, and its function specifically affects the utricular macula. In addition, *pax5* morphants show variable defects in the pattern of SAG processes in the utricle, the severity of which correlates with the degree of hair cell disorganization and death. It seems likely that SAG mispatterning is a secondary consequence of hair cell loss. Together, these changes in utricular architecture seem sufficient to explain the disruption of vestibular function seen in *pax5* morphants.

Some of the above defects could also reflect changes in support cells, which are thought to be necessary for hair cell survival (Haddon et al., 1998). However, there are no substantial deficits in support cells based on the morphology of the sensory epithelia in *pax5* morphants. In addition, about 80% of the dying cells detected in the utricle by AO staining appear to be Pax2-postive hair cells. The remainder are Pax2-negative cells in the basal layer of the utricular sensory epithelium. These could be either newly specified hair cells in the earliest stages of differentiation or support cells (for which there are no markers in zebrafish). For now the involvement of support cells remains an open question.

How *pax5* functions is not yet clear. The early expression of *pax5* in the utricular primordium suggests that it might regulate an essential aspect of early differentiation, without which cells later die. A similar cell death phenotype is seen in *noi* (*pax2a*) mutants (Fig. 3.6). Since *pax2a* is required for expression of *pax5* in the ear (Pfeffer et al., 1998; Fig. 3.7A), the effect of *noi* on cell survival in the utricle could be mediated specifically by loss of *pax5* expression. Alternatively, because *pax2a* and *pax5* are likely to be partially redundant (Bouchard et al., 2000) *pax5* might serve to supplement *pax2a* in promoting hair cell survival in the utricle. In either case, these findings raise the question of why utricular hair cells alone require *pax5* for survival. Presumably the basic ground plan of the sensory epithelium can be modified by specific combinations of multiple factors (combinatorial codes), possibly including Pax5, that confer unique properties and requirement to the utricular macula.

The importance of a combinatorial code is also suggested by the phenotype of *lia* (*fgf3*) mutants. *lia* mutants show strong reduction in *pax5* expression yet do not show cell death or SAG mispatterning in the utricle. This shows that cell death is not an inescapable consequence of reducing *pax5* function in the utricle. Fgf3 presumably regulates other genes that could influence utricular development in conjunction with *pax5*. Indeed, Fgf3 is required to block expression of the posterior marker, *zp23*, in the utricular macula, consistent with a general role for Fgf3 in specifying anterior identity (Kwak et al., 2002). Based on the general morphology of the utricular macula and its SAG projections, *lia* mutants do not show a wholesale conversion of the utricle into a saccule. However, partial readjustment of the combinatorial code in *lia* (e.g. loss of

pax5, ectopic expression of *zp23*) could subtly alter regional identity, thereby making hair cell survival independent of *pax5*.

In mouse, several other genes have been shown to differentially regulate survival of hair cells in different regions. *Brn-3c* is required for the survival of hair cells in all epithelia, although auditory hair cells are affected more severely (Xiang et al., 1998). In a gene expression profiling experiment, *Gfi1* was identified as a downstream target of *Brn-3c* (Hertzano et al., 2004). Although *Gfi1* is expressed in all hair cells, ablation of this gene causes cell death only in cochlear hair cells (Wallis et al., 2003). The cochlear phenotype of $Gfi1^{-/-}$ mutants is very similar to that of $Brn\text{-}3c^{-/-}$ mutants implying that *Brn-3c* regulates maintenance of cochlear hair cells through *Gfi1* function. The fact that *Gfi1* is dispensable for hair cell survival in other sensory patches again suggests that each region is regulated by a specific combination of differentiation and maintenance factors.

Pax2 and *Pax5* functions in other vertebrates

In mouse and chick, the expression and function of *Pax2* have been studied most extensively in the cochlea, although it is also expressed in hair cells in other sensory epithelia (Lawoko-Kerali et al., 2002; Burton et al., 2004; Li et al., 2004a; Sanchez-Calderon et al., 2005). However, its role in hair cell maintenance per se cannot be addressed in the cochlea of *Pax2* null mice because of severe agenesis of this region. The sensory epithelia that do form (utricular macula and cristae) have not been examined

in sufficient detail to determine whether there are defects in hair cell patterning or survival.

Pax5 expression in the otic vesicle has been reported in *Xenopus* (Heller and Brandli, 1999) and recent gene expression profiling data for the chick ear indicate *Pax5* expression in the adult utricle and cochlea (http://hg.wustl.edu/lovett/projects/nohr/inner_ear_ratio.html). In contrast, *Pax5* is not detected in the mouse ear during embryonic development, and *Pax5* null mice have no obvious defects in hearing or balance (Urbanek et al., 1994). It is possible that mouse represents a derived state where in *Pax5* is no longer utilized in otic development.

The pattern of utricular SAG projections

DiI injections into the utricle revealed two patterns of central projections of the SAG, type-1 with discretely organized ascending and descending branches in the hindbrain, and type-2 with diffuse primary branches and several smaller secondary branches. These patterns are independent of age through 7 dpf and do not require vestibular activity, as shown by analysis of *pax5* morphants and *mnl* and *lia* mutants. Variation in neural patterning is often seen during early development and is later corrected by pruning (reviewed by Maklad and Fritzsch, 2003). It therefore seems likely that the type-2 pattern eventually resolves into a more cohesive pattern. Nevertheless it is remarkable that vestibular activity and motor coordination are so effectively integrated in young larvae despite variation in SAG projection patterns.

A fundamental question remaining is how SAG neurons make connections between a given sensory epithelium to the appropriate processing center in the brain. A recent study by Satoh and Fekete (2005) showed that neuroblasts from one region of the ear often innervate sensory patches in another. This suggests that SAG targeting can be regulated after neuroblasts delaminate from the vesicle. For example, SAG neurons might project randomly to different sensory patches, after which regional signals from the sensory patch program the neuron to make appropriate central projections. Changes in the utricle caused by disruption of *pax5* or *fgf3* did not affect central projections, but *noi* mutants showed severely distorted central projections. At present it is not clear whether this reflects changes in otic vesicle or hindbrain. Further analysis of *noi* and other zebrafish mutants could help resolve this issue.

CHAPTER IV

SPATIAL AND TEMPORAL GRADIENT OF FGF CONTROLS DISCRETE STAGES OF STATOACOUSTIC GANGLION DEVELOPMENT IN THE ZEBRAFISH INNER EAR

INTRODUCTION

Sensory neurons of the VIIIth cranial ganglion, statoacoustic ganglion (SAG), innervate hair cells in the sensory epithelia. These bipolar neurons relay auditory (hearing) and vestibular (balance) sensory information to the hindbrain. SAG precursor cells, called neuroblasts, are specified in the otic floor by *neurogenin1* (*neurog1*), a bHLH factor homologous to *atoh1*. Loss of *neurog1* leads to a complete loss of SAG neurons (Ma et al., 1998, Ma et al., 2000; Andermann et al., 2002). In zebrafish, neuroblasts are first specified during placodal stages adjacent to the nascent sensory epithelium, utricular macula (Haddon and Lewis, 1996; Andermann et al., 2002; Radosevic et al., 2011). These neuroblasts leave the otic floor in a process called delamination from the anterolateral margin of the vesicle and from the middle of the floor more posteriorly until 42 hpf (Haddon and Lewis, 1996). Expression of *neurog1* is transient in the precursors and is followed by strong upregulation of neuronal differentiation bHLH gene *neurod* (Korzh et al., 1998, Andermann et al., 2002). Delta-Notch signaling regulates the number of cells committed into entering neuronal differentiation via lateral inhibition. Members of Notch signaling pathway are expressed in the neurogenic domain of the otic

vesicle and disruption of Notch signaling in zebrafish *mindbomb* mutant or in chick by blocking Notch intracellular cleavage leads to excess sensory neuronal precursors (Adam et al., 1998; Haddon et al., 1998; Alsina et al., 2004; Abello et al., 2007).

In chick and mouse, neuroblasts undergo a brief phase of proliferation to expand the precursor population (D'Amico-Martel, 1982; Begbie et al., 2002; Alsina et al., 2003; Matei et al., 2005). This stage of transit-amplification is characterized by the expression of *neurod* and proliferation markers (Camerero et al., 2003). Mitotic cells are observed in the SAG well after delamination has ceased in chick (D'Amico-Martel, 1982). Following proliferation, neuroblasts exit the cell cycle and differentiate into bipolar neurons that innervate hair cells in the sensory epithelia and processing centers in the hindbrain. Maturing SAG neurons in zebrafish express LIM domain/homeodomain transcription factors Islet-1/2 (Korzh et al., 1993; Inoue et al., 1994; Haddon et al., 1998).

Several studies have implicated the role of Fgf signaling at different stages of otic neurogenesis. Fgf10 is expressed in the prospective neurosensory domain of the otic placode and has been shown to promote neuronal determination in chick (Alsina et al., 2004). Fgf2 and 8 expressed in chick otic placode increases the number of migrating and differentiating SAG neurons (Hossain et al., 1996; Adamska et al., 2001). In zebrafish, *fgf3/8* are detected in the hindbrain (rhombomere 4) and by 18 hpf they are expressed in the nascent sensory epithelium (Leger and Brand, 2002; Millimaki et al., 2007). Both *fgf3/8* have been shown to affect SAG development. Expansion of *fgf3* into the posterior segments of the hindbrain in *vhnf1* mutants results in posterior extension of

neurogenic domain (Lecaudey et al., 2007). Loss of Fgf3/8 function in mutants and morphants shows a reduction in SAG markers (Adamska et al., 2000; Leger and Brand, 2002). Because of the importance of Fgfs in otic induction, defects in ear morphogenesis are often associated with SAG defects thus making it difficult to deduce the role of Fgf in otic neurogenesis per se.

Here we study the development of SAG and its regulation by Fgf. We show that Fgf signaling controls each stage of otic neurogenesis by conditionally manipulating Fgf levels. Fgf is necessary for the initial specification of neuroblasts in the otic floor and moderate to low level of Fgf from the adjacent utricle promotes this phase. As SAG development continues, mature neurons express *fgf5* causing an increase in the overall level of Fgf. This serves two roles. First, upon accumulation of sufficient mature neurons the phase of specification is terminated. Second, elevated Fgf signaling stabilizes the transit-amplifying population and delays the differentiation of SAG precursor cells. Thus, a spatial and temporal gradient of Fgf ensures production of the appropriate number of precursors and prevents overproduction of mature neurons.

MATERIALS AND METHODS

Fish strains, misexpression and inhibitor treatment

Wild-type zebrafish strains were derived from the AB line (Eugene OR). The following transgenic lines were used in this study- *Tg(hsp70:fgf8)*^{x17} (Millimaki et al., 2010), *Tg(hsp70I:dnfgfr1-EGFP)pd1* (Lee et al., 2005) and *Tg(-17.6isl2b:GFP)zc7* (Pittman et al., 2008). Embryos were maintained at 28^{o}C, unless otherwise stated, and staged

according to standard protocol (Kimmel et al., 1995). PTU, 1-phenyl 2-thiourea, (0.3mg/ml, Sigma) was added to fish water to prevent melanin formation. For misexpression experiments, embryos were incubated in a re-circulating water bath at specific temperatures and time points described in the results. To block Fgf signaling, embryos were treated in their chorions with SU5402 (Tocris Bioscience) diluted from a 20mM stock in DMSO.

Morpholino injection and RT-PCR

A splice-blocking morpholino targeting intron1-exon2 (I1E2) boundary, 5'-TTTCTCTATCTAGGTGTGC TGGAGC-3' was designed to knock down *fgf5* function. Approximately 5ng morpholino was injected per embryo at one-cell stage. The efficacy of this morpholino was assessed by RT-PCR with primers- P1 (forward), 5'-TCGATGGAAGAGTCAACGGGAGC-3' and P2 (reverse) 5'-GCCTTCCCCTCTTGTTCATGGC-3'. For control *ornithine decarboxylase* (*odc*) was used. Uninjected embryos from the same genetic background were used as controls.

In situ hybridization

Whole-mount in situ hybridization was carried out with methods described previously (Jowett and Yan, 1996). A shorter riboprobe was synthesized for *neurog1* using T7 RNA polymerase to address non-specific binding in *Tg(-17.6isl2b:GFP)zc7* line at sites of *gfp* expression. The in situ hybridization protocol was modified for *fgf5* riboprobe to reduce background. Pre-hybridization was performed at 70^{o}C for 12 hours instead of 67^{o}C for 2

hours. Similarly, hybridization step was done at 70^{o}C and lasted 24 hours instead of 16 hours. Washes on day 2 were as described in Moens, C., (2008).

Immunostaining

Antibody staining was performed as described previously (Riley et al., 1999). Primary antibodies were as follows: anti-Islet1/2 (Developmental Studies Hybridoma Bank 39.4D5, 1:100 for whole-mount, 1:250 for cryosections) and anti-BrdU (Beckton-Dickinson, 1:300). Secondary antibodies were as follows: HRP-conjugated goat anti-mouse IgG (Vector Labs PI-2000, 1:200) and Alexa 546 goat anti-mouse IgG (Invitrogen A-11003, 1: 250).

Cryosectioning and BrdU labeling

Fixed embryos were washed thrice for 5 min each in 1x PBS and then soaked in 20% sucrose solution made in PBS followed by 30% sucrose until they sunk to the bottom of a microcentrifuge tube. Embryos were embedded in tissue freezing medium (Triangle Biomedical Sciences, TFM-C), transverse sections were cut at 10μm thickness using a cryostat and immunostained. Finally, slides were washed twice in 1x PBS and mounted in ProLong Gold (Invitrogen) with a coverslip. For double labeling, whole-mount in situ hybridization was performed first followed by immunostaining on cryosections.

For BrdU labeling, dechorionated embryos were incubated in fish water containing 10mM BrdU in 1% DMSO for the indicated duration. Embryos were rinsed twice for 5 minutes each in fish water prior to fixation. For older stages (96 hpf) 2nl of

10mM BrdU/1% DMSO solution with 3% filtered green food coloring was injected into the brain ventricle of larvae anesthetized in Tricaine (Sigma). Embryos were first processed by whole-mount in situ hybridization for *neurod* and then cryosectioned. Slides were washed thrice for 5 minutes each in PBT (with 0.1% Triton) and incubated in 2N HCl for 45 minutes at 37^{o}C. Slides were rinsed in PBT again, incubated in blocking solution (with 1% Triton for 36 hpf and 3% Triton for 102 hpf) for 2 hours and stained for BrdU.

Laser ablation

Maturing SAG neurons were ablated using a MicroPoint laser, under 40x objective, in *isl2b:GFP* transgenic line that labels this population of cells. Anesthetized embryos were mounted in a dorsolateral orientation beneath a #1 coverslip on a bridge slide made by stacking two #1 coverslips on either side of the embryo. Single round of ablations resulted in only 50% loss of Isl1-positive population possibly because neighboring cells in the GFP domain were photo-bleached during ablation. GFP fluorescence recovers within 1-2 hours. Serial ablation 2-3 hours after the first round results in approximately 90% decrease in Isl1^{+} cell number (data not shown).

RESULTS

Development of the statoacoustic ganglion (SAG)

Otic neurogenesis is a sequential process involving specification, delamination, proliferative expansion and differentiation of precursor cells resulting in the formation of

the SAG (Alsina et al., 2003; Sanchez-Calderon et al., 2007b) as illustrated in figure 4.1A. In zebrafish, neuronal precursors (neuroblasts) are specified in the floor of the otic placode as early as 16 hpf and express *neurog1* (Andermann, 2002; Radosevic et al., 2011). Cells from the anterolateral margin of the vesicle and from the middle of the otic floor more posteriorly delaminate between 17 hpf and 42 hpf in zebrafish (Fig. 4.1C). Delamination begins to slow down after 30 hpf (this study and Haddon and Lewis, 1996). *neurog1* is only transiently expressed in precursors, followed by upregulation of a neuronal differentiation gene, *neurod* (Liu et al., 2000; Andermann et al., 2002). In chick and mouse embryos, neuroblasts proliferate briefly to expand the neural population (D'Amico-Martel, 1982; Begbie et al., 2002; Alsina et al., 2003; Fritzsch et al., 2006). Cells then begin to exit cell cycle and differentiate into mature neurons. In zebrafish, neuroblasts undergo a similar transit-amplification phase as seen by co-expression of *neurod* and cell proliferation marker BrdU (Fig. 4.1D). The presence of a transit-amplifying population explains why neuronal population in the SAG continues to expand at least through 72 hpf although delamination ends at around 42 hpf (Fig. 4.1B). *neurod*-positive precursor cells continue to proliferate even at 4 days post fertilization (dpf) (Fig. 4.1E). As precursor cells exit the cell cycle, they begin to differentiate and express Islet-1 (Isl1) (Fig. 4.1B, F and Haddon et al., 1998; Khorzh et al., 1998). The most mature neurons lose *neurod* expression and are located proximal to the vesicle, plastered against the ventromedial edge of the ear, while the *neurod*-expressing cells undergoing transit-amplification reside more distally (Fig. 4.1I, J). These cell

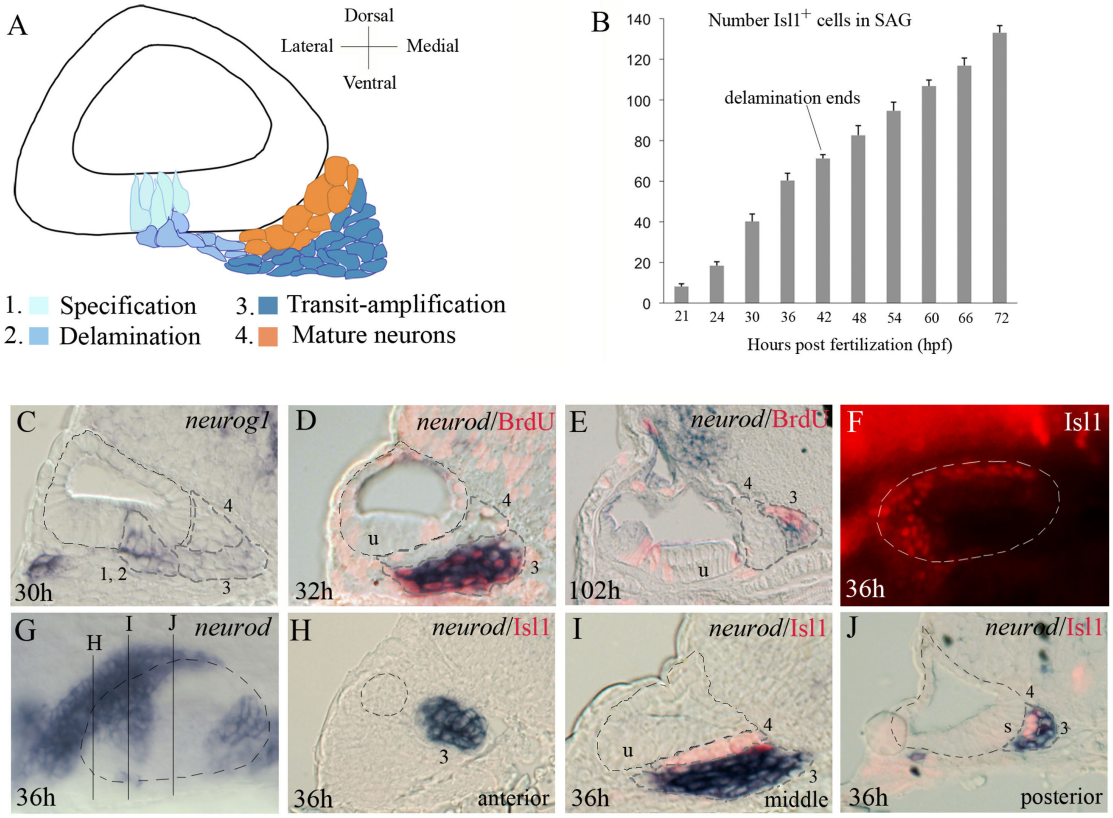

Figure 4.1. Development of statoacoustic ganglion (SAG).
(A) Illustration showing the various stages of SAG development. Neuronal precursors (neuroblasts) that are specified (1) in the otic floor delaminate (2) and accumulate ventromedially between the otic vesicle and hindbrain. They undergo a phase of transit-amplification (3) where they proliferate and eventually differentiate into mature neurons (4). (B) Number of Islet-1-positive mature SAG neurons at indicated stages (mean of total number ± standard deviation, n=20 for each timepoint). (C) *neurog1* expression at 30 hpf. (D-E) Co-expression of *neurod* (blue) and BrdU (red) in embryos exposed to BrdU for 6 hours starting at 26 hpf (D) and 96 hpf (E). (F-J) Expression of *neurod* (blue) and Islet-1 (red) at 36 hpf. Mature neurons are labeled with Islet-1 (F) and precursor cells express *neurod* (G). (H-J) Sections showing co-expression of *neurod* and Islet-1 at regions indicated in (G). All embryos are wild-type. The otic vesicle is outlined in black. Regions representing the different stages of SAG development are demarcated in grey and numbered accordingly. Transverse sections are at the level of anterior (C-E, I) and posterior (J) sensory epithelium indicated by u, utricular and s, saccular maculae. Images of whole-mount specimens (F, G) are dorsolateral (F) and dorsal (G) views with anterior to the left. Images of transverse sections (C-E, H-J) show dorsal to the top and lateral to the left.

populations also show a dynamic spatial distribution along the anterior-posterior axis of the developing SAG: the anterior most region is occupied by *neurod*$^{+}$ precursors followed by a region of *neurod*$^{+}$ and Isl1^{+} cells in the middle that extends mediolaterally, and the posterior region that is narrow and strictly medial (Fig. 4.1H, I, J, respectively and 4.1G). Upon differentiation, Isl1^{+} neurons project dendrites to hair cells in peripheral sensory endorgans, and axons to central targets in the hindbrain.

Fgf regulates neuroblast specification at early and late stages

Several Fgfs expressed in tissues near the developing SAG have been implicated in establishing a neurogenic domain in the ear (reviewed in Wright and Mansour, 2003). In zebrafish, Fgf3/8 are expressed in hindbrain segments adjacent to the otic placode and in the nascent maculae (sensory epithelium) starting at 18 hpf. We hypothesize that high levels of Fgf signaling in the sensory epithelium promotes sensory development whereas lower levels of Fgf specify the neurogenic domain in adjacent otic epithelium. Knockdown of Fgf3/8 in mutants and morphants results in a smaller SAG. However, these embryos also exhibit a smaller otic vesicle and defects in sensory epithelia (Leger and Brand, 2002). To bypass the early requirements of Fgf during otic induction we used a chemical inhibitor, SU5402, to inhibit signaling at later stages of development. Embryos treated with 100μM SU5402 from 14 hpf -18 hpf showed a strong reduction in *neurog1* expression domain (Fig. 4.2A, B). These embryos show severe necrosis within 12 hours of treatment because of ongoing dependence on Fgf for proper embryonic development and this precludes analysis of Isl1 numbers at later stages. Loss of Fgf

signaling at 14 hpf using heat shock-inducible *hs:dnfgfr1* transgenic line activated at 38^{o}C for 30 minutes showed similar results albeit to a lesser extent (Fig. 4.2C). These data confirm that initial specification of the neurogenic domain depends on Fgf signaling. To test our hypothesis that cells in the otic floor that are specified to become neuroblasts respond to a specific low level Fgf signaling we used a heat shock-inducible transgenic line, *hs:fgf8* (Millimaki et al., 2010). To provide a broad shelf of low Fgf sgnaling we misexpressed *hs:fgf8* at a low temperature (35^{o}C, 6 hours) for a prolonged period of time at 18 hpf. As a result a marked expansion in *neurog1* expression domain was observed (Fig. 4.2D-E). There is a subsequent increase in delaminating neuroblasts as seen by *hmx3* expressing cells leaving the vesicle (Fig. 4.2F-G) and in the number of Isl1^{+} cells in the mature SAG (Fig. 4.2H, an average of 63.44 ± 5.98 Isl1^{+} cells were present in the SAG of control embryos compared to 86 ± 3.6 in *hs:fgf8* transgenic embryos, n=15). To evaluate the effects of high level Fgf, *hs:fgf8* embryos were maximally activated (39^{o}C, 30 minutes). Elevated Fgf signaling is inhibitory to SAG development (Fig. 4.2H, an average of 51.2 ± 4.16 Isl1^{+} cells in the SAG, n=15). *neurog1* expression is reduced briefly following heat shock but recovers by 24 hpf (data not shown). These data support the idea that Fgf acts as a morphogen and lower levels promote and higher levels inhibit neuronal precursor specification.

We next examined the effects of Fgf on specification at later stages of development. Misexpression of *hs:fgf8* at 24 hpf resulted in a reduced *neurog1* expression domain at 30 hpf following activation at either 39^{o}C for 30 minutes (Fig.

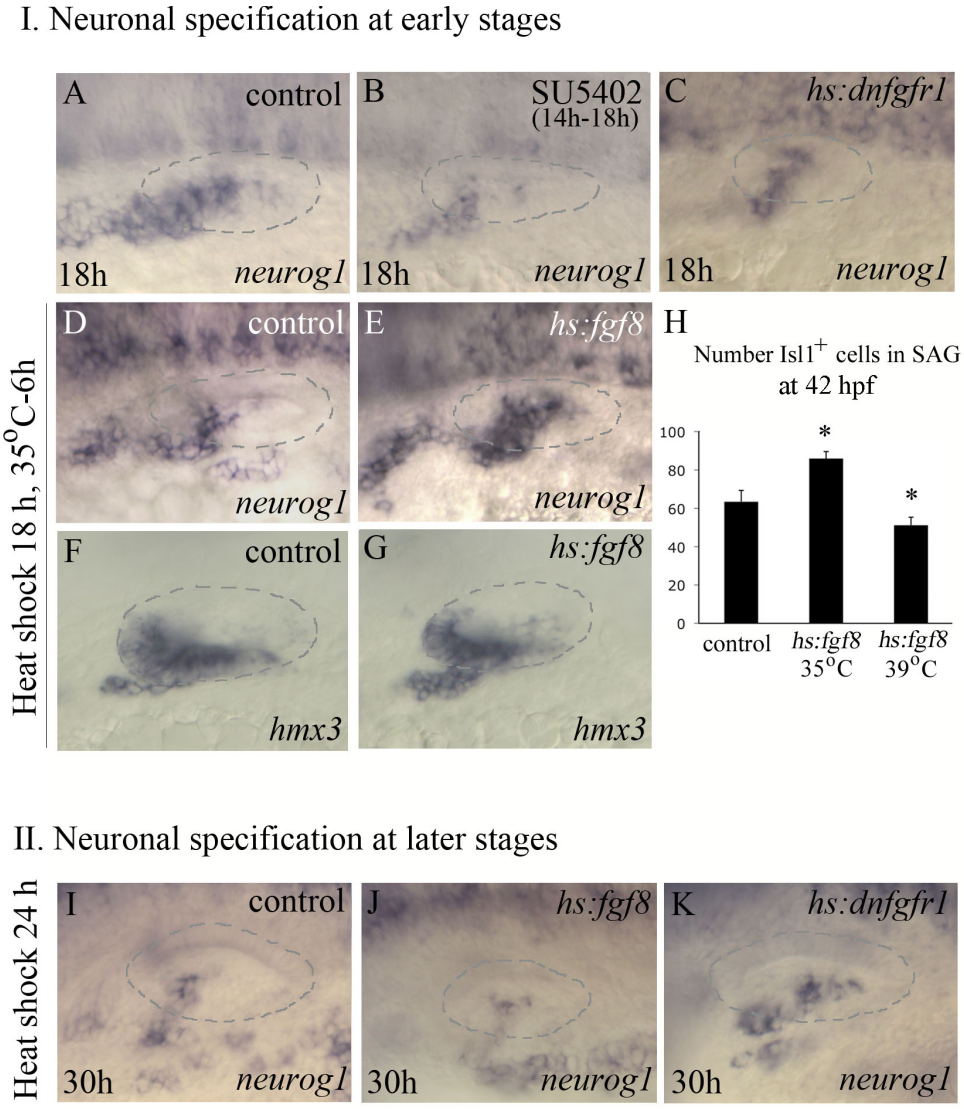

Figure 4.2. Fgf regulates neuroblast specification.
(A-C) *neurog1* expression at 18 hpf in a control (A), SU5402 inhibitor treated (B) and *hs:dnfgfr1* transgenic embryo heat shocked at 14 hpf. (D-G) Expression of *neurog1* (D-E) and *hmx3* (F-G) in control and *hs:fgf8* embryos heat shocked at 18 hpf at 35°C for 6 hours to activate prolonged low level Fgf and fixed immediately. (H) Number of Islet-1-positive cells in the SAG (mean of total number ± standard deviation) at 42 hpf following heat shock activation of *hs:fgf8* at 18 hpf at indicated temperatures. *$p < 0.001$ in comparison to control, analyzed with Student's *t* test. (I-K) *neurog1* expression at 30 hpf following heat shock at 24 hpf in a control embryo (I), *hs:fgf8* embryo heat shocked at 39°C for 30 minutes to strongly over-express Fgf (J) and *hs:dnfgfr1* embryo heat shocked for 2 hours at 35°C and then incubated at 33°C instead of 28.5°C to maintain low level inhibition of Fgf signaling (K). Otic vesicle is outlined in grey. Images show dorsolateral views with anterior to the left.

4.2H, I) or 35^{o}C for 6 hours (data not shown). In keeping with the requirement of Fgf for neuroblast specification, full activation of *hs:dnfgfr1* diminished *neurog1* expression (data not shown). However, weak attenuation of Fgf signaling by activating *hs:dnfgfr1* at a low level, 35^{o}C for 2 hours followed by incubation at 33^{o}C, expanded the *neurog1* expression domain at 30 hpf (Fig. 4.2J). Overall these data suggest that a moderate dose of Fgf promotes neuroblast specification at both early and later stages, and complete blockage of Fgf signaling impairs this process. At later stages, however, the process of specification becomes increasingly sensitive to inhibition by Fgf. This indicates that either otic cells respond more efficiently to Fgf or that the overall level of Fgf increases during development. The latter possibility proved to be correct as described below.

***fgf5* from mature neurons inhibits neuroblast specification**

Our data suggest that SAG specification becomes more sensitive to inhibition by Fgf as development progresses. We speculated that this is because local Fgf levels increase during normal neuroblast development. We therefore surveyed expression of all known *fgf* genes and identified f*gf5* as a strong candidate for a feedback regulator of SAG development. Fgf5, is a member of the Fgf1 superfamily, is expressed in the mouse acoustic ganglion between E12.5 and E14.5 (Goldfarb et al., 1991), however, its function in this context is not known. In zebrafish, *fgf5* is expressed in the SAG (Fig. 4.3A-C) and in other cranial ganglia including trigeminal (V), facial (VII) and vagus (X) (data not shown). *fgf5* mRNA was detected as early as 20 hpf in a small population of

recently delaminated neuroblasts (data not shown). By 24 hpf, expression begins to upregulate in maturing neurons located proximal to the ventromedial floor of the otic

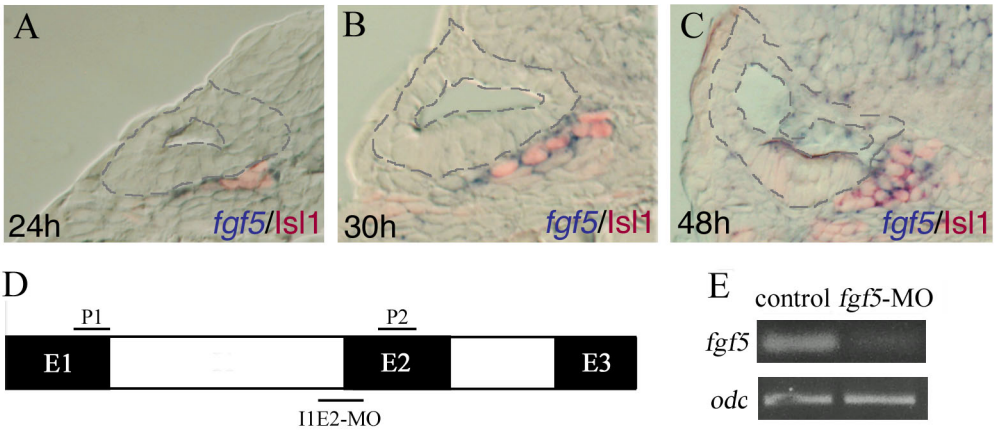

Figure 4.3. Mature neurons express *fgf5*.
(A-C) Co-expression of *fgf5* (blue) and Islet-1 (red) at indicated stages at the level of the anterior sensory epithelium. (D) Schematic of *fgf5* mRNA showing intron (I)-exon (E) structure (not to scale). Binding sites for splice-blocking morpholino at intron1-exon2 junction (I1E2-MO) and PCR primers for RT-PCR (forward P1, reverse P2) are shown. (E) RT-PCR results showing the efficacy of I1E2-MO. *fgf5* transcript levels are severely reduced. *odc* transcript level was used as a control. Otic vesicle is outlined in grey. Images are transverse sections (A-C) with dorsal to the top and lateral to the left.

vesicle as seen by co-localization with Isl1 (Fig. 4.3A). Expression of *fgf5* continues to be restricted to mature SAG neurons at later stages (Fig. 4.3B, C).

We investigated the role of Fgf5 in SAG development by knocking down gene function using a morpholino targeting the intron1-exon2 splice junction (Fig. 4.3D, E). To address the role of *fgf5* in neuroblast specification we examined *neurog1* expression at various stages in morphant embryos. At 24 hpf no obvious difference was observed between morphants and controls (Fig. 4.4A, E) but at 30 hpf, *neurog1* expression was

dramatically expanded in *fgf5* morphants (Fig. 4.4B-C, F-G). The mediolateral expansion of *neurog1* in the otic floor is evident in sections (Fig. 4.4C, G). Although *neurog1* expression also extends along the anterior-posterior axis (Fig. 4.4B, F) the site of delamination did not shift posteriorly in morphants (data not shown). Normally, neuroblast specification begins to slow down after 30 hpf (Andermann et al., 2002 and

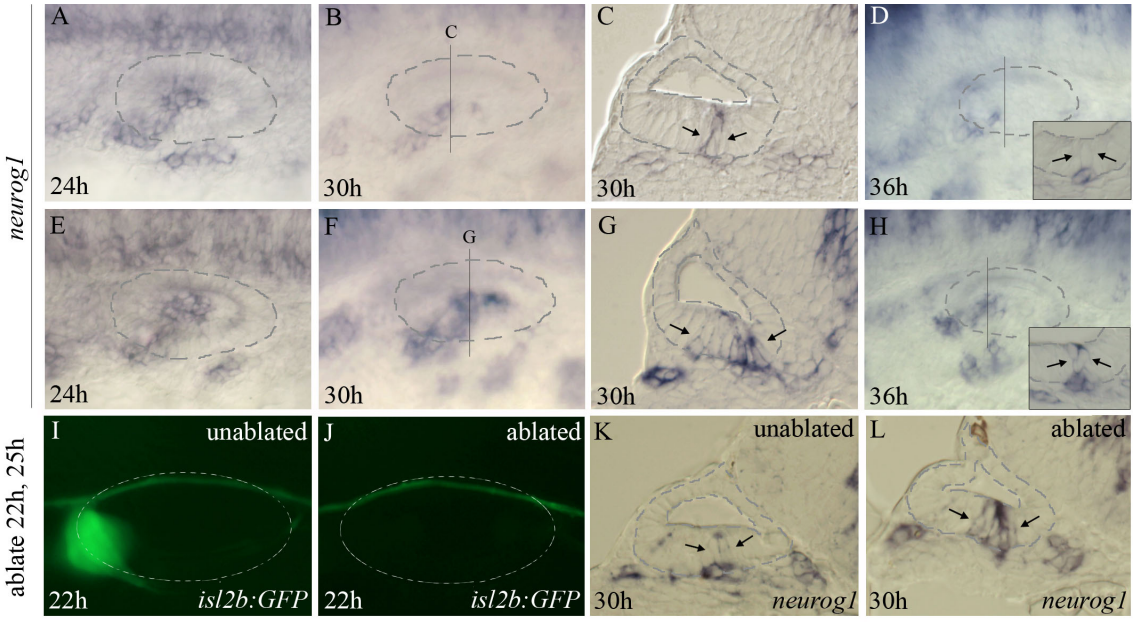

Figure 4.4. *fgf5* from mature neurons terminates the phase of neuroblast specification. (A-H) Expression of *neurog1* in control (A-D) and *fgf5* morphant (E-H) embryos at indicated stages. (I-L) Expression of *isl2b:gfp* (I-J) and *neurog1* (K-L) in unablated (contralateral) control side (I, K) and ablated side (J, L) of the same embryo. GFP-positive mature neurons were serially ablated at 22 and 25 hpf (compare GFP domain in I and J). Otic vesicle is outlined in grey/white. Grey vertical lines in (B, F, D, H) indicate the plane of section in (C, G, inset in D and H). Insets in (D) and (H) show magnified images of the otic floor. Arrows indicate the expanse of *neurog1* domain in the otic floor. Images of whole-mount specimens (A-B, E-F, D, H-J) are dorsolateral views with anterior to the left. Transverse sections (C, G, inset in D and H, K-L) with dorsal to the top and lateral to the left.

Haddon and Lewis, 1996). However, in *fgf5* morphants more *neurog1*-positive cells are detected, both in the otic floor and in the delaminating population, in contrast to controls at 36 hpf indicating a prolonged phase of specification (Fig. 4.4D, H). This data is consistent with the notion that mature SAG cells become a source of elevated Fgf, which eventually exceeds the threshold for termination of specification. This also explains the increased susceptibility to *fgf8* misexpression. To test whether *neurog1* expansion is an indirect effect of altered otic patterning we examined general axial patterning markers and observed no difference between morphant and control embryos. Sensory epithelia development, which is also regulated by Fgf (Millimaki et al., 2007), was normal in *fgf5* morphants (Fig. 4.5, hair cell numbers shown in Table 3).

We used another approach to test whether signals from mature SAG neurons inhibit neuroblast specification. Mature neurons labeled by GFP in *isl2b:gfp* transgenic line were laser-ablated serially at 22 and 25 hpf (Fig. 4.4I-J) and *neurog1* expression at 30 hpf was examined. On the ablated side, *neurog1* expression was expanded relative to the unablated (contralateral) side although to a slightly lesser extent than in *fgf5* morphants (Fig. 4.4K-L, compare with 5G). All together these data suggest that as mature neurons expressing *fgf5* accumulate within the SAG, overall levels of Fgf signaling increase and as a result neuroblast specification is terminated. Differentiating neurons thus regulate the phase of specification to ensure that the appropriate number of SAG precursor cells is produced.

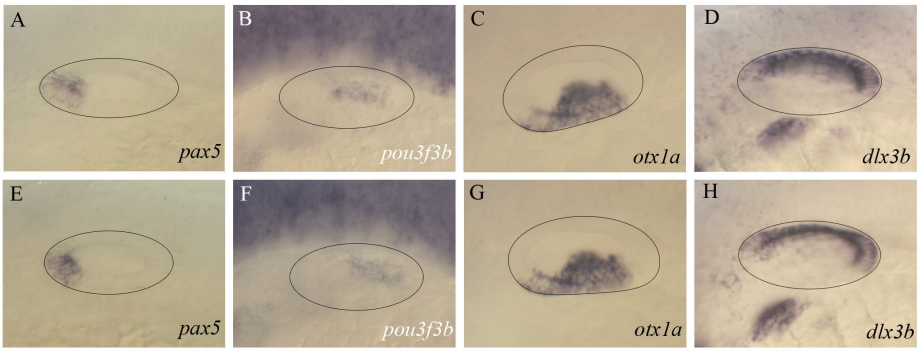

Table 3
Number of hair cells in *brn3c:gfp* embryos at 32 hpf

utricle (anterior)
control 6.6+0.74 *fgf5*MO 7.2+1.01 p = 0.16
saccule (posterior)
control 4.8+0.83 *fgf5*MO 5.1+1.18 p = 0.67

Figure 4.5. Axial pattering in *fgf5* morphants.
(A-H) Expression of various otic markers in control (A-D) and *fgf5* morphant (E-H) embryos. *pax5* (A and E) and *pou3f3b* (B and F) label anterior-posterior axis, respectively. *otx1a* (C and G) labels ventromedial and *dlx3b* (D and H) labels dorsolateral regions of the vesicle. Table 1 shows the number of GFP-positive hair cells (mean of total number ± standard deviation) in the sensory epithelia of *brn3c:gfp* embryos injected with *fgf5* morpholino. Otic vesicle is outlined in black. Images show dorsolateral views with anterior to the left.

Fgf regulates the balance between transit-amplification and differentiation

We next wanted to test the effects of Fgf on later stages of SAG development- transit-amplification and differentiation. We used *neurod* expression to mark precursor cells in the transit-amplification phase, and Isl1 expression plus the absence of *neurod* to mark mature SAG neurons. We examined the expression of these markers under various conditions of gain and loss of Fgf signaling. To better interpret changes in the *neurod* and Isl11 expression domains that are distributed dynamically along the anterior-posterior axis of the SAG, we analyzed transverse sections and grouped them into anterior, middle and posterior (see Fig. 4.1G-J). Misexpression of *hs:fgf8* at 24 hpf resulted in a slight increase in *neurod*$^{+}$ precursor domain in the middle part of the SAG at 36 hpf (Fig. 4.6A-B, I). The posterior part of the SAG is truncated and nearly devoid

of *neurod*$^{+}$ cells (Fig. 4.6E-F, I). This is possibly because the posterior SAG forms later and elevated Fgf prematurely terminates specification of neuroblasts that contribute to the posterior tail of SAG (see Fig. 4.2I-J). Despite the increased population of transit-amplifying cells in the middle region of the SAG, there was a reduction in the *neurod*-negative mature neuronal population (Fig. 4.6A-B, E-F,J). No significant difference was noted in the anterior part of SAG (Fig. 4.6I-J). The total number of Isl1^{+} SAG neurons was reduced in *hs:fgf8* embryos compared to controls (Fig. 4.6K). For loss of function studies, we activated *hs:dnfgfr1* at 24 hpf (38^{o}C-30 minutes) to block all Fgf signaling. As a result a smaller *neurod*$^{+}$ domain was observed at 36 hpf in the middle and posterior regions of SAG compared to controls (Fig. 4.6C,G,I). In contrast to reduction in transit-amplifying population there was a corresponding increase in Isl1^{+} population throughout the anterior-posterior axis of the SAG (Fig. 4.6J,K). The opposing changes in the size of transit-amplifying and differentiating populations could possibly reflect altered cell-cycle progression. To address this, we examined BrdU incorporation following heat shock of *hs:fgf8* and *hs:dnfgfr1* at 24 hpf. Embryos were incubated in BrdU after a 2-hour rest period and processed at 36 hpf. Cells undergoing proliferation in the transit-amplifying population were co-labeled with BrdU^{+}/ *neurod*$^{+}$. Since the size of the *neurod*$^{+}$ transit-amplifying domain varies greatly among control, *hs:fgf8* and *hs:dnfgfr1*, we calculated the relative proportion of BrdU-labeled nuclei in the anterior, middle and posterior regions of the SAG. No significant change was observed suggesting that the rate of proliferation is not altered (data not shown). We then evaluated the number of BrdU^{+} nuclei in the mature neuron population to gauge the progression of precursor cells

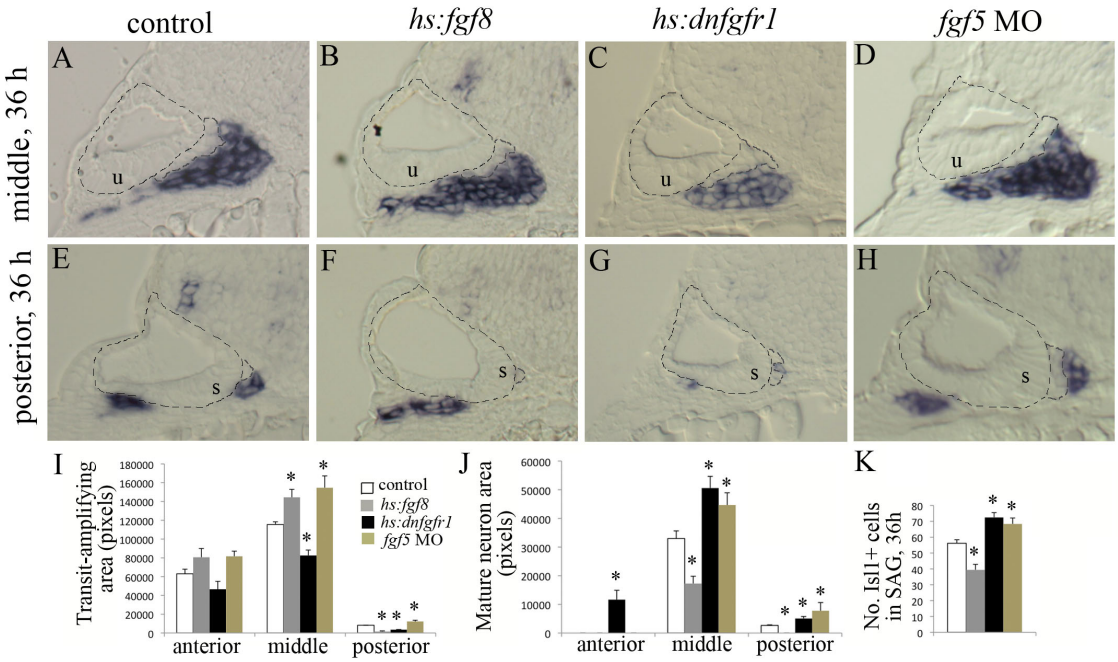

Figure 4.6. Fgf regulates the balance between transit-amplification and differentiation. (A-H) *neurod* expression in control (A, E), *hs:fgf8* (B, F), *hs:dnfgfr1* (C, G) and *fgf5* morphant (D, H) embryos at 36 hpf. (I-K) Quantification of area occupied by neurod^{+} precursor cells (I), neurod^{-}/Isl1^{+} mature neurons (J) in the anterior, middle and posterior region of SAG and the total number of Isl1^{+}cells (K) in the SAG at 36 hpf. (L- S) Isl1 expression in control (L, P), *hs:fgf8* (M, Q), *hs:dnfgfr1* (N, R) and *fgf5* morphant (O, S) embryos at 48 hpf. (T-V) Quantification of the area occupied by neurod^{+} precursor cells (T), neurod^{-}/Isl1^{+} mature neurons (U) in the anterior, middle and posterior region of SAG and the total number of Isl1^{+}cells (V) in the SAG at 48 hpf. *hs:fgf8* embryos activated at 39^{o}C for 30 minutes to strongly over-express Fgf and *hs:dnfgfr1* activated at 38^{o}C for 30 minutes to fully block Fgf signaling. Error bars indicate standard deviation. *$p < 0.05$ in comparison to control, analyzed with Student's *t* test. Otic vesicle is outlined in black. Area occupied by mature neurons is demarcated (A-H) and the limits of SAG are outlined (L-S) in grey. Representative sections from the middle (A-D, L-O) and posterior (E-H, P-S) part of the SAG are shown at the level of the utricular (u) and saccular (s) maculae. Images of transverse sections show dorsal to the top and lateral to the left.

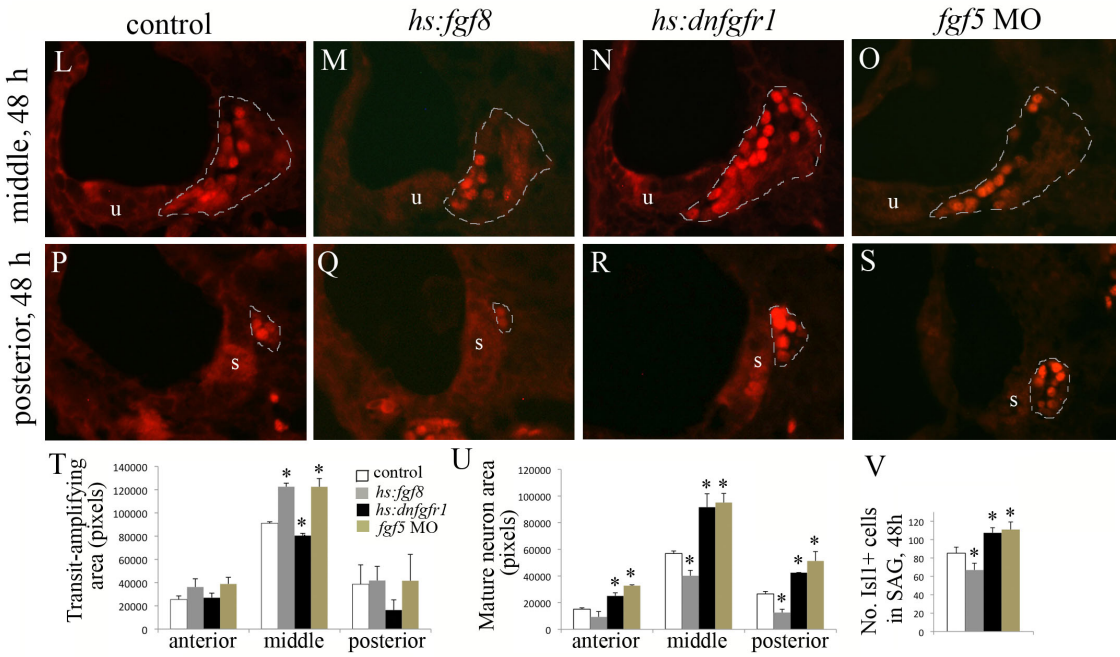

Figure 4.6. (continued) Fgf regulates the balance between transit-amplification and differentiation.

towards differentiation. Fewer $BrdU^+$ nuclei were observed in the middle region of the SAG in *hs:fgf8* than control. In contrast, more $BrdU^+$ nuclei were observed in the middle region of the SAG in *hs:dnfgfr1* (control 17 ± 1.4, *hs:fgf8* 10.7 ± 0.6 and *hs:dnfgfr1* 27.2 ± 5; $p<0.05$, n=4). Overall these data support the idea that Fgf inhibits or delays SAG differentiation, such that blocking Fgf relieves this inhibition thereby accelerating maturation.

We next assessed the role of Fgf5 as a candidate for the endogenous factor from mature SAG that normally inhibits maturation of precursor cells. We examined the distribution of cells in the transit-amplification vs differentiation phase as explained above. The size of *neurod*$^+$ domain was increased in both the middle and posterior

regions of SAG in the embryos (Fig. 4.6D,H, I). There was also an increase in the number of Isl1^{+} neurons in the SAG and the area occupied by mature neurons at 36 hpf in morphant embryos compared to control (Fig. 4.6J,K). No obvious change was observed between controls and *fgf5* morphants in the anterior region of SAG (Fig. 4.6I-J). An increase in both transit-amplification and differentiation is different from what was observed with loss and gain of Fgf function above. This is because *fgf5* morphants showed an increase in transit-amplifying cells due to prolonged phase of specification, but also had an increase in mature SAG due to ongoing maturation. It is important to note that despite the large increase in transit-amplifying population and continued maturation, *fgf5* morphants did not produce more mature neurons than *hs:dnfgfr1* embryos. This suggests that other Fgfs, perhaps Fgf3/8 from the maculae, contribute to SAG regulation and weakly restrain maturation in *fgf5* morphants. In *hs:dnfgfr1* embryos signaling from all Fgfs is impaired and leads to more rapid maturation. In summary, the balance between transit-amplification and differentiation in the developing SAG shifts in response to the overall level of Fgf signaling.

We extended our analysis to a later time point to study how changes in the transit-amplifying and mature neuronal populations at early stages continue to affect SAG development. By 48 hpf more *neurod*$^{+}$ precursors in the transit-amplification phase have differentiated into Isl1^{+} neurons in comparison to 36 hpf. The spatial distribution of these populations remains the same along the anterior-posterior and proximal-distal axes. The distribution of transit-amplifying cells and differentiating neurons, in the middle and anterior region of the SAG, at 48 hpf was similar to what was observed at 36 hpf with

some exceptions (Fig. 4.6T-U). There was no notable difference in the posterior (Fig. 4.6T, compare with 4.6I). As expected, the mature neuronal population was smaller in *hs:fgf8*, and expanded in *hs:dnfgfr1* and *fgf5* morphant embryos both in the middle and posterior regions of the SAG (Fig. 4.6L-N, P-R and U-V). There was, however, an increase in the mature neuronal population in *fgf5* morphant embryos in the anterior region of the SAG (Fig. 4.6U, compare with 4.6J). This possibly reflects maturation of the excessive neuroblasts that were specified during earlier stages of SAG development. These findings strongly support the idea that as the SAG expands, elevated levels of Fgf signaling from mature neurons stabilizes the transit-amplifying population and inhibits these cells from differentiating into neurons, thus regulating the overall size of the ganglion.

DISCUSSION

Otic neurogenesis is a multistep process that gives rise to neurons of the statoacoustic ganglion (SAG). SAG development has been well characterized in chick and mouse. Here we show that zebrafish otic neurogenesis follows similar steps. Neuroblasts are specified in the otic floor that later delaminate. Upon delamination, neuroblasts then undergo a phase of proliferation. The number of neurons in the SAG continue to increase even after delamination ceases owing to growth of a precursor pool. In this study we show that Fgf controls each phase of this complex developmental process. Initially moderate to low level Fgf from the hindbrain and utricular macula specifies neuroblasts. Neuroblasts differentiate into SAG neurons that express *fgf5* and as more neurons

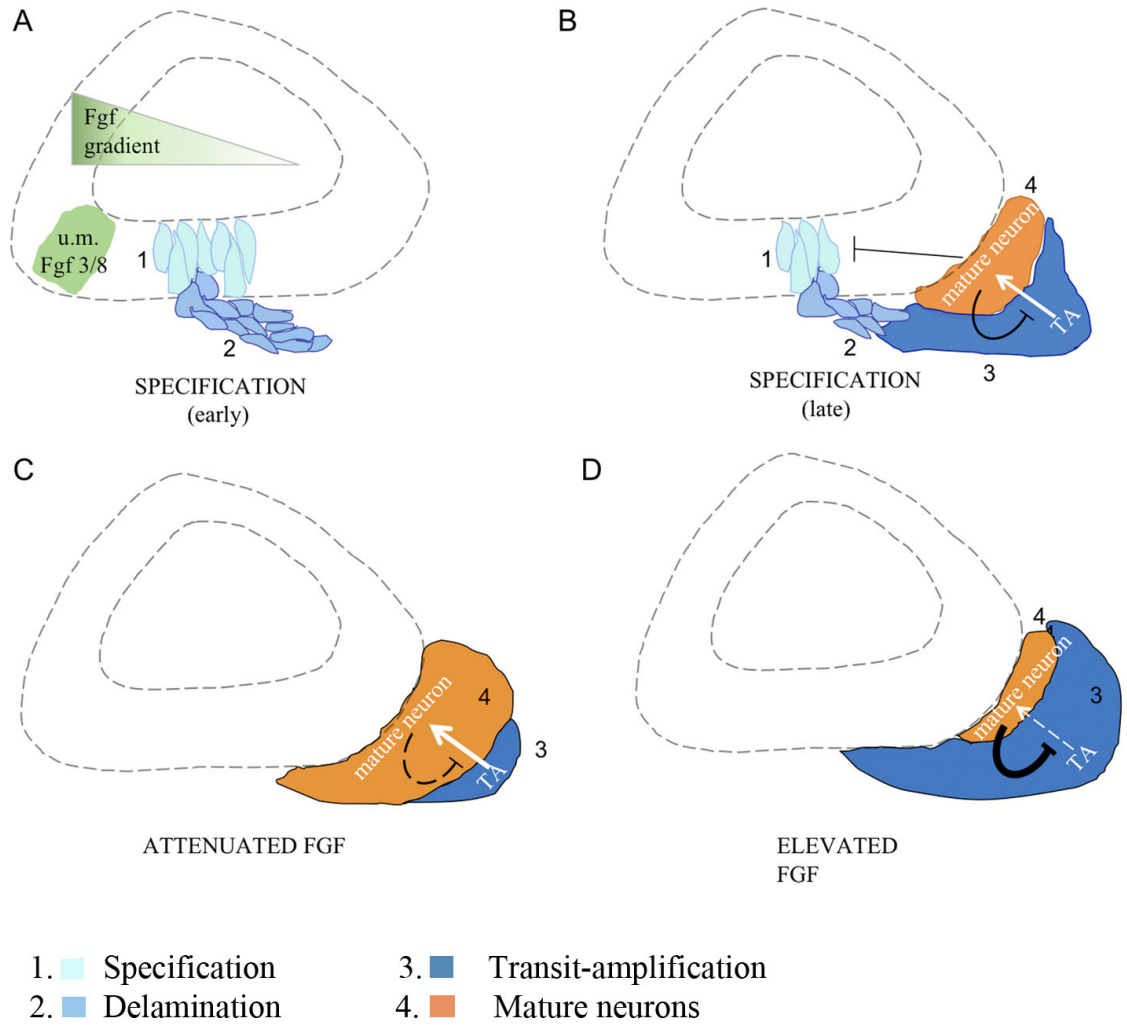

Figure 4.7. Model illustrating regulation of SAG development by Fgf.
(A) Neuroblast specification at early stages. Fgf3/8 gradient from the utricular macula (u.m) specifies neuroblasts in the otic floor that later delaminate. (B) Fgf5 from mature neurons terminated the phase of specification and regulates progression from transit-amplification to differentiation. (C-D) Ongoing Fgf signaling delays maturation of transit-amplifying cells into neurons. Attenuation of Fgf signaling (C) promotes maturation of neurons whereas elevated Fgf (D) delays the progression further. White arrows indicate cell stage progression and black arrows indicate gene function. Transverse sections are represented with dorsal on top and medial to the right.

accumulate, elevated Fgf level in turn terminates the phase of specification. We show that Fgf also regulates the balance between transit-amplification and differentiation. Thus, Fgf signaling renders the SAG system self-organizing and self-maintaining.

Fgf regulates the phase of neuroblast specification

Several studies have implicated a role for Fgfs in neuroblast specification (Alsina et al., 2003; Wright and Mansour, 2003; Alsina et al., 2004). Since Fgfs are also critical in otic induction and patterning, steps foreshadowing establishment of the neurogenic domain, it has been challenging to interpret most of these studies. Blocking Fgf signaling after placode induction resulted in a dramatic loss of neurogenic domain (*neurog1* expression) although it was not completely lost. This is possibly because of incomplete inhibition of Fgf signaling. Blocking Fgf signaling at earlier stages or more strongly is toxic to the embryo (data not shown). We show that Fgf acts as a morphogen with both an upper and lower threshold for SAG specification. Neurogenic domain is induced in response to low level of Fgf emanating from the utricle/hindbrain (Fig. 4.7A). High levels of Fgf, on the other hand, are inhibitory. One possible explanation for the inhibitory action of Fgf is that elevated Fgf induces high levels of *neurog1* initially. *Neurog1* has been shown to negatively autoregulate itself via Notch-mediated lateral inhibition (Haddon et al., 1998; Raft et al., 2007) and elevated Notch activity might shut down the entire process of specification.

At later stages the process of specification becomes more sensitive to the inhibitory effects of Fgf but not until sufficient *fgf5*$^{+}$ SAG neurons have accumulated. As

SAG development progresses the overall levels of Fgf increase further and the phase of specification is terminated (Fig. 4.7B). In *fgf5* morphants, although specification is prolonged it begins to slow down at 36 hpf suggesting that specification might be regulated by multiple mechanisms.

Fgf regulates later stages of otic neurogenesis

We show evidence that Fgf signaling continues to regulate later stages of SAG development. The final number of neurons in the SAG depends on a dynamic balance between transit-amplification and differentiation of precursor cells. As SAG development continues mature neurons express *fgf5* thus elevating levels of Fgf. This in turn inhibits or delays SAG differentiation. Blocking Fgf alleviates this inhibition and accelerates maturation whereas elevated levels delays it further (Fig. 4.7C, D). In *fgf5* morphants, although additional neuroblasts are specified, the number of mature neurons is no different from when Fgf signaling is completely attenuated in *hs:dnfgfr1*. It is possible that Fgf from other adjacent sources such as the maculae play a role in regulating SAG neurogenesis. The possibility that sensory epithelia expansion cooperates with SAG development to regulate neurosensory growth in the inner ear is fascinating. A similar role for Fgf signaling has been shown in minbrain-rhombomere1 development in mouse where conditional knockdown of Fgf receptors results in an increase in differentiated neurons and a concomitant loss of progenitor cells in the ventricular zone. Thus, Fgf is thought to play a role in regulating the balance between progenitor self-renewal and postmitotic differentiation (Saarimaki-Vire et al., 2007). In

another study, high levels of Fgf2 have been shown to maintain proliferation of cultured neural progenitor cells from the human cortex and block differentiation. Low levels of Fgf2, however, enhance neurogenesis. An autoregulatory mechanism mediated by Fgf2 is proposed where levels of Fgf2 increase as neurogenesis proceeds and this in turn prevents further differentiation (Nelson and Svendsen, 2006). In summary our data support a model for SAG regulation mediated by different sources of Fgf during different phases of otic neurogenesis.

CHAPTER V

SUMMARY AND DISCUSSION

SUMMARY OF FINDINGS

This study examines the development of neurosensory components of the zebrafish inner ear. Formation of sensory epithelia, composed of hair cells and support cells, depends on *atoh1* function. In Chapter II, we show that misexpression of *atoh1a* recapitulates expression of markers seen during endogenous sensory epithelia development. This results in the induction of ectopic sensory epithelia. However, the ability of otic tissue to respond to *atoh1a* varies in a spatial and temporal manner. Maximal effects are observed during placodal stages and induction of ectopic sensory epithelia is still limited to the ventromedial region of the otic vesicle. Competence of otic tissue to respond to *atoh1a* can be enhanced by co-misexpression of *fgf8* or *sox2*, genes that normally work in concert with *atoh1a*. As a result ectopic sensory epithelia are induced in the non-sensory lateral wall of the otic vesicle, even at later stages of development. The sensory epithelium expresses several genes that regulate differentiation and maintenance/survival of hair cells. *pax5* is one such gene differentially expressed in the utricular (anterior) macula and its role is examined in Chapter III. *pax5* regulates the maintenance of utricular hair cells and requires *pax2a* and *fgf3* for its expression. Disruption of Pax5 function results in hair cell death in the utricle and not the (posterior) saccule. As a consequence, neurons of the statoacoustic ganglion (SAG) that innervate these hair cells

become disorganized and vestibular, not auditory, function is impaired. Bipolar neurons of the SAG transmit information from sensory endorgans to targets in the hindbrain. Detailed analysis of the development and regulation of SAG is addressed in Chapter IV. Neuronal precursor cells (neuroblasts) are formed in the otic floor in response to a moderate dose of Fgf signaling possibly from the adjacent hindbrain or the utricular macula. These neuroblasts undergo a protracted phase of proliferation prior to differentiating into mature neurons. Mature neurons express *fgf5* and together with *fgf3*/*8* expression in the sensory epithelia increase the overall levels of Fgf signaling as development progresses. We show evidence that Fgf signaling regulates SAG development by first, terminating the phase of neuroblast specification, and later maintaining the balance between proliferation of neuroblasts and their differentiation into neurons. This ensures that sufficient precursors are generated and prevents over-production of neurons, thus controlling the ultimate size of the SAG.

ESTABLISHING THE PROSPECTIVE NEUROSENSORY DOMAIN

Previous studies have shown the requirement of Fgf in establishing the prosensory domain that gives rise to both hair cells and support cells (Pirvola et al., 2002; Millimaki et al., 2007; Hayashi et al., 2008). Fgf is also expressed within the maculae suggesting that high levels of Fgf promote sensory development (Millimaki et al., 2007). Fgf signaling also plays an important role is specifying the proneural domain that gives rise to neurons of the SAG. Our studies using conditional manipulation of Fgf signaling show that neuroblast specification in zebrafish depends on Fgf in a dose-dependent

manner. Cells in the otic floor respond to moderate to low levels of Fgf, emanating from the hindbrain first and then the utricle, whereas high levels are inhibitory.

In mouse and chick, *neurog1* expression foreshadows *atoh1* such that neuroblasts are specified first followed by sensory precursors within the same ventromedial region of the otic palcode. This is different from zebrafish where *atoh1b* expression is seen first in preotic cells in a broad domain as early as 10.5 hpf. This domain is restricted to distinct anterior and posterior regions of the otic placode by 14 hpf. Soon thereafter *neurog1* is expressed in the placode. The role of *atoh1b*, if any, in specifying the proneural domain is not known. Although *atoh1* is expressed before *neurog1* in zebrafish, specification of sensory and neuronal precursors occurs concurrently and not sequentially as seen in chick and mouse. As explained above, Fgf signaling is critical in establishing the proneural and prosensory domains in the ventromedial region of the otic placode. How expression domains of *atoh1* and *neurog1* are spatially restricted within this region is not fully understood. Clues from other systems suggest that differential expression of cofactors might regulate this process. For instance, in mouse, Pax6 plays a role in defining progenitor domains in the lower rhombic lip by limiting *Neurog1* expression domain and promoting *Atoh1* domain. As a result, *Pax6* mutants show an expansion of *Neurog1* expression at the expense of *Atoh1* (Landsberg et al., 2005). In zebrafish, Fgf regulates the expression of Pax2/5/8 family of transcription factors in addition to *atoh1a* and *neurog1*. Pax2/5 are expressed regionally and implicated in hair cell development (Pfeffer et al., 1998; Riley et al., 1999; Kwak et al., 2002; Millimaki et al., 2007; this study). Together with the observation that *pax2a* and *neurog1* transcripts

are distributed in a mutually exclusive fashion in the otic vesicle (Korzh et al., 1998), it is possible that once the general neurosensory domain is set up by Fgf gradient, *pax2a* then sharpens the border analogous to *Pax6*.

SENSORY EPITHELIA DEVELOPMENT AND MAINTENANCE

The proneural gene *atoh1* is both necessary and sufficient for sensory epithelia development. Developing sensory epithelia express several markers that are essential for differentiation and maintenance of hair cells. *sox2*, induced by Fgf and Notch, is co-expressed with *atoh1a/b* at early stages. During sensory epithelia differentiation, *sox2* is downregulated in mature hair cells and maintained in the support cells (Millimaki et al., 2010). *fgf3/8* are also expressed in the sensory epithelia and ongoing Fgf signaling appears to be important for macular expansion. *pax2a* is expressed along the medial wall of the otic palcode in response to Fgf from the hindbrain, and is later upregulated in all utricular hair cells and the first few hair cells in the saccule. Pax2a is required for normal expression of *deltaA* involved in lateral inhibition and in *pax2a* (*noi*) mutants the number of utricular hair cells is doubled (Riley et al., 1999). Pax2a also activates expression of another member of the *pax2/5/8* subfamily, *pax5*. *pax5* is predominantly present in the utricle, and in addition to *pax2a* requires Fgf3 for its expression. Loss of Fgf8 or Atoh1 function does not alter *pax5* expression (Kwak et al., 2002; Millimaki et a., 2007). Our studies show that *pax5* is required for maintenance of utricular hair cells and loss of its function results in vestibular but not auditory defects. However, severe reduction of *pax5* expression does not always lead to cell death. *noi* mutants show elevated cell death in

the utricle whereas *fgf3* (*lia*) mutants do not. One possible explanation is that *lia* mutants express another factor in the utricle that promotes survival. Fgf3 regulates anterior identity in part by suppressing posterior markers such as *pou3f3b. pou3f3b* is expanded anteriorly in *lia* mutant embryos (Kwak et al., 2002) and could account for *pax5*-independent survival in the utricle. In fact, loss of *fgf3* (*lia*) can suppress utricular cell death phenotype in *noi* mutants (unpublished observations). This suggests that each region of the otic vesicle is regulated by a certain combination of factors that promote differentiation and survival.

We show that misexpression of *atoh1a* induces ectopic sensory epithelia in the vicinity of endogenous sensory epithelia, consistent with other studies. By expanding regional identity compatible with sensory development, the overall competence of non-sensory otic regions to respond to *atoh1a* can be enhanced. We achieved this by co-activating *fgf3/8* that work in concert in *atoh1a* normally. As a result, ectopic sensory epithelia are observed in the lateral wall of the otic vesicle. Co-activation of *sox2* and *atoh1a* show similar results. In addition, only this combination of factors induces ectopic sensory epithelia in non-sensory regions at later stages, although still largely limited to the lateral wall. The unique ability of *sox2*, and not *fgf*, to induce sensory epithelia in non-sensory regions could reflect the ability of *sox2* to maintain cells in a pluripotent state, thereby allowing *atoh1a* to promote sensory fate specification. Whether *sox2* alters axial patterning of the vesicle is not known. In the developing inner ear of chick and mouse, *Sox2* is expressed in both neuronal and sensory precursors (Puligilla et al., 2010; Neves et al., 2011). Misexpression of *Sox2* can activate *Atoh1* and induce ectopic

sensory epithelia almost anywhere in the chick otic vesicle by recapitulating early steps of preosensory development. Whether otic cells in mammals respond to factors that alter sensory competence in a similar way remains to be seen.

STATOACOUSTIC GANGLION (SAG) DEVELOPMENT

Development of the SAG or otic neurogenesis involves several stereotypical stages. The region of neural competence or proneural domain is established in the otic tissue by a combination of regionally expressed markers. Fgfs play a critical role in this process. Because of the role of Fgfs in otic induction and patterning it has been a challenge to study the direct effects of Fgf in the development and regulation of SAG. By using inducible transgenic zebrafish lines activated after placode induction we have successfully addressed this issue. We have shown that the anterior ventromedial region of the otic placode expresses *neurog1* in response to moderate to low level of Fgf from adjacent tissue, and gives rise to neuronal precursors (neuroblasts). In mouse, T-box transcription factor *Tbx1* is expressed posterolaterally and anterodorsally in the otic placode, and limits the posterior boundary of the proneural domain. *Tbx1* null mice fail to restrict the neurogenic domain and ectopic neurogenesis is observed. *Tbx1* misexpression on the other hand suppresses neurogenic fates (Raft et al., 2004). *tbx1* is expressed in the posterolateral part of zebrafish otic vesicle and it appears to restrict the posterior limit of the neurogenic domain (Radosevic et al., 2011). Upon specification, neuroblasts delaminate and undergo proliferation even after delamination has ceased, similar to what has been reported in chick (D'Amico-Martel, 1982). SAG precursors in

chick express *Sox2*, known to mark progenitor cells in the central nervous system. However, expression of SoxB1 subfamily members, *sox1/2/3* is not detected in zebrafish SAG precursors during embryonic stages (unpublished results). Proliferating cells are detected in the zebrafish SAG as late as 5 days postfertilization. How these precursor cells remain in an undifferentiated state is not known.

After cell cycle exit, neuroblasts differentiate into bipolar SAG neurons that extend processes to peripheral and central targets. SAG neurons depend on neurotrophic factors from sensory epithelia for differentiation and survival (reviewed in Appler and Goodrich, 2011). With the death of hair cells, afferent fibers of SAG neurons become disorganized and begin to degenerate as seen in *pax5* morphants. It is thus critical to preserve SAG neurons following hair cell insult, by application of neuroprotective factors such as neurotprohins or electrical stimulation, for success with prostheses like cochlear implants and gene/cell-based therapies (Roehm and Hansen, 2005; Shibata et al., 2011). Innervation of newly regenerated hair cells would be a prerequisite for functional recovery. Kawamoto et al. (2003) have shown evidence that some ectopic hair cells induced by *Atoh1* misexpression are innervated in mouse. It is not known whether ectopic sensory epithelia observed in our study are innervated by SAG neurons.

REGULATION OF SAG NEUROGENESIS

This study sheds light on how the total number of postmitotic neurons in the SAG might be regulated. We show that Fgfs from both the differentiated neurons within the SAG and from adjacent tissues like the sensory epithelium mediate this process during

embryonic development. First, Fgf signaling from mature SAG neurons (expressing *fgf5*) terminates the phase of neuroblast specification. During later stages, Fgf signaling also regulates the balance between proliferation and differentiation of precursor cells. Elevated levels of Fgf stabilize precursors and delay differentiation. Similar role for Fgf signaling is seen in minbrain-r1 development in mouse and cultured neural progenitor cells from the human cortex (Nelson and Svendsen, 2006, Saarimaki-Vire et al., 2007). Negative autoregulatory action ensures that the correct number of mature neurons is produced. Whether Fgf from developing sensory epithelia or other adjacent tissue plays a role in regulating the overall size of the SAG needs to be further explored.

Members of the TGFβ superfamily have been known for long to act as negative growth regulators during development and adult tissue homeostasis. Myostatin, or Growth and Differentiation Factor 8 (Gdf8), is secreted by differentiating myoblasts and inhibits proliferation of neighboring muscle precursor cells (Thomas et al., 2000). Gdf11 works in a similar manner in mouse to regulate olfactory neurogenesis (Wu et al., 2003). Understanding the mechanisms by which these factors regulate the balance between progenitor self-renewal and postmitotic differentiation is an important step in designing therapeutic strategies to restore function after neuronal damage in the SAG and elsewhere in the nervous system.

REFERENCES

Abello, G., Khatri, S., Giraldez, F., Alsina, B., 2007. Early regionalization of the otic placode and its regulation by the Notch signaling pathway. Mech. Dev. 124, 631-645.

Adam, J., Myat, A., Le Roux, I., Eddison, M., Henrique, D., Ish-Horowicz, D., Lewis, J., 1998. Cell fate choices and the expression of Notch, Delta and Serrate homologues in the chick inner ear: parallels with Drosophila sense-organ development. Development 125, 4645-4654.

Adamska, M., Leger, S., Brand, M., Hadrys, T., Braun, T., Bober, E., 2000. Inner ear and lateral line expression of a zebrafish *Nkx5-1* gene and its downregulation in the ears of *FGF8* mutant, *ace*. Mech. Dev. 97, 161-165.

Adamska, M., Herbrand, H., Adamski, M., Krüger, M., Brauna, T., Bober, E., 2001. FGFs control the patterning of the inner ear but are not able to induce the full ear program. Mech. Dev. 109, 303-313.

Akagi, T., Inoue, T., Miyoshi, G., Bessho, Y., Takahashi, M., Lee, J.E., Guillemot, F.o., Kageyama, R., 2004. Requirement of multiple basic helix-loop-helix genes for retinal neuronal subtype specification. J. Biol. Chem. 279, 28492-28498.

Alsina, B., Giraldez, F., Varela-Nieto, I., Romand, R., Isabel, V.N., 2003. Growth factors and early development of otic neurons: interactions between intrinsic and extrinsic signals. Curr. Top. Dev. Biol. 57, 177-206.

Alsina, B., Abello, G., Ulloa, E., Henrique, D., Pujades, C., Giraldez, F., 2004. FGF

signaling is required for determination of otic neuroblasts in the chick embryo. Dev. Biol. 267, 119-134.

Alvarez, Y., Alonso, M.T., Vendrell, V., Zelarayan, L.C., Chamero, P., Theil, T., Bosl, M.R., Kato, S., Maconochie, M., Riethmacher, D., Schimmang, T., 2003. Requirements for FGF3 and FGF10 during inner ear formation. Development 130, 6329-6338.

Andermann, P., Ungos, J., Raible, D.W., 2002. Neurogenin1 defines zebrafish cranial sensory ganglia precursors. Dev. Biol. 251, 45-58.

Appler, J.M., Goodrich, L.V., 2011. Connecting the ear to the brain: Molecular mechanisms of auditory circuit assembly. Prog. Neurobiol. 93, 488-508.

Ayaso, E., Nolan, C.M., Byrnes, L., 2002. Zebrafish insulin-like growth factor-I receptor: molecular cloning and developmental expression. Mol. Cell. Endocrin. 191, 137-148.

Baker, C.V.H., Bronner-Fraser, M., 2001. Vertebrate cranial placodes I. Embryonic induction. Dev. Biol. 232, 1-61.

Bang, P.I., Sewell, W.F., Malicki, J.J., 2001. Morphology and cell type heterogeneities of the inner ear epithelia in adult and juvenile zebrafish (*Danio rerio*). J. Comp. Neurol. 438, 173-190.

Bang, I.B., Yelick, P.C., Malicki, J.J., Sewell, W.F., 2002. High-throughput behavioral screening and method for detecting auditory response deficits in zebrafish. J. Neurosci. Methods 118: 177-187.

Barald, K.F., Kelley, M.W., 2004. From placode to polarization: new tunes in inner ear

development. Development 131, 4119-4130.

Beck, J.C., Gilland, E., Tank, D.W., Baker, R., 2004. Quantifying the ontogeny of optokinetic and vestibuloocular behaviors in zebrafish, medaka and goldfish. J. Neurophysiol. 92: 3546-3561.

Begbie, J., Ballivet, M., Graham, A., 2002. Early steps in the production of sensory neurons by the neurogenic placodes. Mol. Cell. Neurosci. 21, 502-511.

Bell, D., Streit, A., Gorospe, I., Varela-Nieto, I., Alsina, B., Giraldez, F., 2008. Spatial and temporal segregation of auditory and vestibular neurons in the otic placode. Dev. Biol. 322, 109-120.

Bertrand, N., Castro, D.S., Guillemot, F., 2002. Proneural genes and the specification of neural cell types. Nat. Rev. Neurosci. 3, 517-530.

Blader, P., Fischer, N., Gradwohl, G., Guillemont, F., Strahle, U., 1997. The activity of neurogenin1 is controlled by local cues in the zebrafish embryo. Development 124, 4557-4569.

Bouchard, M., Pfeffer, P., Busslinger, M., 2000. Functional equivalence of the transcription factors Pax2 and Pax5 in mouse development. Development 127: 3703-3713.

Bricaud, O., Collazo, A., 2006. The transcription factor *six1* inhibits neuronal and promotes hair cell fate in the developing zebrafish (*Danio rerio*) inner ear. J. Neurosci. 26, 10438-10451.

Brignull, H.R., Raible, D.W., Stone, J.S., 2009. Feathers and fins: Non-mammalian models for hair cell regeneration. Brain Res. 1277, 12-23.

Brooker, R., Hozumi, K., Lewis, J., 2006. Notch ligands with contrasting functions: Jagged1 and Delta1 in the mouse inner ear. Development 133, 1277-1286.

Brumwell, C.L., Hossain, W.A., Morest, D.K., Bernd, P., 2000. Role for basic fibroblast growth factor (FGF-2) in tyrosine kinase (TrkB) expression in the early development and innervation of the auditory receptor: in vitro and in situ studies. Exp. Neurol. 162, 121-145.

Burton, Q., Cole, L.K., Mulheisen, M., Chang, W., Wu, D.K., 2004. The role of *Pax2* in mouse inner ear development. Dev. Biol. 272: 161-175.

Bylund, M., Andersson, E., Novitch, B.G., Muhr, J., 2003. Vertebrate neurogenesis is counteracted by Sox1-3 activity. Nat Neurosci. 6, 1162-1168.

Camarero, G., Leon, Y., Gorospe, I., De Pablo, F., Alsina, B., Giraldez, F., Varela-Nieto, I., 2003. Insulin-like growth factor 1 is required for survival of transit-amplifying neuroblasts and differentiation of otic neurons. Dev. Biol. 262, 242-253.

Camarero, G., Villar, M.A., Contreras, J., Fernandez-Moreno, C., Pichel, J.G., Avendano, C., Varela-Nieto, I., 2002. Cochlear abnormalities in insulin-like growth factor-1 mouse mutants. Hear. Res. 170, 2-11.

Chen, P., Johnson, J. E., Zoghbi, H. Y., Segil, N., 2002. The role of *Math1* in inner ear development: Uncoupling the establishment of the sensory primordium from hair cell fate determination. Development 129, 2495-2505.

Cordes, S.P., Barsh, G.S., 1994. The mouse segmentation gene *kr* encodes a novel basic domain-leucine zipper transcription factor. Cell 79, 1025-1034.

Cotanche, D.A., Kaiser, C.L., 2010. Hair cell fate decisions in cochlear development and regeneration. Hear. Res. 266, 18-25.

D'Amico-Martel, A., 1982. Temporal patterns of neurogenesis in avian cranial sensory and autonomic ganglia. . Am. J. Anat. 163, 351-372.

Dabdoub, A., Puligilla, C., Jones, J.M., Fritzsch, B., Cheah, K.S.E., Pevny, L.H., Kelley, M.W., 2008. Sox2 signaling in prosensory domain specification and subsequent hair cell differentiation in the developing cochlea. Proc. Natl. Acad. Sci. 105, 18396-18401.

Daudet, N., Lewis, J., 2005. Two contrasting roles for Notch activity in chick inner ear development: specification of prosensory patches and lateral inhibition of hair-cell differentiation. Development 132, 541-551.

Daudet, N., Ariza-McNaughton, L., Lewis, J., 2007. Notch signalling is needed to maintain, but not to initiate, the formation of prosensory patches in the chick inner ear. Development 134, 2369-2378.

Draper, B.W., Morcos, P.A., Kimmel, C.B., 2001. Inhibition of zebrafish *fgf8* pre-mRNA splicing with morpholino oligos: a quantifiable method for gene knockdown. Genesis 30: 154-156.

Ekker, M., Akimenko, M-A., Bremiller, R., Westerfield, M., 1992a. Regional expression of three homeobox transcripts in the inner ear of zebrafish embryos. Neuron 9: 27-35.

Ekker, S.C., von Kessler, D.P., Beachy, P.A., 1992b. Differential DNA sequence recognition is a determinant of specificity in homeotic gene action. Embo J. 11:

4059-4072.

Fay, R.R., Popper, A.N., 1973. Acoustic stimulation of the ear of the goldfish (*Carassius auratus*). J. Exp. Biol. 61: 243-260.

Fay, R.R., Popper, A.N., 1980. Structure and function in teleosts auditory systems. In Comparative studies of hearing in vertebrates (ed. A. N. Popper and R. R. Fay), Springer-Verlag, Berlin.

Fekete, D.M., Wu, D.K., 2002. Revisiting cell fate specification in the inner ear. Curr. Opin. Neurobiol. 12, 35-42.

Fritzsch, B., Tessarollo, L., Coppola, E., Reichardt, L.F., 2004. Neurotrophins in the ear: their roles in sensory neuron survival and fiber guidance, Prog. Brain Res. 146, 265-278.

Fritzsch, B., Beisel, K.W., Hansen, L.A., 2006. The molecular basis of neurosensory cell formation in ear development: a blueprint for hair cell and sensory neuron regeneration? BioEssays 28, 1181-1193.

Goldfarb, M., Bates, B., Drucker, B., Hardin, J., Haub, O., 1991. Expression and possible functions of the *FGF-5* gene. Ann. N Y Acad. Sci. 638, 38-52.

Gowan, K., Helms, A.W., Hunsaker, T.L., Collisson, T., Ebert, P.J., Odom, R., Johnson, J.E., 2001. Crossinhibitory activities of *Ngn1* and *Math1* allow specification of distinct dorsal interneurons. Neuron 31, 219-232.

Graham, V., Khudyakov, J., Ellis, P and Pevny, L., 2003. SOX2 functions to maintain neural progenitor identity. Neuron 39, 749-765.

Haddon, C., Lewis, J., 1996. Early ear development in the embryo of the zebrafish,

Danio rerio. J. Comp Neurol. 365, 113-128.

Haddon, C., Jiang, Y.J., Smithers, L., Lewis, J., 1998. Delta-Notch signalling and the patterning of sensory cell differentiation in the zebrafish ear: evidence from the *mind bomb* mutant. Development 125, 4637-4644.

Hans, S., Christison, J., Liu, D., Westerfield, M., 2007. Fgf-dependent otic induction requires competence provided by Foxi1 and Dlx3b. BMC Dev. Biol. 7: 5.

Hartman, B.H., Reh, T.A., Bermingham-McDonogh, O., 2010. Notch signaling specifies prosensory domains via lateral induction in the developing mammalian inner ear. Proc. Natl. Acad. Sci. 107, 15792-15797.

Hatch, E.P., Noyes, C.A., Wang, X., Wright, T.J., Mansour, S.L., 2007. *Fgf3* is required for dorsal patterning and morphogenesis of the inner ear epithelium. Development 134, 3615-3625.

Hauptmann, G., Gerster, T., 2000. Combined expression of zebrafish *Brn-1*- and *Brn-2*-related POU genes in the embryonic brain, pronephric primordium, and pharyngeal arches. Dev. Dyn. 218: 345-358.

Hayashi, T., Cunningham, D., Bermingham-McDonogh, O., 2007. Loss of FGFR3 leads to excess hair cell development in the mouse organ of Corti. Dev. Dyn. 235, 525-533.

Hayashi, T., Ray, C.A., Bermingham-McDonogh, O., 2008. *Fgf20* is required for sensory epithelial specification in the developing cochlea. J. Neurosci. 28, 5991-5998.

Heller, N., Brandli, A.W., 1999. *Xenopus Pax-2/5/8* orthologues: novel insights into *Pax*

gene evolution and identification of Pax-8 as the earliest marker for otic and pronephric cell lineages. Dev. Genet. 24: 208-219.

Helms, A. W., Abney, A. L., Ben-Arie, N., Zoghbi, H. Y., Johnson, J. E., 2000. Autoregulation and multiple enhancers control *Math1* expression in the developing nervous system. Development 127, 1185-1196.

Herbrand, H., Guthrie, S., Hadrys, T., Hoffmann, S., Arnold, H.H., Rinkwitz-Brandt, S., Bober, E., 1998. Two regulatory genes, *cNkx5-1* and *cPax2*, show different responses to local signals during otic placode and vesicle formation in the chick embryo. Development 125, 645-654.

Hernandez, R.E., Rikhof, H.A., Bachmann, R., Moens, C.B., 2004. *vhnf1* integrates global RA patterning and local FGF signals to direct posterior hindbrain development in zebrafish. Development 131, 4511-4520.

Hertzano, R., Montcouquiol, M., Rashi-Elkeles, S., Elkon, R., Yucel, R., Frankel, W.N., Rechavi, G., Moroy, T., Friedman, T.B., Kelley ,M.W., Avraham, K.B., 2004. Transcription profiling of inner ears from *Pou4f3(ddl/ddl)* identifies *Gfi1* as a target of the *Pou4f3* deafness gene. Hum. Mol. Genet. 13: 2143-2153.

Herzog, W., Sonntag, C., von der Hardt, S., Roehl, H.H., Varga, Z.M., Hammerschmidt, M., 2004. Fgf3 signaling from the ventral diencephalon is required for early specification and subsequent survival of the zebrafish adenohypophysis. Development 131: 3681-3692.

Higgs, D.M., Souza, M.J., Wilkins, H.R., Presson, J.C., Popper, A.N., 2001. Age- and size-related changes in the inner ear and hearing ability of the adult zebrafish

(*Danio rerio*). J Assoc Res Otolaryngol 3, 174-184.

Hossain, W.A., Zhou, X., Rutledge, A., Baier, C., Morest, D.K., 1996. Basic fibroblast growth factor affects neuronal migration and differentiation in normotypic cell cultures from the cochleovestibular ganglion of the chick embryo. Exp. Neurol. 138, 121-143.

Huang, Y., Chi, F., Han, Z., Yang, J., Gao, W., Li, Y., 2009. New ectopic vestibular hair cell-like cells induced by *Math1* gene transfer in postnatal rats. Brain Res. 1276, 31-38.

Hutson, M.R., Lewis, J.E., Nguyen-Luu, D., Lindberg, K.H., Barald, K.F., 1999. Expression of *Pax2* and patterning of the chick inner ear. J. Neurocytol. 28, 795-807.

Inoue, A., Takahashi, M., Hatta, K., Hotta, Y., Okamoto, H., 1994. Developmental regulation of *islet-1* mRNA expression during neuronal differentiation in embryonic zebrafish. Dev. Dyn. 199, 1-11.

Izumikawa, M., Minoda, R., Kawamoto, K., Abrashkin, K.A., Swiderski, D.L., Dolan, D.F., Brough, D.E., Raphael, Y., 2005. Auditory hair cell replacement and hearing improvement by Atoh1 gene therapy in deaf mammals. Nat. Med. 11, 271-276.

Jacques, B.E., Montcouquiol, M.E., Layman, E.M., Lewandoski, M., Kelley, M.W., 2007. Fgf8 induces pillar cell fate and regulates cellular patterning in the mammalian cochlea. Development 134, 3021-3029.

Jones, J.M., Montcouquiol, M., Dabdoub, A., Woods, C., Kelley, M.W., 2006. Inhibitors

of differentiation and DNA binding (Ids) regulate Math1 and hair cell formation during development of the organ of Corti. J. Neurosci. 26, 550-558.

Jowett, T., Yan, Y.L., 1996. Double fluorescent in situ hybridization to zebrafish embryos. Trends Genet. 12, 387-389.

Kawamoto, K., Ishimoto, S.-I., Minoda, R., Brough, D.E., Raphael, Y., 2003. *Math1* gene transfer generates new cochlear hair cells in mature guinea pigs *in vivo*. J. Neurosci. 23, 4395-4400.

Kiefer, P., Strahle, U., Dickson, C., 1996. The zebrafish *Fgf-3* gene: cDNA sequence, transcript structure and genomic organization. Gene 168: 211-215.

Kiernan, A.E., Ahituv, N., Fuchs, H., Balling, R., Avraham, K.B., Steel, K.P., de Angelis. M.H., 2001. The Notch ligand *Jagged1* is required for inner ear sensory development. Proc. Natl. Acad. Sci. 98, 3873-3878.

Kiernan, A.E., Pelling A.L., Leung, K.K.H., Tang, A.S.P., Bell, D.M., Tease,C., Lovell-Badge, R., Steel, K.P., Cheah, K.S.E., 2005. *Sox2* is required for sensory organ development in the mammalian inner ear. Nature 434, 1031-1035.

Kiernan, A.E., Xu, J., Gridley, T., 2006. The Notch ligand JAG1 is required for sensory progenitor development in the mammalian inner ear. PLOS Genetics 2(1), e4.

Kimmel, C.B., Ballard, W.W., Kimmel, S.R., Ullman, B., Schilling, T.F., 1995. Stages of embryonic development of the zebrafish. Dev. Dyn. 203: 253-310.

Korzh, V., Edlund, T., Thor, S., 1993. Zebrafish primary neurons initiate expression of the LIM homeodomain protein Isl-1 at the end of gastrulation. Development 118, 417-425.

Korzh, V., Sleptsova, I., Liao, J., He, J., Gong, Z., 1998. Expression of zebrafish bHLH genes *ngn1* and *nrd* defines distinct stages of neural differentiation. Dev. Dyn. 213, 92-104.

Koundakjian, E.J., Appler, J.L., Goodrich, L.V., 2007. Auditory neurons make stereotyped wiring decisions before maturation of their targets. J. Neurosci. 27, 14078-14088.

Kwak, S.J., Phillips, B.T., Heck, R., Riley, B.B., 2002. An expanded domain of *fgf3* expression in the hindbrain of zebrafish *valentino* mutants results in mis-patterning of the otic vesicle. Development 129, 5279-5287.

Kwak, S.J., Vemaraju, S., Moorman, S.J., Zeddies, D., Popper, A.N. and Riley, B.B., 2006. Zebrafish *pax5* regulates development of the utricular macula and vestibular function. Dev. Dyn. 235, 3026-3038.

Ladher, R.K., Anakwe, K.U., Gurney, A.L., Schoenwolf, G.C., Francis-West, P.H., 2000. Identification of synergistic signals initiating inner ear development. Science 290, 1965-1967.

Ladher, R.K., Wright, T.J., Moon, A.M., Mansour, S.L., Schoenwolf, G.C., 2005. FGF8 initiates inner ear induction in chick and mouse. Genes Dev. 19, 603-613.

Landsberg, R.L., Awatramani, R.B., Hunter, N.L., Farago, A.F., DiPietrantonio, H.J., Rodriguez, C.I., Dymecki, S.M., 2005. Hindbrain rhombic lip is comprised of discrete progenitor cell populations allocated by *Pax6*. Neuron 48, 933-947.

Lanner, F., Rossant, J., 2001. The role of FGF/Erk signaling in pluripotent stem cells. Development 137, 3351-3360.

Lawoko-Kerali, G., Rivolta, M.N., Holley, M., 2002. Expression of the transcription factors GATA3 and Pax2 during development of the mammalian inner ear. J. Comp. Neurol. 442: 378-391.

Lecaudey, V., Ulloa, E., Anselme, I., Stedman, A., Schneider-Maunoury, S., Pujades, C., 2007. Role of the hindbrain in patterning the otic vesicle: A study of the zebrafish *vhnf1* mutant. Dev. Biol. 303, 134-143.

Lee, Y., Grill, S., Sanchez, A., Murphy-Ryan, M., Poss, K.D., 2005. Fgf signaling instructs position-dependent growth rate during zebrafish fin regeneration. Development 132, 5173-5183.

Leger, S., Brand, M., 2002. Fgf8 and Fgf3 are required for zebrafish ear placode induction, maintenance and inner e. Mechanisms of Developement 119, 91-108.

Lewis, R.R., Leverenz, E.L., Bialek, W.S., 1985. The Vertebrate Inner Ear, CRC Press, Boca Raton, FL.

Li, Y., Allende, M.L., Finkelstein, R., Weinberg, E.S., 1994. Expression of two zebrafish *orthodenticle*-related genes in the embryonic brain. Mech. Dev. 48: 229-244.

Li, S., Price, S.M., Cahill, H., Ryugo, D.K., Shen, M.M., Xiang, M., 2002. Hearing loss caused by progressive degeneration of cochlear hair cells in mice deficient for the *Barhl1* homeobox gene. Development 129, 3523-3532.

Li, H., Liu, H., Corrales, C.E., Mutai, H., Heller, S.. 2004a. Correlation of Pax-2 expression with cell proliferation in the developing chicken inner ear. J. Neurobiol. 60: 61-70.

Li, H., Liu, H., Sage, C., Huang, M., Chen, Z.-Y., Heller, S., 2004b. Islet-1 expression in the developing chicken inner ear. J. Comp. Neurol. 477, 1-10.

Liu, M., Pereira, F.A., Price, S.D., Chu, M.-j., Shope, C., Himes, D., Eatock, R.A., Brownell, W.E., Lysakowski, A., Tsai, M.-J., 2000. Essential role of BETA2/NeuroD1 in development of the vestibular and auditory systems. Genes Dev. 14, 2839-2854.

Lun, K., Brand, M., 1998. A series of *no isthmus* (*noi*) alleles of the zebrafish *pax2.1* gene reveals multiple signaling events in development of the midbrain-hindbrain boundary. Development 125: 3049-3062.

Ma, Q., Kintner, C., Anderson, D.J., 1996. Identification of *neurogenin*, a vertebrate neuronal determination gene. Cell 87, 43-52.

Ma, Q., Chen, Z., del Barco Barrantes, I., de la Pompa, J.L., Anderson, D.J., 1998. *neurogenin1* is essential for the determination of neuronal precursors for proximal cranial sensory ganglia. Neuron 20, 469-482.

Ma, Q., Anderson, D.J., Fritzsch, B., 2000. *Neurogenin 1* null mutant ears develop fewer, morphologically normal hair cells in smaller sensory epithelia devoid of innervation. J. Assoc. Res. Otolaryngol. 1, 129-143.

Mackereth, M. D., Kwak, J.-J., Fritz, A., Riley, B. B., 2005. Zebrafish *pax8* is required for otic placode induction and plays a redundant role with Pax2 genes in the maintenance of the otic placode. Development 132, 371-382.

Maklad, A., Fritzsch, B., 1999. Incomplete segregation of endorgan-specific vestibular ganglion cells in mice and rats. J. Vestib. Res. 9, 387-399

Maklad, A., Fritzsch, B., 2003. Development of vestibular afferent projections into the hindbrain and their central targets. Brain Res. Bul. 60, 497-510.

Maroon, H., Walshe, J., Mahmood, R., Kiefer, P., Dickson, C., Mason, I., 2002. Fgf3 and Fgf8 are required together for formation of the otic placode and vesicle. Development 129, 2099-2108.

Matei, V., Pauley, S., Kaing, S., Rowitch, D., Beisel, K.W., Morris, K., Feng, F., Jones, K., Lee, J., Fritzsch, B., 2005. Smaller inner ear sensory epithelia in *Neurog1* null mice are related to earlier hair cell cycle exit. Dev. Dyn. 234, 633-650.

Matsui, J.I., Ryals, B.M., 2005. Hair cell regeneration: an exciting phenomenon…but will restoring hearing and balance be possible? J. Rehab. Res. Dev. 42, 187-198.

Millimaki, B. B., Sweet, E. M., Dhason, M. S., Riley, B. B., 2007. Zebrafish *atoh1* genes: Classic proneural activity in the inner ear and regulation by Fgf and Notch. Development 134, 295-305.

Millimaki, B.B., Sweet, E.M., Riley, B.B., 2010. Sox2 is required for maintenance and regeneration, but not initial development, of hair cells in the zebrafish inner ear. Dev. Biol. 338, 262-269.

Moens, C., 2008. Whole mount RNA in situ hybridization on zebrafish embryos: hybridization. Cold Spring Harb. Protoc. 8, pdb.prot5037.

Morsli, H., Tuorto, F., Choo, D., Postiglione, M.P., Simeone, A., Wu, D.K., 1999. *Otx1* and *Otx2* activities are required for the normal development of the mouse inner ear. Development 126: 2335-2343.

Nasevicius, A., Ekker, S.C., 2000. Effective targeted gene 'knockdown' in zebrafish. Nat. Genetics 26: 216-220.

Nelson, A.D., Svendsen, C.N., 2006. Low concentrations of extracellular FGF-2 are sufficient but not essential for neurogenesis from human neural progenitor cells. Mol. Cell. Neurosci. 33, 29-35.

Neves, J., Parada, C., Chamizo, M., Giráldez, F., 2011. Jagged 1 regulates the restriction of Sox2 expression in the developing chicken inner ear: a mechanism for sensory organ specification. Development 138, 735-744.

Nornes, H.O., Dressler, G.R., Knapik, E.W., Deutsch, U., Gruss, P., 1990. Spatially and temporally restricted expression of Pax2 during murine neurogenesis. Development 109, 797-809.

Nyeng, P., Bjerke, M.A., Norgaard, G. A., Qu, X., Kobberup, S., Jensen, J., 2011. Fibroblast growth factor 10 represses cell differentiation during establishment of the intestinal progenitor niche. Dev. Biol. 349, 20-34.

Oxtoby, E., Jowett, T., 1993. Cloning of the zebrafish *krox-20* gene (*krx-20*) and its expression during hindbrain development. Nucleic Acids Res. 21: 1087-1095.

Pan, W., Jin, Y., Stanger, B., Kiernan, A. E. (2010). Notch signaling is required for the generation of hair cells and supporting cells in the mammalian inner ear. Proc. Natl. Acad. Sci. 107, 15798-15803.

Pauley, S., Wright, T.J., Pirvola, U., Ornitz, D., Beisel, K., Fritzsch, B., 2003. Expression and function of FGF10 in mammalian inner ear development. Dev. Dyn. 227, 203-215.

Pfeffer, P.L., Gerster, T., Lun, K., Brand, M., Busslinger, M., 1998. Characterization of three novel members of the zebrafish *Pax2/5/8* family: dependency of *Pax5* and *Pax8* expression on the *Pax2.1* (*noi*) function. Development 125, 3063-3074.

Phillips, B.T., Bolding, K., Riley, B.B., 2001. Zebrafish *fgf3* and *fgf8* encode redundant functions required for otic placode induction. Dev. Biol. 235, 351-365.

Pirvola, U., Spencer-Dene, B., Xing-Qun, L., Kettunen, P.i., Thesleff, I., Fritzsch, B., Dickson, C., Ylikoski, J., 2000. FGF/FGFR-2(IIIb) signaling is essential for inner ear morphogenesis. J. Neurosci. 20, 6125-6134.

Pirvola, U., Ylikoski, J., Trokovic, R., Hebert, J.M., McConnell, S.K., Partanen, J., 2002. FGFR1 is required for the development of the auditory sensory epithelium. Neuron 35, 671-680.

Pittman, A.J., Law, M.Y., Chien, C.B., 2008. Pathfinding in a large vertebrate axon tract: isotypic interactions guide retinotectal axons at multiple choice points. Development 135, 2865-2871.

Popper, A.N., Hoxter, B., 1984. Growth of a fish ear: 1. Quantitative analysis of hair cell and ganglion cell proliferation. Hear. Res. 15, 133-142.

Popper, A.N., Fay, R.R., 1993. Sound detection and processing by fish: critical review and major research questions, Brain Behav. Evol. 41: 14-38.

Popper, A.N., Fay, R.R., Platte, C., Sand, O., 2003. Sound detection mechanisms and capabilities of teleosts fishes. In Sensory processing in aquatic environments (ed. S. P. Collin and N. J. Marshall) Springer-Verlag, New York. pp. 3-38.

Presson, J.C., Popper, A.N., 1990. A ganglionic source of new eighth nerve neurons in a post-embryonic fish. Hear. Res. 46, 23-28.

Puligilla, C., Feng, F., Ishikawa, K., Bertuzzi, S., Dabdoub, A., Griffith, A.J., Fritzsch, B., Kelley, M.W., 2007. Disruption of *Fibroblast Growth Factor Receptor 3* signaling results in defects in cellular differentiation, neuronal patterning, and hearing impairment. Dev. Dyn. 236, 1905-1917.

Puligilla, C., Dabdoub, A., Brenowitz, S.D., Kelley, M.W., 2010. Sox2 induces neuronal formation in the developing mammalian cochlea. J. Neurosci. 30, 714-722.

Quint, E., Furness, D.N., Hackney, C.M., 1998. The effect of explantation and neomycin on hair cells and supporting cells in organotypic cultures of the adult guinea-pig utricle. Hear Res.118: 157-167.

Radde-Gallwitz, K., Pan, L., Gan, L., Lin, X., Segil, N., Chen, P., 2004. Expression of Islet1 marks the sensory and neuronal lineages in the mammalian inner ear. J. Comp. Neurol. 477, 412-421.

Radosevic, M., Robert-Moreno, A., Coolen, M., Bally-Cuif, L., Alsina, B., 2011. Her9 represses neurogenic fate downstream of Tbx1 and retinoic acid signaling in the inner ear. Development 138, 397-408.

Raft, S., Nowotschin, S., Liao, J., Morrow, B.E., 2004. Suppression of neural fate and control of inner ear morphogenesis by Tbx1. Development 131, 1801-1812.

Reifers, F., Bohli, H., Walsh, E.C., Crossley, P.H., Stainier, D.Y.R.. 1998. *Fgf8* is mutated in zebrafish *acerebellar* (*ace*) mutants and is required for maintenance

of midbrain-hindbrain boundary and somitogenesis. Development 125, 2381-2395.

Riccomagno, M.M., Takada, S., Epstein, D.J., 2005. Wnt-dependent regulation of inner ear morphogenesis is balanced by the opposing and supporting roles of Shh. Genes & Dev. 19, 1612-1623.

Riley, B.B., Grunwald, D.J., 1996. A mutation in zebrafish affecting a localized cellular function required for normal ear development. Dev. Biol. 179: 427-435.

Riley, B. B., Chiang, M.Y., Farmer, L., Heck, R., 1999. The *deltaA* gene of zebrafish mediates lateral inhibition of hair cells in the inner ear and is regulated by *pax2.1*. Development 126, 5669-5678.

Riley, B.B., Moorman, S.J., 2000. Development of utricular otoliths, but not saccular otoliths, is necessary for vestibular function and survival in zebrafish. J. Neurobiol. 43, 329-337.

Riley, B.B., Phillips, B.T., 2003. Ringing in the new ear: resolution of cell interactions in otic development. Dev. Biol. 261, 289-312.

Roehm, P.C., Hansen, M.R., 2005. Strategies to preserve or regenerate spiral ganglion neurons. Curr. Opin. Otolaryngol. Head Neck Surg. 13, 294-300.

Sanchez-Calderon, H., Martin-Partido, G., Hidalgo-Sanchez, M., 2005. *Pax2* expression patterns in the developing chick inner ear. Gene Expr. Patterns. 5, 763-773.

Sanchez-Calderon, H., Francisco-Morcillo, J., Martin-Partido, G., Hidalgo-Sanchez, M., 2007a. Fgf19 expression patterns in the developing chick inner ear. Gene Expr. Patterns. 7, 30-38.

Sanchez-Calderon, H., Milo, M., Leon, Y., Varela-Nieto, I., 2007b. A network of growth and transcription factors controls neuronal differentiation and survival in the developing ear. Int. J. Dev. Biol. 51, 557-570.

Saarimaaki-Vire, J., Peltopuro, P., Lahti, L., Naserke, T., Blak, A.A., Vogt Weisenhorn, D.M., Yu, K., Ornitz, D.M., Wurst, W., Partanen, J., 2007. Fibroblast growth factor receptors cooperate to regulate neural progenitor properties in the developing midbrain and hindbrain. J. Neurosci. 27, 8581-8592.

Sapede, D., Pujades, C., 2010. Hedgehog signaling governs the development of otic sensory epithelium and its associated innervation in zebrafish. J. Neurosci. 30, 3612-3623.

Satoh, T., Fekete, D.M., 2005. Clonal analysis of the relationships between mechanosensory cells and the neurons that innervate them in the chicken ear. Development 132: 1687-1697.

Schuck, J. B., Smith, M. E., 2009. Cell proliferation follows acoustically-induced hair bundle loss in the zebrafish saccule. Hear. Res. 253, 67-76.

Schlueter, P.J., Peng, G., Westerfield, M., Duan, C., 2007. Insulin-like growth factor signaling regulates zebrafish embryonic growth and development by promoting cell survival and cell cycle progression. Cell Death Differ. 14, 1095-1105.

Shibata, S.B., Budenz, C.L., Bowling, S.A., Pfingst, B.E., Raphael, Y., 2011. Nerve maintenance and regeneration in the damaged cochlea. Hear. Res. (in press).

Shou, J., Zheng, J.L., Gao, W.Q., 2003. Robust generation of new hair cells in the

mature mammalian inner ear by adenoviral expression of Hath1. Mol. Cell. Neurosci. 23, 169-179.

Smeti, I., Savary, E., Capelle, V., Hugnot, J.P., Uziel, A., Zine, A., 2011. Expression of candidate markers for stem/progenitor cells in the inner ears of developing and adult GFPA and nestin promoter-GFP transgenic mice. Gene Expr. Patterns. 11, 22-32.

Sobkowicz, H.M., August, B.K., Slapnick, S.M., 1992. Epithelial repair following mechanical injury of the developing organ of Corti in culture: an electron microscopic and autoradiographic study. Exp. Neurol. 115: 44-49.

Sobkowicz, H.M., August, B.K., Slapnick, S.M., 1997. Cellular interactions as a response to injury in the organ of Corti in culture. Int. J. Dev. Neurosci. 15: 463-485.

Stoick-Cooper, C.L., Weidinger, G., Riehle, K.J., Hubbert, C., Major, M.B., Fausto, N., Moon, R.T., 2007. Distinct Wnt signaling pathways have opposing roles in appendage regeneration. Development 134, 479-489.

Streit, A., 2004. Early development of the cranial sensory nervous system: from a common field to individual placodes. Dev. Biol. 276, 1-15.

Sun, Y., Jan, L.Y., Jan, Y.N., 1998. Transcriptional regulation of *atonal* during development of the *Drosophila* peripheral nervous system. Development 125, 3731-3740.

Sun, Z., Hopkins, N., 2001. *vhnf1*, the MODY5 and familial GCKD-associated gene, regulates regional specification of the zebrafish gut, pronephros, and

hindbrain. Genes Dev. 15, 3217-3229.

Thomas, M., Langley, B., Berry, C., Sharma, M., Kirk, S., Bass, J., Kambadur, R., 2000. Myostatin, a Negative Regulator of Muscle Growth, Functions by Inhibiting Myoblast Proliferation. J. Biol. Chem. 275, 40235-40243.

Tucker, E.S., Lehtinen, M.K., Maynard, T., Xirsinger, M., Dulac, C., Rawson, N., Penvy L., LaMantia, A.S., 2010. Proliferative and trancscriptional identity of distinct classes of neural precursors in the mammalian olfactory epithelium. Development 137, 2471-2481.

Uchikawa, M., Kamachi, Y., Kondoh, H., 1999. Two distinct subgroups of Group B Sox genes for transcriptional activators and repressors: their expression during embryonic organogenesis of the chicken. Mech. Dev. 84, 103-120.

Urbanek, P., Wang, Z.Q., Fetka, I., Wagner, E.F., Busslinger, M., 1994. Complete block of early B cell differentiation and altered patterning of the posterior midbrain in mice lacking Pax5/BSAP. Cell 79: 901-912.

Varela-Nieto, I., Morales-Garcia, J.A., Vigil, P., Diaz-Casares, A., Gorospe, I., Sanchez-Galiano, S., Canon, S., Camarero, G., Contreras, J., Cediel, R., Leon, Y., 2004. Trophic effects of insulin-like growth factor-I (IGF-I) in the inner ear. Hear. Res. 196, 19-25.

Vasquez-Echeverria, C., Domininguez-Frutos, E., Charnay, P., Schimmang, T., Pujades, C., 2008. Analysis of mouse *kreisler* mutants reveals new roles of hindbrain-

derived signals in the establishment of the otic neurogenic domain. Dev. Biol. 322, 167-178.

Vendrell, V., Carnicero, E., Giraldez, F., Alonso, M.T., Schimmang, T., 2000. Induction of inner ear fate by FGF3. Development 127, 2011-2019.

Wallis, D., Hamblen, M., Zhou, Y., Venken, K.J.T., Schumacher, A., Grimes, H.L., Zoghbi, H.Y., Orkin, S.H., Bellen, H.J., 2003. The zinc finger transcription factor Gfi1, implicated in lymphomagenesis, is required for inner ear hair cell differentiation and survival. Development 130, 221-232.

Whitfield, T.T., Riley, B.B., Chiang, M.Y., Phillips, B., 2002. Development of the zebrafish inner ear. Dev. Dyn. 223, 427-458.

Woods, C., Montcouquiol, M., Kelley, M. W., 2004. Math1 regulates development of the sensory epithelium in the mammalian cochlea. Nat. Neurosci. 7, 1310-1318.

Wright, T.J., Mansour, S.L., 2003. FGF signaling in ear development and innervation, Curr. Top. Dev. Biol. 57, 225-259.

Wright, T.J., Ladher, R., McWhirter, J., Murre, C., Schoenwolf, G.C., Mansour, S.L., 2004. Mouse FGF15 is the ortholog of human and chick FGF19, but is not uniquely required for otic induction. Dev. Biol. 269, 264-275.

Wu, H.H., Ivkovic, S., Murray, R.C., Jaramillo, S., Lyons, K.M., Johnson, J.E., Calof, A.L., 2003. Autoregulation of neurogenesis by GDF11. Neuron 37, 197-207.

Xiang, M., Gao, W.Q., Hasson, T., Shin, J.J., 1998. Requirement for Brn-3c in maturation and survival, but not in fate determination of inner ear hair cells. Development 125, 3935-3946.

Xiao, T., Roeser, T., Staub, W., Baier, H., 2005. A GFP-based genetic screen reveals mutations that disrupt the architecture of the zebrafish retinotectal projection. Development 132, 2955-2967.

Yang, H., Xie, X., Deng, M., Chen, X., Gan, L., 2010. Generation and characterization of *Atoh1-Cre* knock-in mouse line. Genesis 48, 407-413.

Zeddies, D.G., Fay, R.R., 2005. Development of the acoustically evoked behavioral response in zebrafish to pure tones. J. Exp. Biol. 208: 1361-1372.

Zheng, J.L.,Gao, W.Q., 2000. Overexpression of *Math1* induces robust production of extra hair cells in postnatal rat inner ears. Nat. Neurosci. 3, 580-586.

Zhou, X., Hossain, W.A., Rutledge, A., Baier, C., Morest, D.K., 1996. Basic fibroblast growth factor (FGF-2) affects development of acoustico-vestibular neurons in the chick embryo brain in vitro. Hear. Res. 101, 187-207.

VITA

Shruti Vemaraju
Department of Biology, 3258 TAMU
Texas A&M University, College Station 77843
svemaraju@mail.bio.tamu.edu

Education:

B.Tech., Biotechnology, Guru Gobind Singh Indraprastha University, 2003
Ph.D., Biology, Texas A&M University, 2011

Publications:

Su-Jin Kwak, **Shruti Vemaraju**, Stephen J. Moorman, David Zeddies, Arthur N. Popper, Bruce B. Riley (2006). Zebrafish *pax5* regulates development of the utricular macula and vestibular function. Dev. Dyn. 235, 3026-3038.

Elly M. Sweet, **Shruti Vemaraju**, Bruce B. Riley (2011). Sox2 and Fgf interact with Atoh1 to promote sensory competence throughout the zebrafish inner ear. Dev. Biol. 358, 113-121.

Manuscripts in preparation:

Shruti Vemaraju and Bruce B. Riley. Spatial and temporal gradient of Fgf controls discrete stages of statoacoustic ganglion development in the zebrafish inner ear. (In preparation).